Technical University of Crete
Department of Chemical and Environmental Engineering

Postgraduate Thesis

“Occupant Behaviour optimisation towards thermal comfort and energy efficiency in Buildings”

by

Thodoris Maximilianos Chytis

Supervisor: Asst. Professor Nikolaos A. Diangelakis

Thesis Committee:

Professor Dionysia Kolokotsa

Assoc. Professor Tryfon Daras

Chania 2024

Abstract

Occupant behaviour impact is under-recognized in the design and operation of buildings. Conventional approaches address thermal comfort and energy efficiency typically relying on rule-based and schedule-based systems. This study combines innovative dynamic methods and shifts focus on occupant behaviour and its impact on building conditions, thermal comfort, and energy efficiency. A framework is introduced to simulate building occupant behaviours and thus provide decision making support tools for low carbon communities while prioritising occupant comfort and satisfaction. The primary objectives include advancing scholarly understanding in building energy efficiency and indoor environmental quality, in the context of occupant-centric and regulated interventions and adjustments. Optimisation towards thermal comfort maximisation and energy consumption minimisation supports the base for an occupant-centric decision support system. In the interest of achieving the aforementioned goals, we employ a methodology, which comprises of (i) building energy simulations (EnergyPlus), (ii) occupant actions modelling, (iii) Python simulation coupling, (iv) machine learning (ReLU-based Artificial Neural Networks) and (v) mixed integer optimisation techniques. The optimisation techniques applied, utilise the concept of the “rolling horizon”, in order to determine strategies of (sub)optimal behaviours of a singular occupant over time. Outcomes include a comprehensive understanding of the intricate interplay between occupant thermal comfort adjustment actions, building thermal conditions, and building energy consumption under exposure to location specific weather conditions.

Acknowledgements

I wish to express my gratitude to my academic supervisor Asst. Prof. Nikolaos A. Diangelakis, whose unwavering motivation, support, and technical expertise, guided me throughout my postgraduate studies.

Special thanks to Prof. Dionysia Kolokotsa, Dr. Nikolaos Kampelis, Dr. Konstantinos Gobakis, Filippos Lygerakis, members of the “Energy Management in the Built Environment” (EMBER) Lab, for sharing their technical, theoretical knowhow, offering useful guidance to support the completion of the interdisciplinary approach that characterises this postgraduate thesis.

I am thankful for the financial support provided by the Pancretan Foundation scholarship program for funding the postgraduate thesis.

To my family, whose unwavering support has been my pillar of strength, I am deeply thankful.

Finally, to my close friends, whether near or far, your presence and encouragement meant the world to me.

Contents

I. List of Abbreviations

Acronym	Description
ABM	Agent-Based Modelling
AHU	Air Handling Unit
AM	Approximate Model
AML	Algebraic Modelling Languages
ANN	Artificial Neural Network
API	Application Programming Interface
ASHRAE	Society of Heating, Refrigeration and Air-Conditioning Engineers
B&B	Branch-and-Bound
BEM	Building Energy Modelling
CI	Computational intelligence
DX	Direct Expansion
E+	EnergyPlus™
EC	Energy Consumption
EN	European Standards
GA	Genetic Algorithms
GBD	Generalized Benders decomposition
GHG	Green House Gas
HVAC	Heating, ventilation, and air conditioning
IAQ	Indoor Air Quality

Acronym	Description
IEQ	Indoor environmental quality
IoT	Internet of Things
LEED	Leadership in Energy and Environmental Design
LP	Linear Programming
MAS	Multi-Agent Systems
MIQP	Mixed Integer Quadratic Programming
ML	Machine Learning
MOGA	Multi-Objective Genetic Algorithm
MOO	Multi-objective optimisation
MPC	Model predictive control
NN	Neural Network
NREL	National Renewable Energy Laboratory
nZEB	nearly Zero Energy Buildings
OA	Outer approximation
OB	Occupant Behaviour
OWC	Outdoor weather conditions
P	Zone Air Vapor Pressure
PMV	Predicted Mean Vote
PSO	Particle Swarm Optimisation
Pyomo	Python Optimisation Modeling Objects

Acronym	Description
QCP	Quadratically Constrained Programming
QP	Quadratic Programming
ReLU	Rectified Linear Unit
RES	Renewable Energy Sources
RH	Rolling Horizon
T	Zone Mean Air Temperature
TC	Thermal Comfort
TMY	Typical Meteorological Year
Tr	Zone Radiant Temperature
TZ	Thermal Zone
XML	eXtensible Markup Language

II. List of Figures

List of Tables

1. Introduction

1.1. Research Problem

The heightened focus on energy and climate concerns, both in public discourse and academic research, reflects growing awareness of the risks posed to human and natural systems due to escalating greenhouse gas (GHG) emissions stemming from increased primary energy consumption (EC) [1]. This includes increasing severity and frequency of extreme weather across the globe such as heat and cold waves, flash floods and tropical cyclones [2]. Over the past decade, there has been a notable increase in EC, with approximately one-third attributed to the building sector. For instance, buildings in the United Kingdom account for 39% of energy usage compared to other European nations, slightly exceeding the average EC of 37% [3]. The operational phase of a building's life cycle accounts for over 80% of its EC [4]. Therefore, while buildings serve as essential facilities meeting human needs and offering numerous societal advantages, they have also exerted detrimental effects on the environment in recent decades [5]. As a results, minimum performance standards and building energy codes are expanding and becoming stricter worldwide, while the adoption of efficient and renewable building technologies is gaining momentum. However, the building sector requires faster transformations to align with the Net Zero Emissions by 2050 (NZE) Scenario. The current decade is critical for implementing the necessary measures to meet the objectives of having all new buildings and 20% of the existing building stock ready for zero-carbon emissions by 2030 [6]. To ensure a global transition to a low-carbon future, accelerating the transformation to energy-saving practices in the building industry is crucial [7]. Annual EC shows a rising trend toward greater energy demand [8]. Efforts to reduce EC in buildings have focused on energy-efficient building systems. To enhance energy performance in buildings, the installation of efficient energy systems should be complemented by suitable operational and management tactics. However, the anticipated decline in energy use per capita in buildings has not been realised [9]. Furthermore, recent studies in the United Kingdom suggest that for various reasons, over 40% of the population is reluctant to purchase and adopt energy-saving technologies [10]. Additionally, through monitoring building EC, scholars have observed a significant disparity between predicted and actual energy usage by occupants [11]. Research has been conducted to investigate how the actual presence of occupants affects building energy usage [12]. Accurately predicting the impact of occupants on EC requires more than just considering the number of occupants in the building. Incorporating realistic occupancy information could enhance the accuracy of energy prediction [13]. Previous experimental studies have validated the effectiveness of occupant behavioural efficiency, with improvements ranging from 4% to 30%. Compared to retrofitting existing buildings,

behavioural education emerges as an efficient and cost-effective method. However, current categorisations of behavioural energy styles, such as "austerity," "standard," and "wasteful," are overly generalised. These vague descriptions are inadequate for effectively categorizing behavioural energy styles and incorporating behavioural impacts into building energy prediction [4]. The clear importance of achieving energy efficiency is clear, though it should not arrive at the expense of indoor environmental quality (IEQ). Four primary components—thermal comfort (TC), indoor air quality (IAQ), sound, and visual comfort—along with emotional and psychological needs, are essential for determining IEQ. Studies indicate that poor IEQ can lead to illnesses and negatively impact employee or occupant well-being and productivity. Among these factors, TC significantly influences occupants' comfort and productivity [14]. Therefore, it is essential to achieve the optimum occupant behaviour that results in maximum building energy efficiency while preserving and considering IEQ and specifically TC.

1.2. Energy Efficiency in Buildings

An energy-efficient building provides a suitable living environment while minimising energy usage and waste, thereby maximising energy preservation [15]. The energy efficiency of a building is fundamentally determined by the rate of energy loss through its physical envelope and the effectiveness of energy utilisation to meet occupants' needs and comfort. These two aspects are intricately linked, as the design and structure of a building, in conjunction with local weather conditions, strongly influence the choice and efficiency of energy systems. Therefore, any initiatives aimed at enhancing building energy efficiency necessitate a comprehensive consideration of both factors [16]. According to the International Energy Agency - Energy in the Buildings and Communities Program (IEA-EBC) Annex 53, EC in buildings is affected by six factors: (1) climatic conditions, (2) building structure, (3) energy and service systems within the building, (4) interior design specifications, (5) building operation and maintenance practices, and (6) occupant behaviours [17].

Figure 1. Key factors influencing accurate building Energy Prediction [17]

1.3. Thermal Comfort in Buildings

Thermal comfort, a subjective assessment of satisfaction with the thermal environment, hinges on an individual's perception and satisfaction regarding the ambient environment, often characterized by a sensation of neutrality without perspiration. Achieving optimal TC within buildings necessitates a holistic approach, considering factors such as the building's geographical location, internal activities, architectural design, and IAQ. The commonly employed method for evaluating TC is the Predicted Mean Vote (PMV) technique, initially introduced by Fanger in the 1970s, which operates on the principle of a constant state model. PMV values are derived from the aggregated thermal sensation responses of a large sample population habituated to specific environmental conditions. To accurately quantify PMV, six variables influencing TC must be computed: air temperature, humidity, air velocity, mean radiant temperature, occupants' metabolic rate, and fabric insulation (CLO value). These factors (Figure 2) encompass both environmental parameters and personal characteristics essential for an objective assessment of TC [18] [19]. Figure 3 depicts the evolution of the PMV modelling techniques and recommendations throughout the years, according to the International Organisation for Standardisation (ISO), the American Society of Heating, Refrigeration and Air-Conditioning Engineers (ASHRAE) and European Standards (EN). The TC scale quantifying thermal sensation by utilizing the PMV is shown in Table 1 [20].

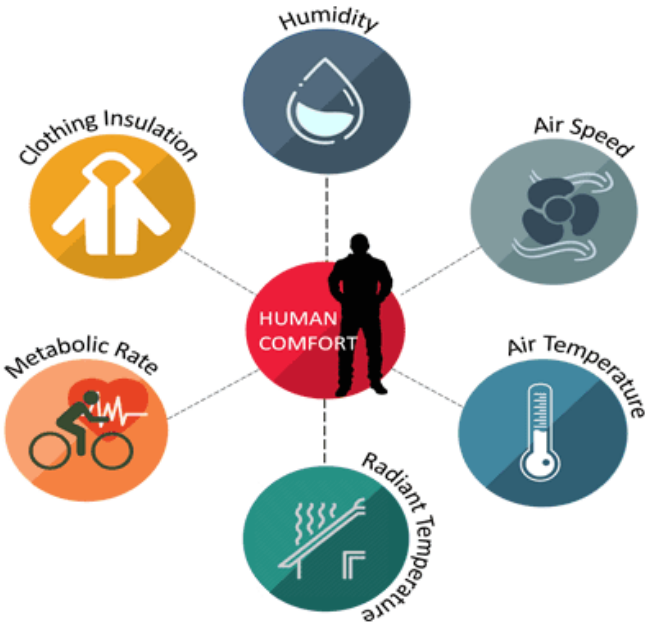

Figure 2. Variables influencing thermal comfort acquired from [21].

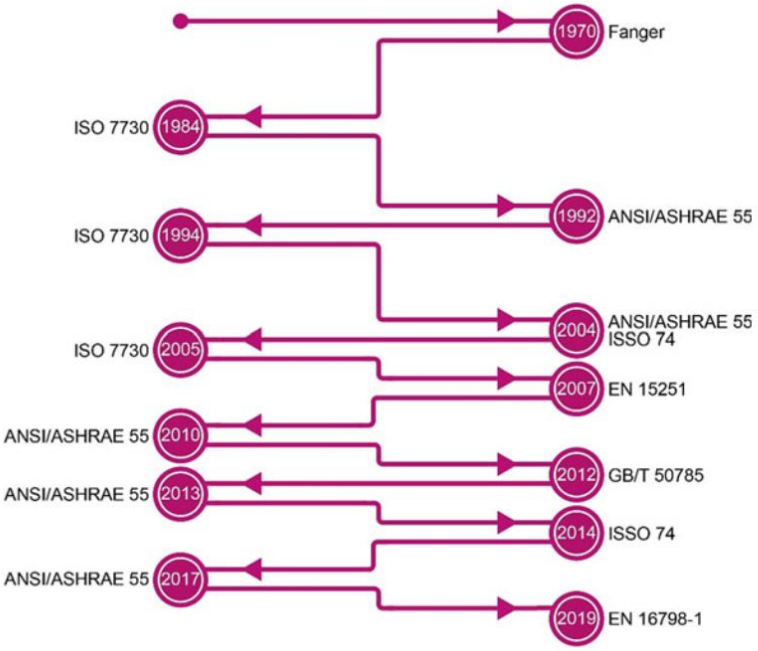

Figure 3. PMV timeline adapted from [22].

Table 1. ASHRAE PMV Thermal sensation scale [20].

PMV INDEX	Thermal sensation
-3	Cold
-2	Cool

-1	Slightly cool
0	Neutral
1	Slightly warm
2	Warm
3	Hot

1.4. Occupant Behaviour in Buildings

The term of occupant behaviour (OB) encompasses various phenomena related to how building occupants react to factors influenced by the building's physical attributes, indoor and outdoor environmental conditions, projected state of building systems, time of day, as well as their individual characteristics and physiological, psychological, social, and stochastic factors. In particular, environmental and time-related factors may play a crucial role on the behaviours of inhabitants [23]. OBs are often characterised by energy-related actions, such as managing systems and appliances like Heating, ventilation, and air conditioning (HVAC), windows, blinds, and lighting. Recent research underscores the significant role of OB in decreasing building EC [11].

1.5. Building Energy Modelling

Building energy modelling (BEM) and prediction are fundamental to major use cases. It is utilised in various architectural and engineering applications to enhance building efficiency and performance. Architects use BEM to design energy-efficient structures, balancing initial construction costs with operational energy expenses, often reducing both. In HVAC design, BEM assists mechanical engineers in creating systems that efficiently meet thermal demands and in testing control strategies. For building performance rating, BEM evaluates a building's inherent efficiency, aiding in code compliance, green certifications, and financial incentives. Additionally, BEM supports the development of energy codes and large-scale energy-efficiency programs through building stock analysis for organisations like utilities and local governments [24]. Existing models can be classified as purely physics-based (white box) models, purely data-driven (black box) models, and hybrid models that combine elements of both (grey box models) [25].

1.5.1. Physics-based Models

White-box models, also known as physics-based models, are grounded in fundamental principles of physics and engineering. They intricately replicate the energy dynamics of buildings by accounting for the physical behaviours of different components and systems. A

BEM program inputs detailed descriptions of a building, including its geometry, construction materials, lighting, HVAC, refrigeration, water heating, and renewable energy systems, as well as their component efficiencies and control strategies. It also incorporates information on the building's usage and operation, including schedules for occupancy, lighting, plug loads, and thermostat settings [26]. By integrating these inputs with local weather data, a BEM program uses physics-based equations to calculate thermal loads, how systems respond to those loads, and the resulting EC. Notable examples of white-box modelling tools include EenergyPlus™, TRNSYS, and IDA-ICE. These platforms enable detailed and accurate simulations of building energy performance, offering insights into how various elements interact and influence overall efficiency [27] (Figure 4).

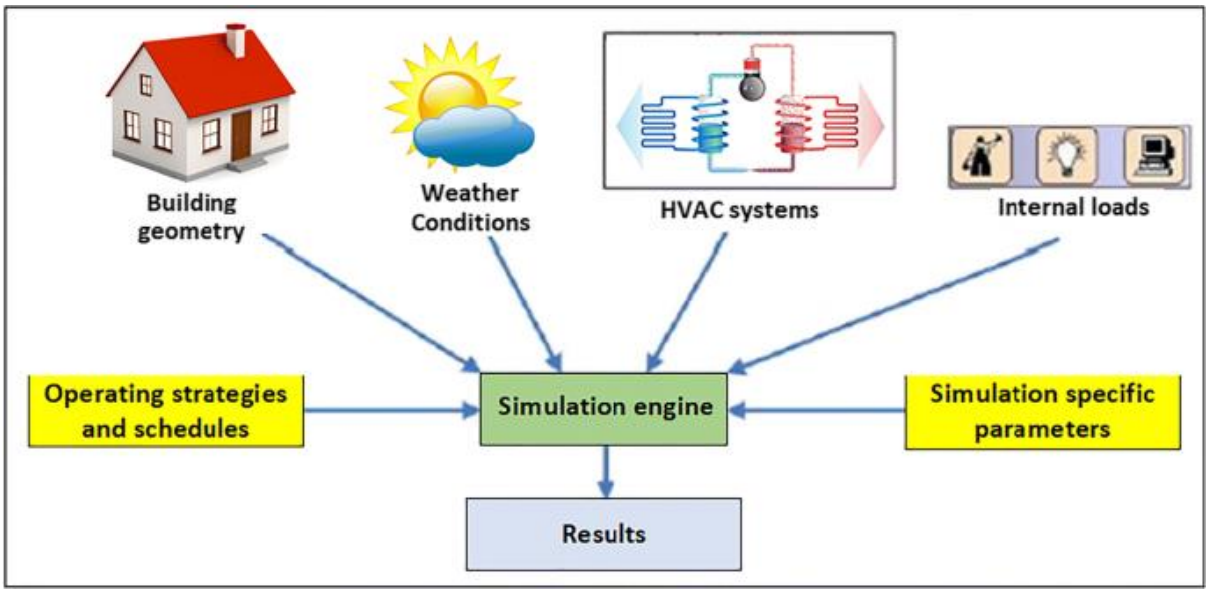

Figure 4. General data flow of building energy simulation models acquired from [26].

1.5.2. Data-driven Models

Black-box models rely on empirical and data-driven methodologies, often incorporating machine learning algorithms and statistical techniques. These models leverage historical data to forecast building energy consumption and behaviour. Prominent examples of black-box tools include Support Vector Machines, Random Forest, and Artificial Neural Networks (ANNs) [28] (see 1.5.2.1). Statistical and ML models are utilised to directly capture the relationship between building EC and operational data. These models require on-site measurements collected over a specific period to train them, enabling accurate predictions of building performance under varying conditions. Black-box models tend to be easy to build and computationally efficient [25]. These methodologies excel at capturing complex relationships within the data but may lack the transparency of white-box models due to their reliance on computational methods rather than explicit physical principles [27].

1.5.2.1. Artificial Neural Networks

Neural networks a subcategory of black-box models, are designed to mimic the human brain, replicating the way real neurons communicate. The objective of simulating the human brain in a neural network is to create a machine learning model capable of performing tasks that are difficult for traditional computing methods. The human brain excels at processing vast amounts of information, recognising patterns, and making decisions processes input data, applies weights, incorporates a bias, and generates an output, based on incomplete or ambiguous data. A neural network is composed of layers of nodes, which include an input layer, one or more hidden layers, and an output layer. Each node is interconnected and has an associated weight and threshold value. When a node's output surpasses its threshold, it activates and sends data to the next layer in the network.

Two essential processes are fundamental to the operation of a neural network, each playing a distinct yet interconnected role. Forward propagation involves processing data to generate an output, while back propagation focuses on learning from errors to enhance the network's accuracy.

Neural networks can be classified based on their learning type: supervised learning, unsupervised learning. Supervised learning involves the machine learning from labelled datasets under supervision, where the model makes predictions based on the known outcomes. In contrast, unsupervised learning allows the machine to learn from data that is neither classified nor labelled, enabling the algorithm to work without supervision. Here, the device aims to categorise unstructured information based on similarities, patterns, and differences [29].

A Feed-Forward Neural Network (Figure 5) is the most common type of neural network, where information flows in a single direction—from the input layer, through various hidden layers, and finally to the output layer. This network acts as a gateway to larger neural networks, processing input data through multiple layers of artificial neurons.

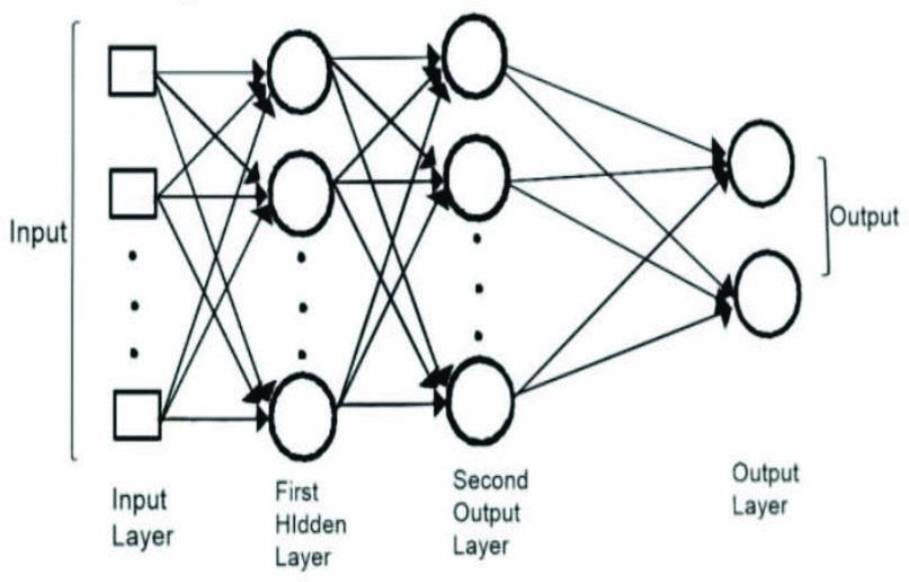

Figure 5. Feedforward Neural Network acquired from [29]

1.5.3. Hybrid Models

Hybrid or grey-box modelling strategies merge aspects of both physical and data-driven prediction models, aiming to capitalise on the strengths of each while mitigating their drawbacks. In grey-box models, certain internal parameters and equations retain physical interpretability. Moreover, grey-box models often demonstrate superior performance when compared to both black-box and white-box models [30].

1.6. Optimisation

Optimisation plays a pivotal role in process integration, exerting substantial influence by selecting the most advantageous solution from a range of possible options. Evaluation of solution quality is conducted through an objective function, typically aimed at either minimising or maximising a specific criterion such as cost. This quest for the optimal solution takes place within the framework of a system model and associated constraints. In essence, optimisation seeks to improve the value of a defined function, referred to as the objective function, while satisfying a multitude of constraints, including both equality and inequality constraints [31].

1.6.1. Convex Optimisation and Linear Programming

Convex optimisation is a subfield of optimisation that focuses on minimising convex functions over convex sets. Many convex optimisation problems can be solved in polynomial time. This area has wide applications, benefiting from the effectiveness of approximation methods. Recent advancements in computing and optimisation algorithms have made solving convex programming problems almost as straightforward as linear programming (LP) [32]. LP is a

mathematical technique used to optimise a linear objective function while adhering to constraints that are expressed as linear equalities and inequalities. LP can effectively manage a substantial number of continuous variables and constraints, delivering precise solutions. By employing Branch-and-Bound (B&B) methods, it can be adapted into mixed-integer LP to incorporate integer variables. The formulation of LP necessitates a clear definition of the optimisation problem, and the objective function must be assessed using linear models. When using LP to optimise energy-flexible systems, the models often need to be simplified [33].

1.6.2. Mixed integer Linear

A mixed integer linear programming (MILP) problem is an optimisation task involving a linear objective function and linear constraints, incorporating both integer and continuous decision variables [34]. MILP, operates as a search-based algorithm commonly referred to as B&B. This method swiftly explores numerous potential scenarios, samples, or situations to identify the optimal solution that optimises the objective function. Notably, MILP accommodates both the continuous and discrete characteristics of controlled and manipulated variables, while adhering to stringent constraints, including hard constraints (e.g., lower and upper bounds) and soft constraints (e.g., targets) [35].

1.6.3. Mixed integer Non-Linear

Mixed-integer non-linear programming (MINLP) is a mathematical optimisation approach that deals with non-linearities in both objective functions and constraints [34]. Regarding its solution, the B&B algorithm becomes too computationally expensive to implement. Thus, an alternative solution approach, comprises problem decomposition strategies like Generalized Benders decomposition (GBD) or Outer approximation (OA). Both algorithms are effective for solving MINLP problems due to their ability to handle nonlinearity and integer variables by breaking the problem into smaller, more manageable sub-problems, namely into NLP problems and MILP problems. GBD primarily focuses on decomposing utilising Lagrange multipliers to generate Benders cuts for tightening the MILP solution space. OA utilises outer approximations (linear or piecewise linear) to iteratively refine the feasible region of the MINLP problem. The NLP problems define the upper bound and MILP problems define the lower bound of the MINLP problem. During the algorithm the gap between the upper and lower bounds is checked. If the gap is within a predefined tolerance, the algorithm converges, indicating that the optimal solution has been found. If the gap is still large, the process iterates, refining the bounds. The possible convexity of the NLP subproblem, ensures that the solutions found in each iteration are globally optimal, leading to more reliable convergence to the global optimum of the original problem [36].

1.6.4. Multi-objective

Multi-objective optimisation (MOO), also known as multi-objective programming, is a branch of multiple-criteria decision-making that deals with mathematical optimisation problems that includes multiple objective functions that must be optimised at the same time [37]. MOO has risen as the preferred methodology for addressing sustainability challenges. Typically, the outcome of MOO models manifests as a collection of Pareto optima, symbolising optimal trade-offs among specified criteria. However, selecting the ultimate Pareto solution from this set for practical implementation presents a formidable challenge, especially in scenarios involving multiple criteria and decision-makers. [38].

1.6.5. Pareto Planes

Pareto optimality stands as a fundamental concept within optimisation. In single objective optimisation problems, the Pareto optimal solution is unique as the focus is on the decision variable space. However, MOO as mentioned above, expands upon this theory by enabling the simultaneous optimisation of multiple objectives. The MOO is considered as a mathematical process looking for a set of alternatives that represents the Pareto optimal solution. Thus, in brief, the Pareto optimal solution comprises a set of 'non-inferior' feasible solutions in the objective space defining a boundary beyond which none of the objectives can be improved without sacrificing at least one of the other objectives [39].

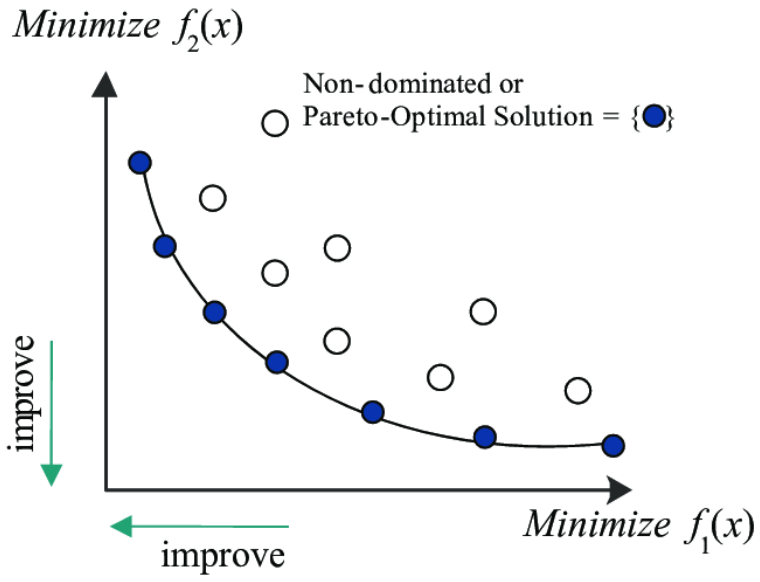

Figure 6. Pareto optimal solutions diagram acquired from [40].

1.6.6. Rolling Horizon

The term rolling horizon is used to indicate that in a time-dependent model, iterative solving occurs, and the planning interval progresses forward in time with each step of solution. At each

time step, decisions are made based on the current state of the system and the available information, without the need to consider the entire future horizon. As time progresses, the horizon shifts forward by one discretisation time-interval, and the optimisation process is re-executed to update decisions based on the latest information. Then, just the decision variable values obtained for the next discrete time instant are used, and the procedure is repeated successively [41].

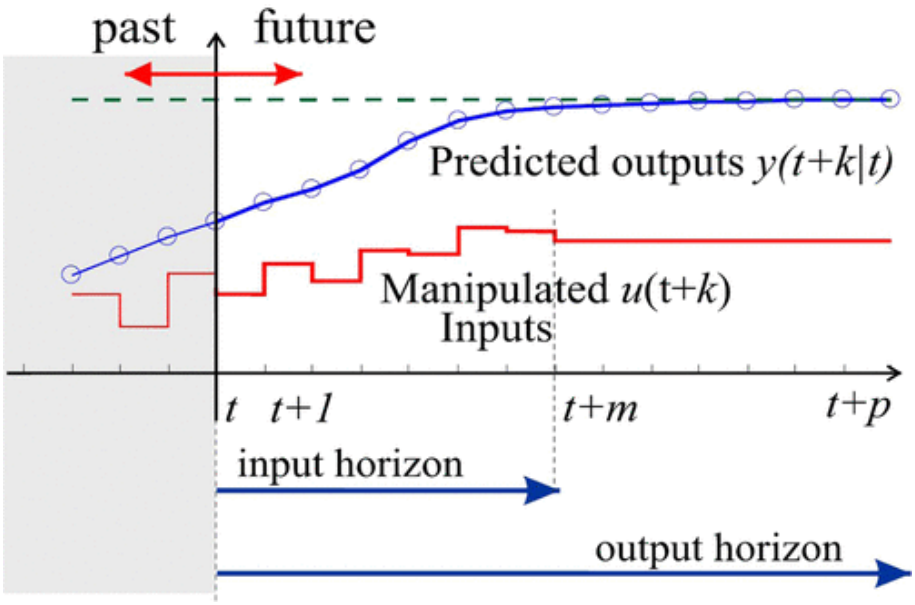

Figure 7. A typical rolling horizon approach acquired from [41].

1.7. Objectives of the Study

The overarching goal of this study is the development of an occupant-centric decision support methodology for the built environment, which shifts the focus to OB and its impact on EC and TC. This study aims to underscore and investigate the critical role of OB in influencing building energy performance and TC, addressing a significant gap in current research. To achieve this, the study will create a novel optimisation framework that integrates physics-based and data-driven models, providing a comprehensive tool for simulating and optimising the interplay between OB, building indoor conditions, and EC.

Employing cutting-edge dynamic modelling techniques, the study seeks to accurately predict and optimise occupant interactions with building systems on a timestep scale. Another key objective is to develop and validate a methodology that balances the dual goals of minimising EC and maximising occupant TC through multi-objective optimisation and Pareto analysis. The study aims to map the dynamics between occupant actions, building conditions, and EC, and utilise that map, to develop strategies for optimal OB that are adapted to location-specific weather conditions. To account for location specific weather, the framework is applied to a

validated specific case study building model, underlining its potential effectiveness on real-world applications, thereby providing actionable insights and decision-making support for stakeholders.

1.8. Scope and Limitations

The scope of this study encompasses the analysis of OB in residential buildings and its impact on energy efficiency and TC. The research will focus on developing a methodology that can optimise building energy performance, and occupant comfort, by considering data on occupant actions, building conditions, and external weather conditions. The study will include the use of building energy simulations, machine learning techniques, and mixed-integer optimisation methods to achieve its objectives.

However, the study incorporates several assumptions and simplifications in its models, such as constant metabolic rates and predefined clothing insulation values for occupants, which may not fully capture real-world variations and complexities. The findings and validations are specific to the case study building (Leaf House, see section 4.1) and may not be directly transferable to other buildings with different designs and systems. Implementing advanced dynamic modelling and optimisation techniques requires significant computational resources, which may limit the scalability and applicability of the approach to larger or more complex buildings. Finally, while the study aims to model and optimise OB, the inherent variability and unpredictability of human actions pose ongoing challenges in consistently achieving optimal energy efficiency and TC.

1.9. Organisation of the Thesis

The rest of the Thesis is structured as follows: Section 2 provides insight into the State of the Art regarding the thesis' topic, Section 3 presents the software tools used and the methodology followed in this study. Section 4 discusses the case study and Section 5 presents the results. Finally, Section 6 provides some concluding remarks and discusses further research pathways.

2. State of the Art

The optimisation of OB in the built environment is crucial for enhancing energy efficiency and improving occupant comfort. With buildings accounting for a significant portion of global EC, optimising how occupants interact with building systems can lead to substantial energy savings and a more sustainable environment. This state-of-the-art review delves into the role of OB, and the impacts of these behaviours on building energy performance, the advancements in computational intelligence (CI), control techniques, and data-driven HVAC optimisation approaches, illustrated through relevant case studies.

2.1. Occupant Behaviour, building energy performance and comfort

Occupancy refers to the presence and activities of occupants within a building. It encompasses the number of occupants, their arrival and departure times, duration of stay, and spatial distribution within the building. Accurate occupancy data is essential for realistic EC predictions, as the number of occupants and their behaviour significantly influence the use of HVAC systems, lighting, and other energy-consuming devices [4]. The presence of occupants in a building is dynamic and varies over time. Traditional static occupancy models, such as those in ASHRAE standards, often fail to capture this variability, leading to discrepancies in EC predictions. Advanced methods, including deep learning and Agent-Based Modelling (ABM) methods, have been developed to improve the accuracy of occupancy data by incorporating real-time and historical data [42], [43]. Realistic occupancy data includes spatial and temporal dimensions of occupant presence. Spatial data involves the location and movement of occupants within the building, while temporal data includes the timing and duration of occupancy events [44]. This data is crucial for understanding occupancy patterns and their impact on energy usage.

Occupants interact with various building systems, including HVAC, lighting, electrical appliances, and windows. These interactions significantly affect building EC. Occupant interactions with HVAC systems include adjusting thermostats, opening or closing windows, adjusting shading devices, and using personal heating or cooling devices. Studies have shown that incorporating realistic occupancy and behaviour data into HVAC control strategies can lead to substantial energy savings [45]. OB related to lighting involves turning lights on or off, adjusting brightness, and using daylight. The use of electrical appliances by occupants varies widely and can be influenced by individual preferences and habits. Window opening behaviour affects both natural ventilation and HVAC performance. While this behaviour is less common in centrally air-conditioned buildings, it can have a significant impact on EC in naturally ventilated buildings [46].

Behavioural efficiency refers to changes in OB that lead to reduced EC [47]. It emphasises increasing occupant awareness and encouraging energy-efficient practices through educational interventions and feedback mechanisms. Providing feedback to occupants about their energy usage is one of the most effective ways to promote behavioural efficiency. Feedback can be delivered through various means, including smart meters, mobile applications, and in-home displays, to help occupants identify inefficient behaviours and make informed decisions about energy use. The adoption of smart technologies, such as automated control systems, CI optimisation systems, and Internet of Things (IoT) devices, can enhance behavioural efficiency by providing real-time data and enabling automated responses to occupancy and usage patterns. However, the awareness and acceptance of these technologies among occupants need to be increased to realise their full potential [48]. Figure 8 shows how Occupancy, Interactions, and Behavioural efficiency, as mentioned above, affect Building Energy Performance.

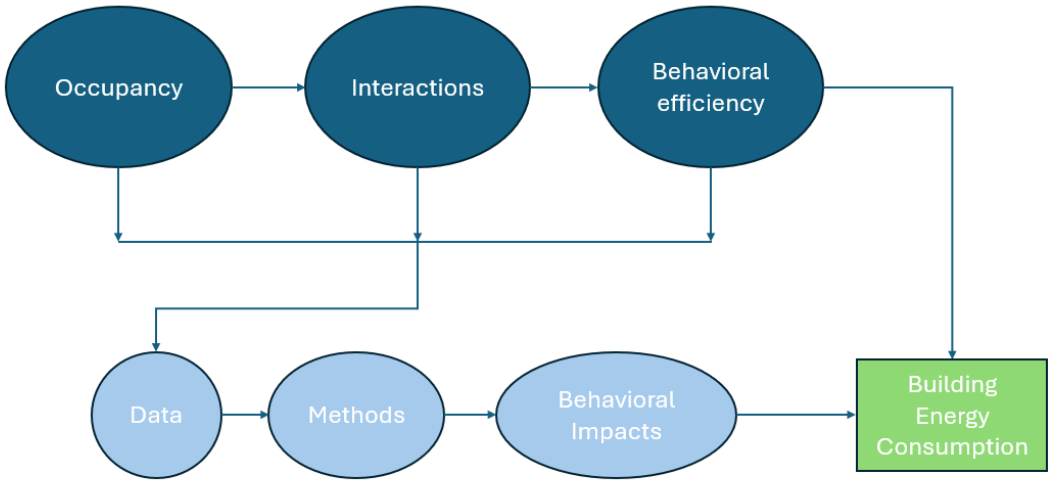

Figure 8. Occupant impact on Building Energy Consumption adjusted from [4].

Various modelling methods are used to simulate the impact of OB on building EC. Agent-Based Modelling, simulates interactions between occupants and their environment, capturing the complexities and uncertainties of occupant behaviour. It is particularly useful for modelling individual and group behaviours within buildings. Stochastic modelling accounts for the random nature of occupant behaviour, predicting long-term and short-term occupancy patterns and their impacts on energy use. Data mining techniques analyse large datasets to identify patterns and correlations in OB. This approach is valuable for understanding long-term behaviour trends and their implications for EC. Statistical analysis, including regression analysis and surveys, questionnaires is used to quantify the relationships between OB and

energy use. This method helps identify key factors influencing EC and predict behaviour patterns [45], [46], [49].

Integrating occupancy and occupant behaviour models into building energy simulations is crucial for improving prediction accuracy. Several studies have focused on developing dynamic occupancy schedules and individualised behaviour models to better represent the diversity and complexity of OB in simulations [46]. In [50], [51] the Drivers, Needs, Actions, and Systems framework, which standardises the definition of OBs was developed. Drivers are environmental factors that motivate occupants to meet physical, physiological, or psychological needs. These needs encompass both physical and non-physical requirements essential for occupant satisfaction with their environment. Actions refer to the interactions or activities occupants undertake to achieve environmental comfort. Systems are the equipment or mechanisms within the building that occupants interact with to maintain or restore their environmental comfort. This framework can be integrated into an obXML schema to effectively differentiate realistic occupant presence data. The obXML (Figure 9) is an XML (eXtensible Markup Language) schema designed to standardise the representation and exchange of OB models for building performance simulation.

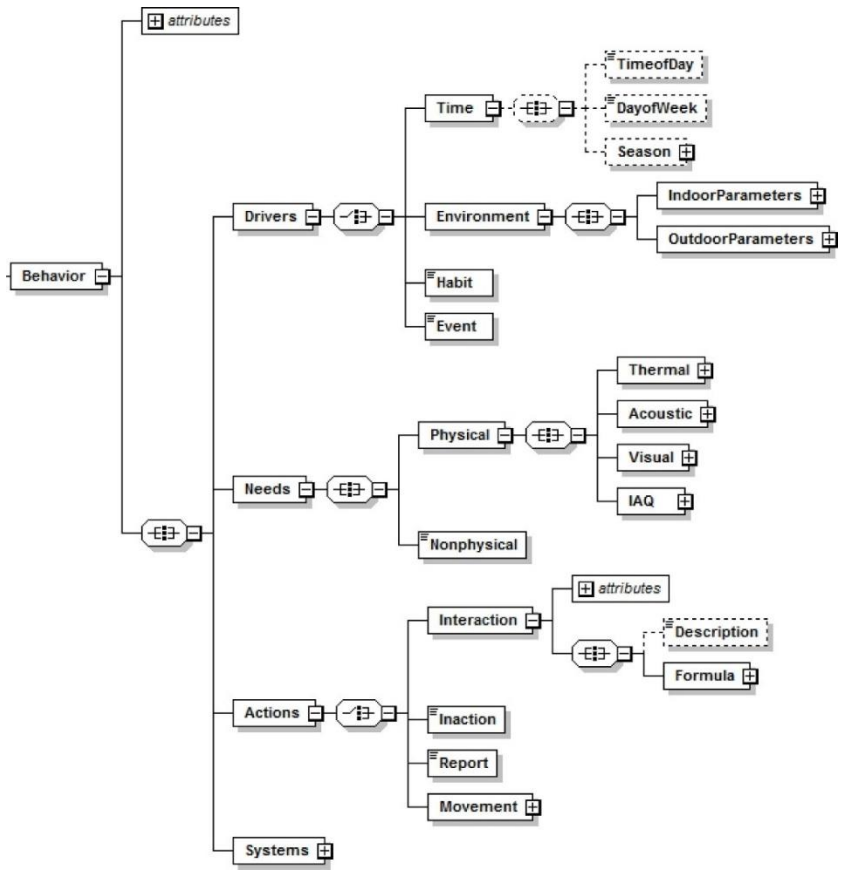

Figure 9. Overview of the obXML schema acquired from [46].

Cross-disciplinary research in energy and social sciences is essential for comprehending OB and attaining low-energy buildings, as the human aspect of building EC cannot be fully understood through a single discipline, given that human-building interactions typically involve both technological and social factors [52]. In [11] study presented an interdisciplinary framework, drawing on theories and insights from both energy and social sciences, to explore interactions between building occupants and their environments in various office settings and cultural contexts. The interdisciplinary framework proposed, incorporates psychological aspects of behaviour, individual motivational drivers, societal norms, and group interactions. This framework leverages multidisciplinary knowledge from social sciences and data science.

2.2. Methods and Techniques used in HVAC control and optimisation

Computational intelligence (CI) and control techniques have revolutionised the optimisation of HVAC systems by providing advanced methods to enhance energy efficiency and occupant comfort. These techniques encompass a range of methodologies, including Artificial Neural Networks (ANN), Genetic Algorithms (GA), Fuzzy Logic, Multi-Agent Systems (MAS), Model predictive control (MPC) and hybrid approaches that combine multiple CI techniques for superior performance [53], [54].

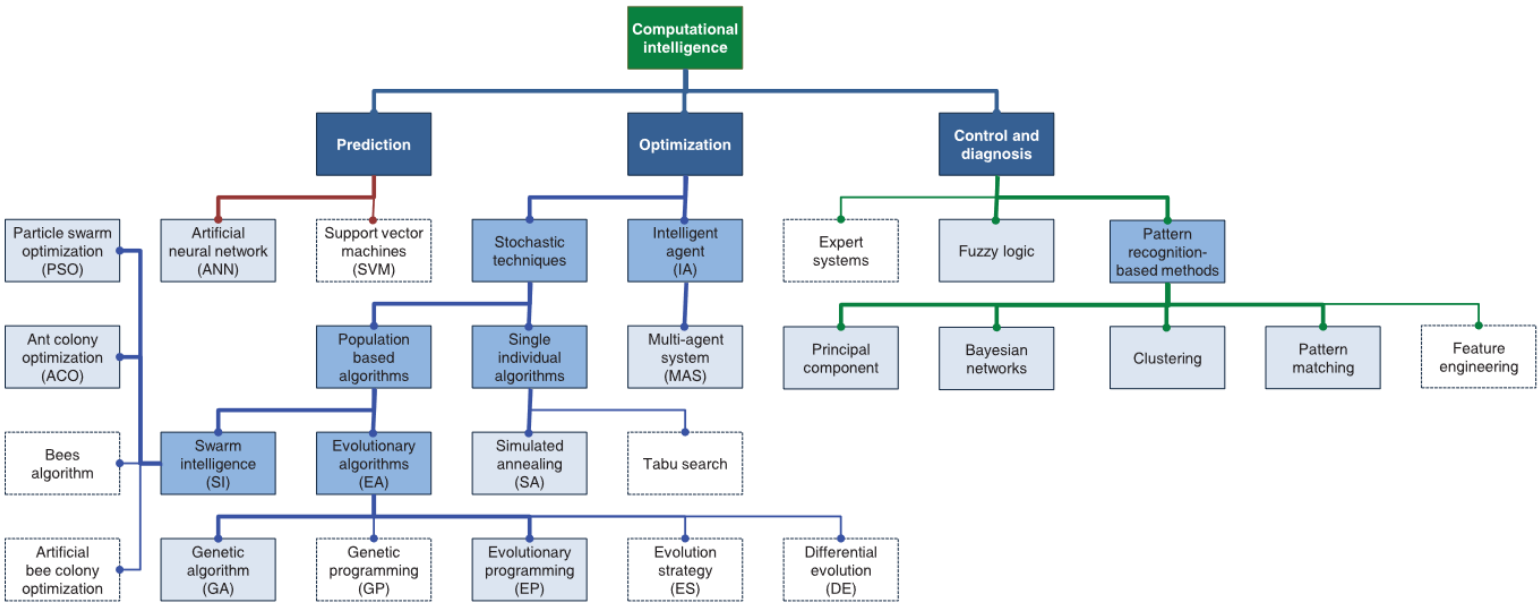

Figure 10. Classification diagram depicting computational intelligence techniques acquired from [54].

Artificial Neural Networks (ANNs) as mentioned in section 1.5.2.1 are inspired by the human brain's neural structure and are widely used for predictive control in HVAC systems. ANNs can model complex, nonlinear relationships between various parameters, such as indoor temperature, humidity, and EC, enabling more accurate predictions and efficient control strategies. In [55] a neural network (NN)-based optimisation method that integrated NN

techniques with model-based predictions was developed. The study aimed to determine optimal set-points for a variable air volume system. Two distinct zones were considered: one where cooling load was primarily influenced by internal gains and another where outdoor air conditions had a predominant impact on cooling load. Results demonstrated that both the night setback strategy (operation of HVAC at less energy-demanding setpoints during the night) and the ANN control effectively maintained indoor air temperature within desired limits. However, the ANN-based approach achieved lower energy costs compared to the night reset strategy. The ANN controller increased fan energy usage by leveraging colder outdoor temperatures in the morning to pre-cool the building. Simulation comparisons with conventional night reset operations indicated that the ANN controller achieved up to approximately 19% energy savings [55].

Particle Swarm Optimisation (PSO) is a method inspired by the social behaviour of birds flocking or fish schooling. It is used for optimising complex functions by iteratively improving candidate solutions with regard to a given measure of quality. In the context of HVAC systems, PSO can be employed to find the optimal settings of building control parameters that minimise EC while maximising occupant comfort. By simulating a population of potential solutions (particles) that explore the search space, PSO adjusts the positions of these particles based on their own experiences and those of their neighbours. This collaborative search process allows PSO to efficiently converge towards the optimal solution. In [56], a study combining the EnergyPlus™ simulation program with a hybrid optimisation algorithm that integrated Particle Swarm Optimization (PSO) with the Hooke-Jeeves method to determine the optimal settings for a chilled water system was conducted. The PSO component was used to address the local search optimisation problem, though it exhibited a slow convergence rate and inefficiencies in the search process. To mitigate these issues, PSO was paired with the Hooke-Jeeves algorithm. The study implemented two strategies to highlight the robustness of the hybrid approach. In the first strategy, constant optimal chilled and cooling water temperatures were set as the set-points, while in the second strategy, these set-points were allowed to vary over time. The simulation results for four summer and four winter days indicated that EC decreased by 9.4% during the summer and 11.1% during the winter compared to conventional settings.

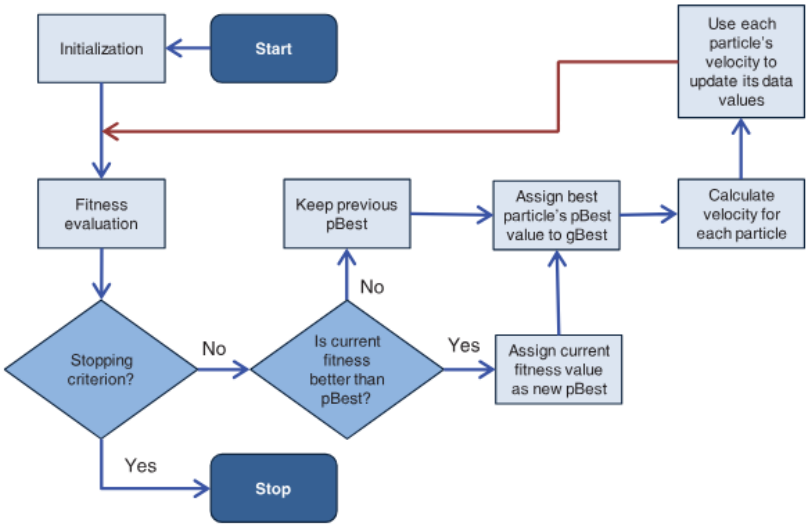

Figure 11. Flow chart depicting Particle Swarm Optimisation acquired from [54].

Genetic Algorithms (GAs) are metaheuristic algorithms. They are optimisation techniques based on the principles of natural selection and genetics. GAs are particularly effective in finding optimal solutions for complex problems by iteratively evolving a population of candidate solutions through selection, crossover, and mutation. In [57] a multi-objective genetic algorithm (MOGA) approach aimed at balancing energy cost and thermal discomfort was proposed. Their study simulated a single-zone HVAC system comprising heating and cooling coils, a fan, and a heat exchanger over a three-day period. Various constraints were applied to coil design, system capacity, and fan performance to optimise system operation. Results from the MOGA were compared against those from a single-objective optimisation approach, showing that the single-objective optimiser outperformed the MOGA, as expected.

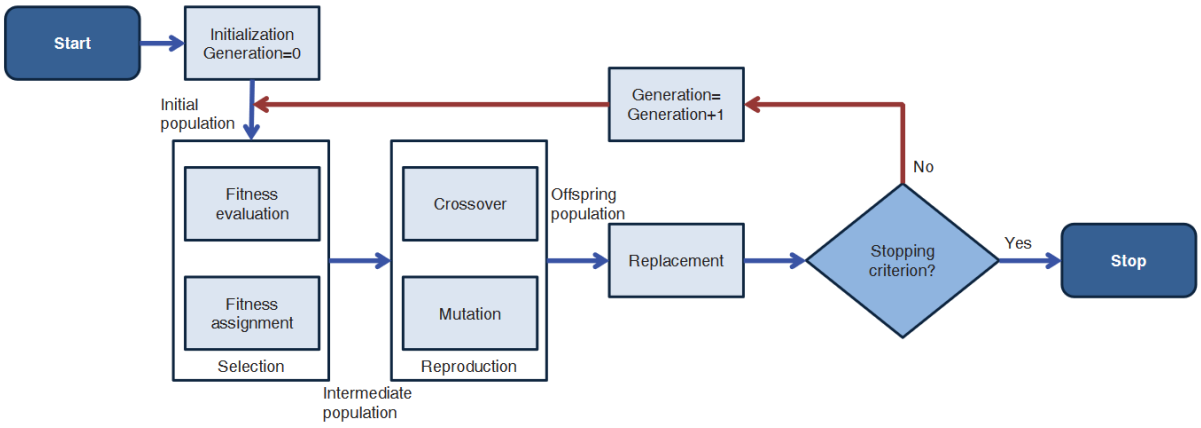

Figure 12. Flow chart of a genetic algorithm optimisation acquired from [54].

Fuzzy logic systems are designed to handle uncertainty and imprecision, making them ideal for controlling HVAC systems in environments with fluctuating occupancy and external conditions. Fuzzy logic controllers use linguistic variables and a set of rules to make decisions, offering a flexible approach to HVAC control. In [58], a control scheme based on fuzzy logic to regulate temperature and humidity in an occupied space using a central air conditioning unit was introduced. The fuzzy logic controller determined adjustments based on deviations between actual and desired temperature and humidity levels. The effectiveness of this scheme was evaluated in two laboratory spaces sharing the same air handling unit (AHU). The results indicated that the fuzzy logic controller not only reduced EC but also proved straightforward to implement [58].

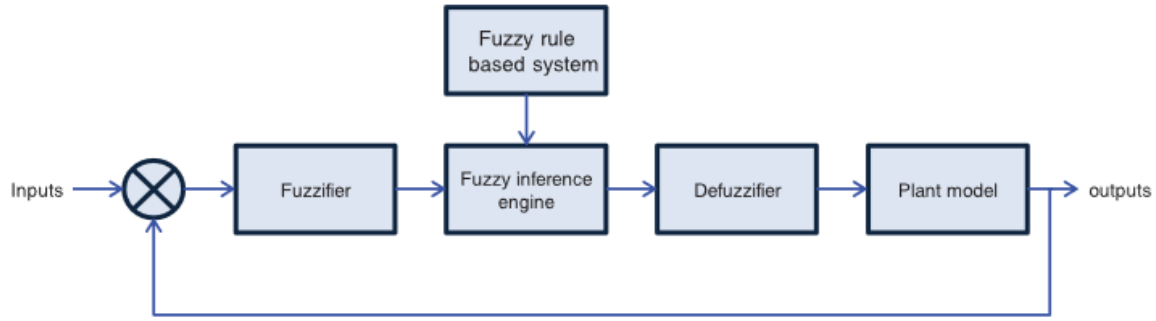

Figure 13. Schema of a fuzzy logic controller acquired from [54].

Multi-Agent Systems (MAS) involve multiple interacting agents, each responsible for specific aspects of HVAC control, such as temperature regulation, airflow, and humidity control. MAS can enhance the coordination and efficiency of HVAC systems by distributing control tasks among specialised agents.

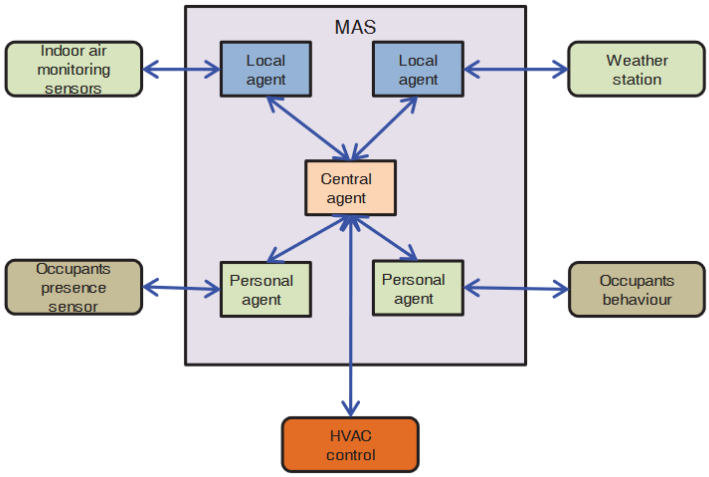

Figure 14. Multi-agent system for building applications acquired from [54].

In [59] a multi-agent control system for a multi-zone building, consisting of three types of agents: central, zone, and local was implemented. They incorporated a particle swarm optimizer within the central agent to determine the optimal solution for achieving the highest overall comfort level throughout the building. In [60] an ARTMAP-based multi-agent Building Management System was introduced. ARTMAP, a type of ANN, enables incremental learning, mimicking human memory and learning processes without forgetting previously learned information. ARTMAP's ability to perform classification and prediction simultaneously makes it superior for agent adaptation compared to traditional methods like ANN and fuzzy logic. This system was applied to the UCLan Samuel Lindow Building, which utilises a ground source heat pump and a gas-fired boiler for heating (GSHP). The existing MAS Building management system was underperforming and couldn't fully exploit the GSHP's capabilities. The authors added a layer of mediator agents between the source and user agents to better categorise the energy sources. Simulations showed promising results, with the ARTMAP-based MAS and additional mediator layer outperforming the existing MAS-based Building management system.

Model Predictive Control (MPC) is a well-established method for constrained control, gaining significant attention from researchers in the context of building and active component control. MPC integrates feedback control principles with numerical optimisation. By leveraging predictions of future disturbances (such as internal gains and weather) and given requirements (such as comfort ranges), MPC can anticipate a building's energy needs and optimise its thermal behaviour based on defined control goals. Constraints are directly incorporated into the optimisation problem, which is solved at each sampling step [61]. Accurately accounting for user comfort can not only ensure proper room conditions but also reduce energy costs. This can be achieved by closing the control loop based on user feedback instead of a fixed temperature setpoint. A Learning-Based MPC approach, utilising user feedback via a smartphone app, is proposed in [62]. This adaptive control method estimates the desired temperature at different times of the day based on simple feedback like "too cold" or "too hot." Experimental results indicate that this approach maintains user comfort throughout the day without needing explicit temperature set points or times. Although [58] focuses on feedback from a single user, it is suggested that the approach could be extended to include multiple users

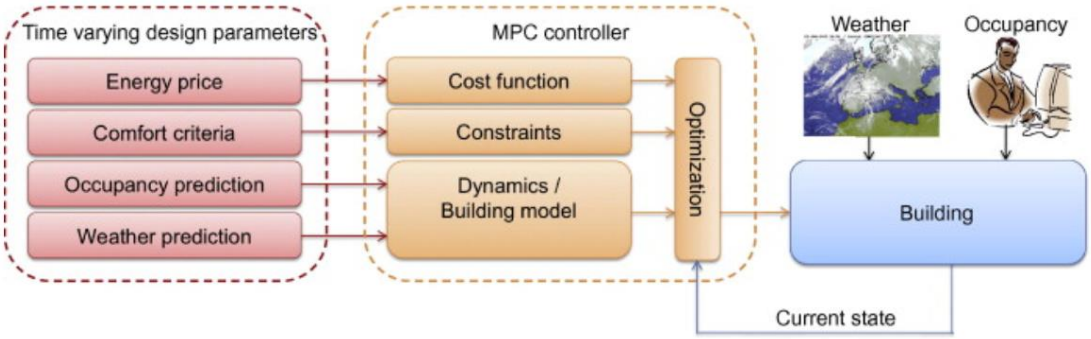

Figure 15. Schematic of model predictive control for buildings acquired from [63].

Hybrid CI techniques combine various CI methodologies to leverage their strengths and mitigate their weaknesses. These approaches can offer more robust and effective solutions for HVAC optimisation. In [64] an analytical model of an HVAC system was developed and an intelligent controller based on a Fuzzy Supervised Neuro-Control approach was implemented. This controller comprised two main components: neuro-control and fuzzy logic control. The neuro-controller, which was a single-layer ANN, was responsible for generating the volumetric airflow rate and the water flow rate of the chiller/heater. To address the issue of saturation, a Mamdani-type fuzzy logic controller was introduced to supervise the neuro-controller. The fuzzy logic controller would activate to supervise and adjust the neuro-controller whenever it approached saturation, ensuring stable and efficient system operation. In [65] a multi-objective PSO to achieve an optimal balance between energy efficiency and occupant comfort was applied. They introduced a multi-agent control system comprising two main types of agents: a central coordinator agent and local controller agents. The central coordinator agent collaborated with the optimizer to ensure that TC for occupants met the desired standards. The local controller agents were responsible for regulating temperature, illuminance, and CO2 concentration within the building. However, the study did not provide detailed information about the building's performance.

2.3. Future directions for optimisation of occupant behaviour towards energy efficiency and thermal comfort in buildings

The advancements in optimising OB for energy efficiency and TC in buildings highlight several critical research avenues. Firstly, developing universal HVAC optimisation approaches adaptable to diverse atmospheric weather conditions, building types, and locations is essential. This includes evaluating the performance of machine learning methods, model predictive control schemes, and optimisation algorithms. Particularly promising is the integration of neural networks, MPC-based controls, and genetic algorithms or particle swarm optimisers [54].

Ensemble learning methods, combining diverse base learners such as NNs, show potential for robust HVAC system modelling. Moreover, integrating electricity price dynamics into HVAC modelling and optimisation frameworks remains an underexplored area, crucial for balancing energy savings with operational costs [53].

Emerging building trends like nearly Zero Energy Buildings (nZEB) and modern construction materials necessitate novel, adaptable HVAC modelling, control, and optimisation approaches. The role of HVAC systems in demand response (DR) within smart grids, especially considering renewable energy sources (RES), requires further investigation. This involves understanding the dynamic interactions between RES and HVAC systems to develop efficient modelling and control strategies [66].

Furthermore, integrating real-time feedback mechanisms into HVAC control systems holds promise for dynamically adjusting environmental conditions based on occupant presence and comfort feedback. This adaptive approach can enhance both comfort and energy efficiency by responding proactively to changing occupancy patterns and individual comfort requirements [67].

Human-centred design principles, including user-centred interfaces and personalised comfort settings, should guide the development of next-generation HVAC systems. This involves leveraging IoT technologies and cloud computing for real-time, adaptive control that enhances both comfort satisfaction and energy efficiency [45].

Advanced data acquisition techniques for big energy data analysis offer opportunities to enhance building energy performance through realistic and timely data utilisation and model validation. Standardising behavioural models and categorising behavioural energy impacts across different building types are imperative for assessing and improving behavioural performance effectively [53], [49] .

Furthermore, addressing empirical gaps at larger city scales and understanding OB in socio-economic and policy contexts are crucial for effective building energy efficiency strategies. Practical validation of HVAC optimisation strategies on commercial systems in real-time environments is essential to confirm scalability and effectiveness [45].

Ultimately, advancing occupant TC research requires interdisciplinary collaboration between building scientists, psychologists, and data scientists. By integrating human-centred approaches with cutting-edge technologies, future HVAC systems can achieve optimal TC conditions while minimising EC in diverse building environments [46].

3. Methodology

3.1. Software tools

EnergyPlus™ (E+) is a computer program that simulates building thermal loads under exposure to location specific weather conditions over a pre-specified time period and calculates energy use and related metrics. The existing E+ Python Application Programming Interfaces (APIs) allow for configuration, simulation, and data retrieval during simulation, at a sub hourly timestep scale. Furthermore, the Python Scikit-learn and Keras libraries are utilised to preprocess the E+ simulation output files and build and train an ANN based off of the E+ Building Model simulation data [68]. The Python Optimisation Modeling Objects (Pyomo) software assists in recasting the ANN into an Approximate Building Model (AM) and supports the formulation of multi-objective Mixed Integer Quadratic Programming (MIQP) Rolling Horizon (RH) optimisation problems. The optimisation problem is solved using the Gurobi solver, a state-of-the-art optimisation tool designed from the ground up to exploit modern architectures and multi-core processors.

3.1.1. Energy Plus

The EnergyPlus™ (E+) is a computer program that is a comprehensive software tool utilised by engineers, architects, and researchers to simulate EC and water usage in buildings. The development of EnergyPlus began in 1996 with funding from the United States Department of Energy (DoE) in partnership with the National Renewable Energy Laboratory (NREL) and several National Laboratories, including Berkeley Lab and Oak Ridge. It was first released in 2001 and has since undergone continuous updates. E+ integrates comprehensive building physics algorithms covering heat transfer (radiation, convection, and conduction), air and moisture movement, light distribution, and water flow. This enables the modelling of diverse building and mechanical system setups and scenarios. It boasts advanced simulation capabilities like sub hourly time steps, simultaneous resolution of zone conditions and HVAC system actions, a modular HVAC framework, and a runtime scripting language for customisable control strategies. Moreover, E+, is recognised for USGBC LEED certification. LEED (Leadership in Energy and Environmental Design) is the world's most widely used green building rating system [23]. Along with OpenStudio, E+ is part of BTO’s (Building Technologies Office) BEM program portfolio. An API has been developed to allow access to internal E+ functionality and open up the possibility for new workflow opportunities around E+, An API has been created to provide access to the internal functionalities of E+, opening up new possibilities for workflow enhancements. Initially, a C API was developed to expose the underlying C++ functions, followed by the creation of Python bindings to further enhance

accessibility. The resulting Python APIs for EnergyPlus enable configuration, simulation, and data retrieval throughout the simulation process, utilising a subhourly timestep scale [69].

3.1.2. Keras and scikit-learn

TensorFlow is a versatile and scalable software library designed for numerical computations utilising dataflow graphs. It empowers users to effectively develop, train, and deploy neural network and other Machine Learning (ML) models for production environments. The underlying algorithms of TensorFlow are predominantly implemented in optimised C++ and Compute Unified Device Architecture (CUDA), facilitating parallel computing on NVIDIA graphics processing units (GPUs). Moreover, TensorFlow offers APIs in multiple languages, with the Python API being the most comprehensive and reliable option [70]. Keras, developed by Francois Chollet [68], is a high-level deep learning framework and TensorFlow API for Python, that can be built on top of TensorFlow. Its primary advantage lies in its user-friendly yet efficient high-level APIs, which save time and facilitate rapid prototyping of ideas. By abstracting away complexities, Keras simplifies the implementation of TensorFlow principles, eliminating the need for boilerplate code when creating deep learning models. Its success is attributed to its flexibility and ease of use, offering access to specialised libraries while leveraging the strengths of the TensorFlow ecosystem [71].

Python's Scikit-Learn is one of the most popular ML libraries. It is built on Python libraries NumPy, SciPy, and Matplotlib. The library is well-documented, open source, commercially usable, and a great vehicle to get started with machine learning. It is also very reliable and well-maintained, and its vast collection of algorithms can be easily incorporated into projects. Scikit-Learn is focused on modelling data rather than loading, manipulating, visualising, and summarising data. For such activities, other libraries such as NumPy, pandas, Matplotlib, and seaborn are chosen. The Scikit-Learn library is imported into a Python script as sklearn [72].

3.1.3. Pyomo

Pyomo, the Python Optimization Modeling Objects software, facilitates the creation and examination of mathematical models for intricate optimisation scenarios. This functionality is often linked with Algebraic Modelling Languages (AMLs), which enable the representation and scrutiny of mathematical models using a high-level language. While many AMLs utilise proprietary modelling languages, Pyomo's modelling objects are embedded within Python, a full-featured high-level programming language that contains a rich set of supporting libraries. Pyomo has garnered recognition, receiving awards from both the R&D100 organisation and the Institute for Operations Research and the Management Sciences Computing Society (INFORMS). Pyomo support scripting with model objects, which facilitates the custom analysis

of complex problems in an object-oriented approach. Additionally, there are packages of Pyomo that define interfaces to solvers like CPLEX and Gurobi [73].

3.1.4. Gurobi Optimizer

The Gurobi™ Optimizer, developed by Gurobi Optimization, LLC, serves as a prescriptive analytics platform and decision-making technology. Widely known as "Gurobi," it functions as a solver, employing mathematical optimisation techniques to compute solutions to various problems. Gurobi was established in 2008 by Dr. Zonghao Gu, Dr. Edward Rothberg, and Dr. Robert Bixby, who derived the name by merging the initial letters of their last names. Gurobi is renowned for its capabilities in various optimisation domains, including linear programming (LP), quadratic programming (QP), quadratically constrained programming (QCP), mixed-integer linear programming (MILP), mixed-integer quadratic programming (MIQP), and mixed-integer quadratically constrained programming (MIQCP) [74]. The Gurobi Optimizer is written in C, and it is available, on all computing platforms and accessible from several programming languages including Python. Standard independent modelling systems including Pyomo (see section 3.1.3) can be used to define and to model problems.

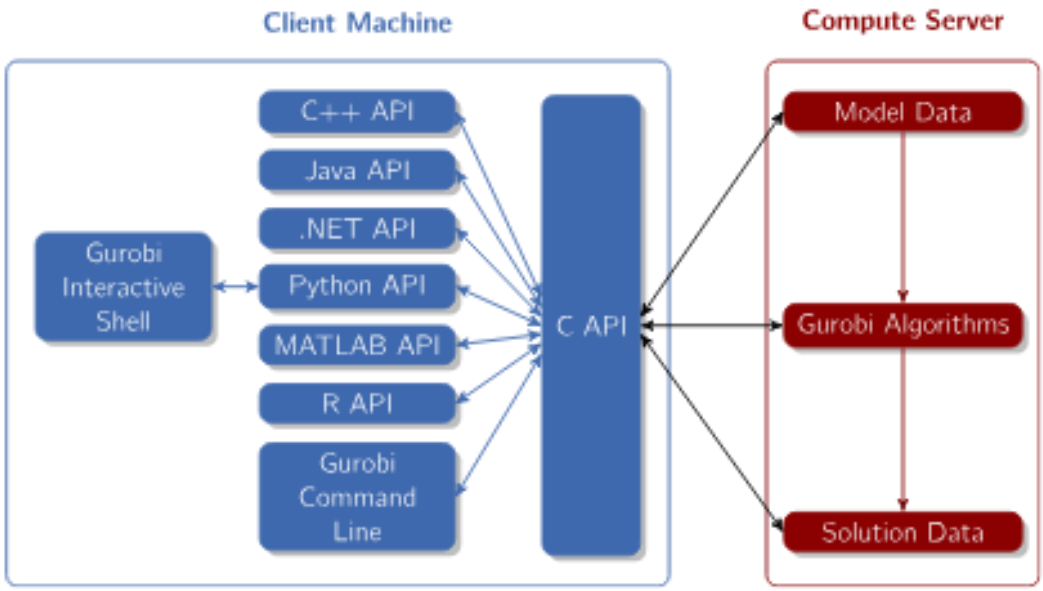

Figure 16. Gurobi Client API [74].

3.2. Methods

The above-mentioned software tools are utilised to implement the sequence of methods as shown in Figure 17. Weather data is fed into E+ to provide location specific weather conditions. E+, through python coupling and configuration allows for the random application and simulation of modelled single OB actions. The resulting dataset, obtained through the black box (E+ building simulation software), is then utilised to create a hybrid building energy model by applying ML modelling through ANN utilisation. To solve occupant centric Optimisation problems, the ML model is exactly reformulated into a piecewise linearised AM. Therefore, in the end, by utilising the AM structure, optimal occupant actions, and therefore OB profiles, can be derived by directly feeding thermal zone (TZ) conditions, occupant conditions and weather data into a well-defined optimisation problem.

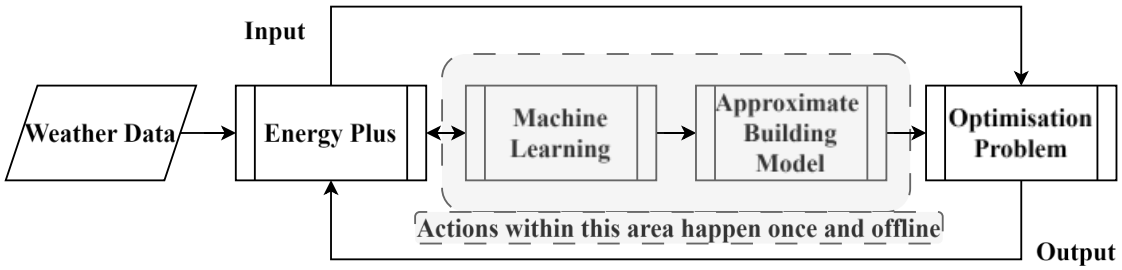

Figure 17. Summary of the methodology.

3.2.1. Building Energy Model exposed to Occupant Actions

In E+ software, building TZs and potential single occupant adaptive TC behaviours are simulated with a 30-minute timestep. Throughout the simulation, the TZ experiences annual OWC (Outdoor Weather Conditions), while occupant actions are randomly applied at a half-hourly frequency. One or more occupant actions can be applied concurrently. This allows for the simultaneous consideration of both (a) OWC and OBs on the building's thermal conditions and subsequent (b) EC, while transitioning from timestep t to t+1. Most occupant actions are represented using E+ components that can be configured, controlled, and monitored via the E+ Python API to generate dynamically adjustable schedules for (i) blind state, (ii) window, and (iv) HVAC operation. Notably, an additional occupant action, the adaptation of (v) occupant clothing insulation does not necessitate modelling within E+.

(i) **Window Blind** operation is modelled using the E+ “Window Shading Control” component. Exterior blinds reduce the amount of solar radiation entering through the window, into the thermal zone of interest (Figure 18). Blinds are either retracted (no window coverage) or activated (glazed window coverage), through a control mechanism allowing on demand blind usage behaviour simulation.

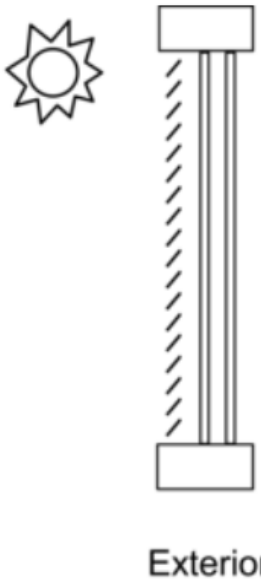

Figure 18. Exterior window shading control representation acquired from E+ Input Output Reference.

(ii) **Window operation** is modelled using the E+ “Ventilation by Wind and Stack with Open Area” component. The ventilation air flow rate is a function of wind speed and thermal stack effect (Figure 19), along with the area of the opening being modelled. The natural ventilation flow rate can be controlled, thus allowing to simulate opening or closing the window on demand.

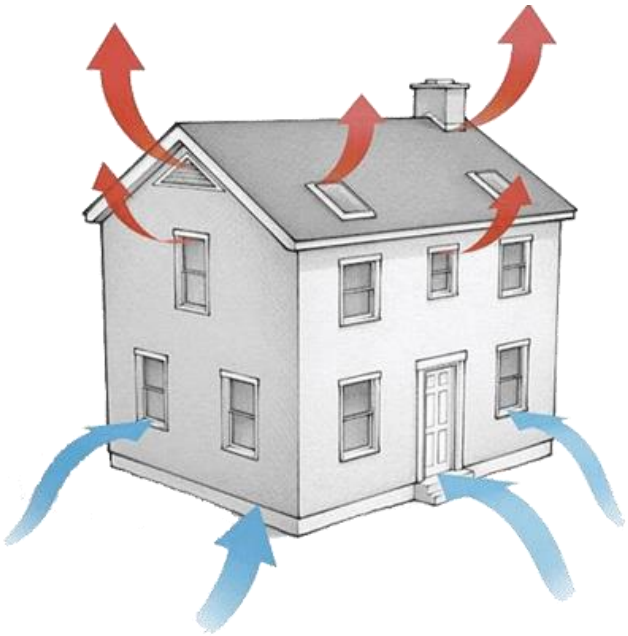

Figure 19. Open Stack Phenomenon depiction, leading to natural ventilation acquired from [75].

(iii) To simulate **HVAC operation** the E+ “Packaged Terminal Heat Pump (PTHP)” component is used. The compound object consists of an outdoor air mixer, direct expansion (DX) cooling coil, DX heating coil, supply air fan, and a supplemental heating coil. The HVAC power switch {ON, OFF} and the heating/cooling thermostat can all be configured dynamically allowing to model PTHP operation on demand.

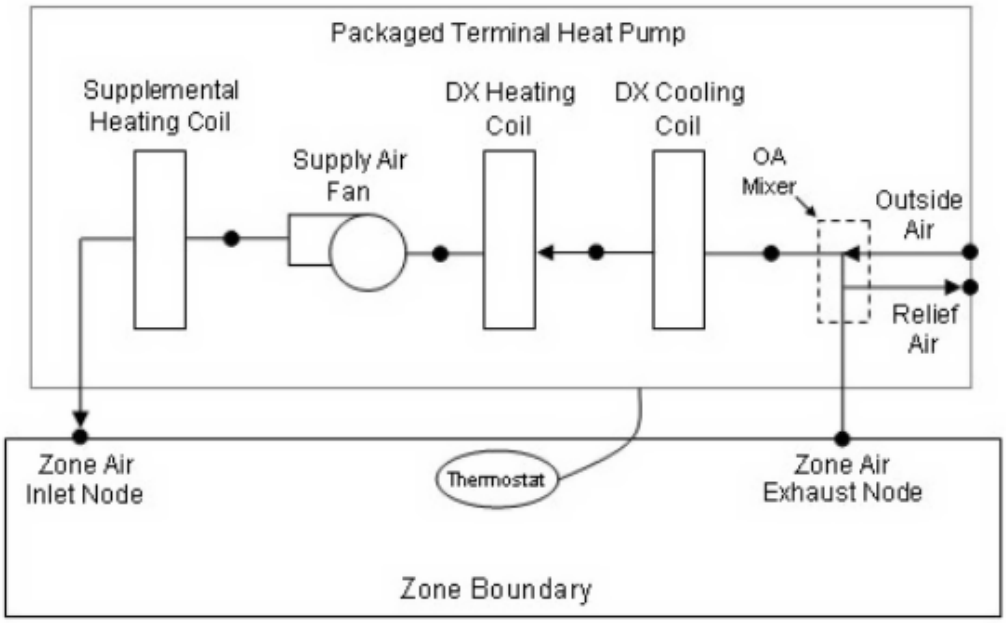

Figure 20. Schematic of a packaged terminal heat pump acquired from E+ Input Output Reference [69].

The amount of thermal insulation/ clothing (clo) worn by a person has a significant impact on its TC. It is acceptable to define a complete clothing ensemble using a combination of the garments (Table 13). (iv) **Occupant clothing** is thus allowed to receive any given clo value in rational bounds. Furthermore, in the adaption of the occupant clothing value action, there is no need to use any E+ component, as the application of different clothing values does not impact the TZ indoor conditions, but only the TC sensation of the occupants themselves. Therefore, it will be treated separately as a decision variable regarding the optimisation towards occupant TC (see section 3.2.4.3.1).

3.2.2. Machine Learning

3.2.2.1. Thermal Zone Artificial Neural Network

The dataset obtained from the E+ simulation consists of sequential information regarding the OWCs, the building thermal conditions, and the applied occupant actions. First, the dataset is pre-processed to examine correlations between occupant actions and building conditions that

affect TC, and EC and then the E+ variables that best capture the above dynamics on consecutive time steps, i.e. from $t \rightarrow t+1$ are retrieved. Afterwards, an ANN is built and trained on the derived variables of interest to allow for single timestep prediction: $y_t = f(C_t, W_t, A_t)$, where C: TZ conditions, W: OWC, A: actions as mentioned in 3.2.1. We define: $y_t = C_{t+1}$, therefore: $C_{t+1} = f(C_t, W_t, A_t)$. In plain words, the TZ conditions in the next time step, is approximated via ML as a function of the variables in Table 2 at the current timestep. Note, regarding C, relative humidity is obtained from the E+ simulation output file but is converted to air vapor pressure for ANN training purposes, Annex II, Figure 53.

Normalisation is applied based on the minimum and maximum values of the dataset. In an ANN, the activation function is a vital component in determining the output of a neural network. It introduces non-linearity into the network, enabling it to recognise intricate patterns in the data. Essentially, the activation function receives the weighted sum of inputs and applies a non-linear transformation to it before passing it on to the next layer of the network. The rectified linear unit (ReLU) activation function in the ANN nodes is employed as $y = max\{0, Gx + b\}$ to discern non-linear data relationships and facilitate piecewise linearisation of system dynamics [76]. The above formulation implies that the value of an output y can either be positive and equal to $Gx + b$ or 0, where G and b are the weights and biases of the ANN.

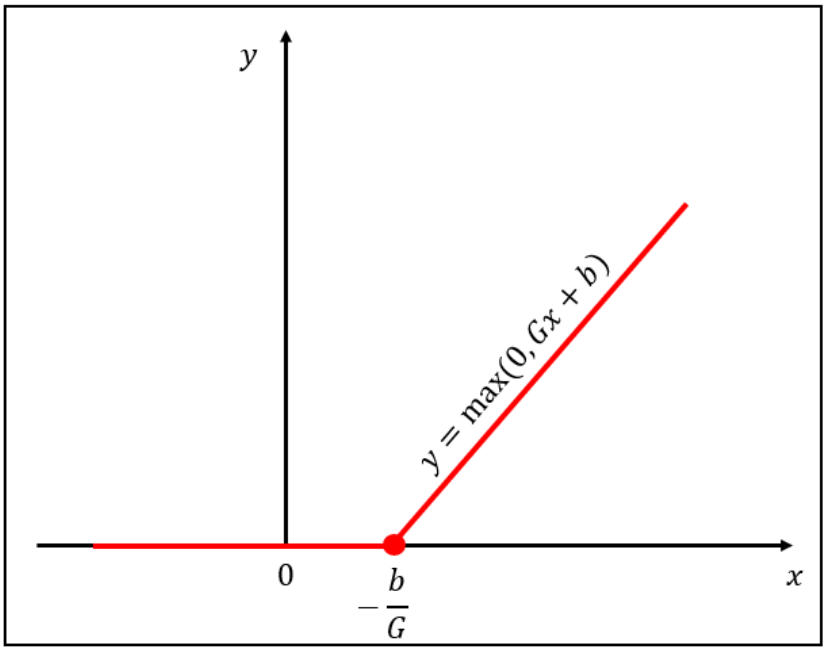

Figure 21. Representation of ReLU activation function.

Hyperparameter tuning of the ANN is conducted via Bayesian Optimisation. K-Fold Validation is employed to enhance model generalisation. Early stopping is implemented to prevent

overtraining and mitigate overfitting of the model. The resulting ReLU based ANN approximates the original non-linear model with only piece-wise linear functions, thus creating a trade-off between complexity reduction and accuracy.

Table 2. Thermal Zone Artificial Neural Network Variables

Variable Symbol	Variable name
W_t	Site Outdoor Air-Dry Bulb Temperature, Site Outdoor Air Dewpoint Temperature, Site Outdoor Air Relative Humidity, Site Outdoor Air Barometric Pressure, Site Wind Speed, Site Wind Direction, Site Diffuse Solar Radiation Rate Per Area, Site Direct Solar Radiation Rate Per Area, Site Horizontal Infrared Radiation Rate Per Area, Site Solar Altitude Angle.
A_t	Window schedule, Blind schedule, PTHP operation schedule, Heating schedule thermostat value, Cooling schedule thermostat value.
C_t	Zone Mean Air Temperature (T), Zone Air Vapor Pressure (P), Zone Mean Radiant Temperature (Tr), Zone Packaged Terminal Heat Pump Electricity Rate (EP, see section 3.2.4.3.2).

3.2.3. Approximate Model

Complex physics-based models like E+ (section 1.5.1, section 3.1.1), or nonlinear black-box models, like ANNs (section 1.5.2.1) are typically not solvable through linear programming (LP) (section 1.6.1), as Neural networks are nonlinear and nonconvex functions. Recent studies have demonstrated that neural networks with rectified linear units (ReLU), can be precisely reformulated as a mixed-integer linear program (MILP) [77], [78]. This transformation converts the nonlinear behaviour into piecewise linear segments. Therefore, in this case, the ReLU activation functions allow to exactly reformulate the ANN AM into a Mixed Integer Optimisation Program. Importing and utilising the weights and biases from the trained ANN model allows integration of the ANN into optimisation problems, albeit with added complexity from managing binary variables. The binary variables in the linear reformulation contribute to modelling the control-flow statements of the ReLU function. Specifically, the $\max\{\cdot\}$ operator present in the ReLU activation function is exactly reformulated via the use of binary variables ($y \in \{0,1\}$) and auxiliary continuous variables ($x \in \mathbb{R}$) as follows in Equation (1).

$$x_k = \max\{0, G_k\, x_{k-1} + b_k\} \Rightarrow \begin{aligned} & x_{k,p}^{aux} + x_{k,n}^{aux} = G_k\, x_{k-1} + b_k \\ & -(1-y)M \le G_k\, x_{k-1} + b_k \le yM \\ & 0 \le x_{k,p}^{aux} \le yM \\ & -(1-y)M \le x_{k,n}^{aux} \le 0 \end{aligned} \quad (1)$$

Where, x_k: output of current ANN layer k, x_{k-1}: output of the previous layer, G_k: matrix of weights for layer k, b_k: the vector of biases for layer k, $x_{k,p}^{aux}$, $x_{k,n}^{aux}$: auxiliary positive and negative values of $G_k\, x_{k-1} + b_k$, M: large scalar value.

As depicted in Table 3, in both cases the resulting $x_{k,p}^{aux}$ value is modelling the output of the ReLU activation functions.

Table 3. Use of binary y to model Equation (1).

Case	y	$x_{k,p}^{aux}$	$x_{k,n}^{aux}$	$G_k\, x_{k-1} + b_k$
A	0	0	$-M \le x_{k,n}^{aux} \le 0$	$x_{k,n}^{aux}$
B	1	$\mathbf{0 \le x_{k,p}^{aux} \le M}$	0	$x_{k,p}^{aux}$

In the case of the TZ ANN, Equation (1) models a single time step of the dynamic simulation. In the case of the Predicted Mean Vote ANN (PMV ANN) (section 3.2.4.3.1), Equation (1) models a single TC index state, utilising the outputs derived from the reformulated TZ ANN into TZ AM (see section 3.2.4.3.1).

A RH concept (see section 1.6.6) is applied for the entire time horizon of interest, solely by utilising the surrogate TZ, PMV ANN models.

3.2.4. Optimisation

The TZ ANN reformulation into a MILP, the quadratic terms of the optimisation objective (section 3.2.4.3, Equation (4)) function, and the RH approach result in a MIQP RH optimisation problem with linear constraints. As MIQP is a subcategory of MINLP, the Gurobi solver (see section 3.1.4), utilises methods based on the approaches mentioned in 1.6.3 . The resulting MIQP RH optimisation problem based on the TZ ANN considers building physics as constraints, accounts for OWC as uncertainties, tries to identify the (sub)optimal adaptive TC actions towards TC maximisation and EC minimisation (section 3.2.4.3, Equation (4)). The Parameters include the outdoor weather parameters that are fed into the optimisation problem from the E+ weather file as disturbance, the initial state TZ conditions, and the metabolic rate of the occupant.

3.2.4.1. Variable Bounds

The decision variables that comprise the adaptive TC actions in the optimisation problem are clothing insulation, window state, blind state adjustment and HVAC system control as described in section 3.2.1, and are bounded between specific values. More specifically, the occupant clothing variable is a real, continuous bounded variable. The window operation action is modelled with a binary decision variable taking values between 0 and 1 signifying the closed and the open window state respectively. Similarly, the blind usage is also modelled with a binary variable, 0 signifying no blind use and 1, full blind use. On the other hand, to model HVAC-PTHP operation, two decision variables are used. The first one, y_{OP}, is binary and states the operation of the PTHP unit 0: OFF and 1: ON. The second PTHP decision variable x_{SP} is continuous and states the zone temperature thermostat setpoint. The setpoint variable is real, continuous, bounded between $[\mathrm{x}_{\mathrm{SP}}^{\min}, \mathrm{x}_{\mathrm{SP}}^{\max}] \rightarrow [17{,}27]$ when the system is running, representing the setpoint temperature in °C. In the case of non-operation $(y_{OP} = 0)$ the setpoint variable assumes a value d outside the aforementioned bounds $(x_{SP} = d)$. Further auxiliary binary and continuous variables are utilised in the definition of the different applied constraints as described below. All variables, parameters are normalised throughout the definition, parametrisation, and solution of the optimisation problem, due to the training procedure of both ANN models (TZ ANN, PMV ANN) where the scikit-learn [72] MinMaxScaler is utilised. Therefore, all variables, binary and continuous and all parameters in the MIQP RH optimisation problem are bounden between 0 and 1. Exceptions are the auxiliary variables $x_{k,n}^{aux}$ mentioned in 3.2.3 that support the modelling of the negative outputs of the ReLU function.

3.2.4.2. Constraints

The MIQP RH Optimisation Problem at hand, is subject to multiple constraints, including i) TZ ANN reformulation into ANN TZ AM that models dynamics between building physics, OWC and occupant actions, ii) PMV ANN reformulation into ANN PMV AM that models the calculation of occupant TC sensation, iii) correctly configured operation of PTHP system within desired bounds, iv) rate-of change limitation of PTHP system thermostat temperature setpoint value.

Equation (1) models i) and ii) as explained in sections 3.2.3, and 3.2.4.3.1 respectively.

Equation (2) models iii), the operation of the PTHP system utilising y_{OP} and x_{SP} as mentioned in section 3.2.4.1.

$$(1 - y_{OP})d + y_{OP}\,\mathrm{x}_{\mathrm{SP}}^{\min} \leq x_{SP} \leq (1 - y_{OP})d + y_{OP}\,\mathrm{x}_{\mathrm{SP}}^{\max} \quad (2)$$

Investigating the above constraint (Equation (2), Table 4) in regard to the use of the binary variable y_{OP} it is clear that when $y_{OP} = 0$, x_{SP} is given the out of bounds ($x_{SP} = d$), in contrast to when $y_{OP} = 1$ and thus x_{SP} can receive values between the temperature thermostat bounds.

Table 4. Use of binary y_{OP} to model Equation (2).

Case	y_{OP}	x_{SP}
A	0	$d \leq x_{SP} \leq d \rightarrow x_{SP} = d$
B	1	$y_{OP}\,\mathrm{x}_{\mathrm{SP}}^{\min} \leq x_{SP} \leq y_{OP}\,\mathrm{x}_{\mathrm{SP}}^{\max}$

Furthermore Equation (3) models iv). To ensure smooth and gradual adjustments in the HVAC system's operation, a rate-of-change constraint is imposed on the thermostat setpoint x_{SP} value. This constraint limits the magnitude of changes allowed between consecutive time steps, Δx_{SP}, promoting stability, and minimising abrupt fluctuations, i.e. $|\Delta x_{SP}| \leq \Delta \mathrm{x}_{\mathrm{SP}}^{\max}$. Furthermore, this rate-of-change constraint must only be implemented when the PTHP system is in operation for consecutive timesteps in order to not hinder its ON/OFF switching. This is mathematically expressed as follows assisted via the use of the binary variable $y_p \in \{0,1\}$.

$$\begin{gathered} \Delta x_{SP} = x_{SP,t} - x_{SP,t-1} \\ -M\left(1 - y_p\right) - \Delta x_{\mathrm{SP}}^{\max} \leq \Delta x_{SP} \leq M\left(1 - y_p\right) + \Delta x_{\mathrm{SP}}^{\max} \\ y_p \leq y_{OP,t-1} \\ y_p \leq y_{OP,t} \\ y_p \geq -M\left(1 - y_{OP,t-1}\right) - M\left(1 - y_{OP,t}\right) + 1 \end{gathered} \quad (3)$$

Investigating the above constraint (Equation (3),Table 5) in regard to the use of the binary variables it is clear that y_p models the multiplication of $y_{OP,t}$ and $y_{OP,t-1}$. Thus, only when the PTHP system is enabled for consecutive timesteps ($y_p = 1$), Δx_{SP} is bounded. In all other cases Δx_{SP} remains unbounded in order to allow ON/OFF switching in PTHP operation ($y_{OP} = 0 \rightarrow x_{SP} = \mathrm{d}$).

Table 5. Use of binaries $y_{OP,t}$, $y_{OP,t-1}$,y_p to model Equation (3).

Case	$y_{OP,t}$	$y_{OP,t-1}$	y_p	Δx_{SP}
A	0	0	0	$-M - \Delta x_{\mathrm{SP}}^{\max} \leq \Delta x_{SP} \leq M + \Delta x_{\mathrm{SP}}^{\max}$
B	0	1	0	$-M - \Delta x_{\mathrm{SP}}^{\max} \leq \Delta x_{SP} \leq M + \Delta x_{\mathrm{SP}}^{\max}$
C	1	0	0	$-M - \Delta x_{\mathrm{SP}}^{\max} \leq \Delta x_{SP} \leq M + \Delta x_{\mathrm{SP}}^{\max}$
D	1	1	1	$-\Delta x_{\mathrm{SP}}^{\max} \leq \Delta x_{SP} \leq +\Delta x_{\mathrm{SP}}^{\max}$

Convexity of Constraints: Under the hypothesis that, the binary variables are either fixed or relaxed (i.e. can assume values between 0 and 1), the constraints are convex because they are linear functions of the variables [36].

3.2.4.3. Objective function

Over a specific time horizon, the MIQP RH optimisation problem intends to maximise the occupant TC and minimise the PTHP EC. Furthermore, a stabilisation term is incorporated in the objective function. This term aims to minimise variations or fluctuations in the operational status {ON/OFF} of the HVAC-PTHP system by imposing a cost. The penalty term is introduced in the objective function to discourage high frequency of transitions between the PTHP system's ON and OFF states, thereby incentivising smoother and more stable operation. When $y_{OP} = 0 \rightarrow x_{SP} = d$. Thus when exactly one of $x_{SP,t}, x_{SP,t-1}$ is d then ${\Delta x_{SP}}^2$ receives relatively high values. Therefore ${\Delta x_{SP}}^2$ comprises the penalty term (see section 3.2.4.2). The below Equation (4) presents the optimisation problem.

$$\begin{aligned} &\underset{x_k, y}{\mathrm{Min}} \sum_{i=0}^{H} \left\{ QR\left[a\,(PMV_i)^2 + (1-a)\,{EP_i}^2 \right] + R{\Delta x_{SP}}^2 \right\} \\ &\text{s.t.} \quad \text{Equation (1),} \\ &\qquad \text{Equation (2),} \\ &\qquad \text{Equation (3),} \\ &\qquad \text{Applied for the entire time horizon} \\ &\qquad y \in \{0,1\}^n \\ &\qquad x_k \in \mathbb{R}^m \end{aligned} \tag{4}$$

Where: H: length of time horizon, PMV_i: deviation of PMV TC term from its optimum desired value (see Equation (5) below), EP_i: PTHP electric power, (direct output of the TZ AM), (QR, R): weighting coefficients between the primary objectives and the penalty term objective, a: weighting parameter. Notably, α is the trade-off parameter between TC and EC. By prioritising

either, and deriving an optimal action/behaviour, different values of a define different OB profiles.

To account for inherent discrepancies between the original E+ model and the ANN AM, a correction term is incorporated to penalise deviations between predicted and actual outcomes for the TC index. As a result, the PMV_i mentioned in Equation (4) is structured as follows.

$$CT = PMV_0^{calc} - PMV_0^{pred} \tag{5}$$

$$PMV_i = PMV_i^{pred} + CT$$

Where, CT: the correction term, PMV_0^{calc}: the actual PMV value at the current timestep, as calculated through the ISO script (see Annex I , Figure 53), PMV_0^{pred}: the PMV value predicted through the Approximate PMV model (PMV AM) (section 3.2.4.3.1).

To retrieve the decision variables utilising the RH concept we strive to minimise the sum towards our objectives over i horizon timesteps. This is accomplished by updating the thermal zone's initial state condition parameters at each subsequent horizon timestep, as predicted through the derived TZ AM from the previous horizon [41].

Convexity of objective function: Under the hypothesis that, the binary variables are either fixed or relaxed (i.e. can assume values between 0 and 1), the objective function is convex semidefinite because, by construction, the eigenvalues of the involved variables are either positive or zero [36].

3.2.4.3.1. Thermal Comfort ANN index

A very clear limitation of PMV regarding its usage in the design of controllers is that there exists no explicit function of the six variables affecting TC. Calculation of PMV requires the utilisation of an iterative algorithm, which poses a challenge for the deterministic optimisation of model-based controllers [79]. Therefore, an explicit input-output relationship as the one mentioned in section 3.2.4 is necessary. In order to tackle the above limitation, and to align the components of the methods used in this framework, the TC PMV model utilised in the objective function of the above-defined optimisation problem is derived based on the flowchart in Figure 22.

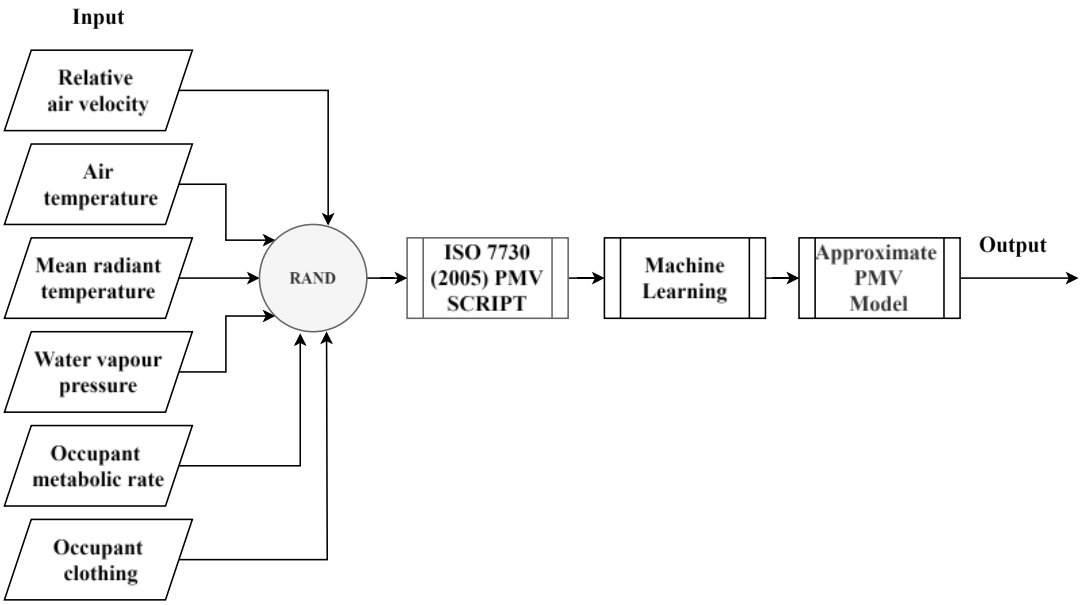

Figure 22. PMV Approximate Model derivation methodology.

First, random values of the PMV calculation input parameters are generated. Notably, most input parameters, which depend, and characterise the TZ conditions are inputs and outputs of the TZ ANN (Table 2). Subsequently, the values of all random input parameters, are within the bounds derived by the initial E+ black-box simulation for the case specific TZ of interest. Clothing, metabolic rate and air velocity which are not output variables of TZ ANN, are assigned rational bounds. These values are fed into a python script (Annex II, Figure 53) which has been refactored from the initial BASIC program provided in ISO 7730, 2005 [80].

The dataset obtained that includes both the PMV parameters and the resulting PMV values is utilised to train an ANN that allows the prediction of the PMV value based on the thermal zone condition at the current timestep. Thus, $PMV_t = f(TZ_t, O_t)$, where TZ_t: thermal zone conditions and O_t: occupant conditions. In plain words, the TC index PMV_t of the occupant in the current time step is approximated via ML as a function of the input variables shown in Table 6.

Table 6. Predicted Mean Vote ANN Input Variables

Variable Dependence	Variable Names
Thermal Zone conditions	Relative air velocity, Air Temperature, Mean radiant temperature, Water vapour pressure
Occupant conditions	Metabolic rate, Occupant clothing

The TZ ANN (section 3.2.2.1) is trained to predict TZ condition variables (Table 2) of the next timestep. This way, through the reformulation of both the TZ ANN, and the PMV ANN, into the optimisation problem, the resulting AM is able to predict the occupant PMV of the next timestep and incorporate TC maximisation (by minimising the PMV value deviation from 0, see Table 1), as one of the objectives of the optimisation function in Equation (4).

3.2.4.3.2. Energy Consumption

The variable to measure EC, is the E+ output variable “Zone Packaged Terminal Heat Pump Electricity Rate”. This E+ output field represents the rate of electricity consumption for the PTHP, measured in Watts. It includes the electricity used by the compressor (including the crankcase heater), fans (both indoor supply air fan and condenser fan), and the supplemental electric heating coil. This value is calculated for each PTHP system timestep during simulation, and the results are averaged for the reported timestep.

The TZ ANN in section 3.2.2.1 is trained to forecast this output variable (Table 2) for the next timestep. By transforming the ANN into an optimisation problem, the TZ AM model can predict EC of the next timestep and include its minimisation as one of the objectives of the optimisation function.

4. Case Study

4.1. Building

The building envelope of Leaf House, situated in Angeli di Rosora in the province of Marche and owned by the Loccioni Group, comprises external walls with a total thermal transmittance (U-value) of $0.41\ W/(m^2\mathrm{K})$ and windows with a U-value of $1.1\ W/(m^2\mathrm{K})$. Leaf House serves as a research and innovation hub across various sectors, including energy and the environment, with its E+ Building energy model validated in [81]. The specific TZ being examined is a small office located on the 2nd floor of the building, facing west. This TZ covers an area of 9.16 m^2 and a volume of 24.74 m^3, featuring a west-facing external window with a U-value of $1.1\ W/(m^2\mathrm{K})$ and an area of 2.40 m^2. As part of this case study, the thermal zone is equipped with a HVAC system, namely a PTHP, with a Heating Coefficient of Performance (COP) of 5 and a Cooling COP of 3, which has been automatically sized using a Typical Meteorological Year (TMY) derived design days file for the region of interest, prior to this study.

During the simulation of the thermal zone, the x_{SP} thermostat temperature setpoint can receive values between $[17,27]$, when in operation, and Δx_{SP} as defined in 3.2.4 can receive values within $[0,3]$. It is assumed that one building occupant is present in the TZ with a constant metabolic rate of 1 met. The sum of nominal internal heat gains accounts to 11.5 W/m^2 including lighting and electricity load. The occupant clothing insulation can vary between $[0,1.5]$ $(1\ clo = 0.155\ Km^2/W)$. Indoor air velocity in regard to occupant thermal sensation calculation is set to 0.2 m/s as E+ cannot calculate this variable. Further information regrading the simulation set up of the TZ for this specific case study can be found in the Appendix.

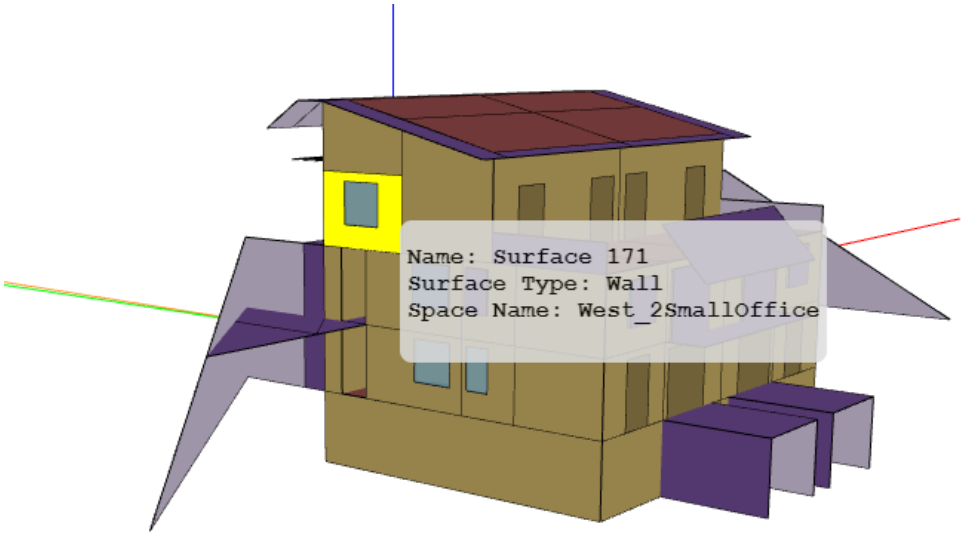

Figure 23. Leaf House Energy Model (OpenStudio graphic interface –Thermal zone shown in yellow).

Figure 24. Leaf House Building as depicted in Google Maps Street View

Table 7. External wall thermal and physical characteristics

Description	Thickness	Thermal Conductivity	Density	U-Value
Inside to Outside	cm	W/mK	kg/m^3	W/m^2K
Gypsum mortar for plasters	2.00	0.29	600	14.29
Porotron Block	30.00	0.21	950	0.70
Polysterine-Rofix EPS 100	18.00	0.036	93	0.2
Plastic Plaster coat	0.50	0.30	1300	100

4.2. Weather

For E+ simulations, a standard weather format input file, known as EPW, is required. This format, initially developed for use with E+ and Energy System Research Unit (ESP-r) simulation programs, has become widely adopted by various building simulation tools. Weather information for the case study building is represented using Ancona, Italy as the location due to its geographical proximity, and its corresponding TMY as the simulation weather input. The EPW weather file operates on an hourly timestep and includes variables for various weather parameters (see Table 9).

To introduce uncertainty into the weather files' variable, random deviations from the actual TMY values are incorporated at each hourly timestep (Figure 25). Note, dew point temperature can be directly calculated from the relative humidity and dry-bulb temperature [82].

$$Wv_{dev} = Wv_{init} + (-1)^{r\{0,1\}} r.ufm(0, Quantile_{.95}(S)), \text{where} \quad (6)$$

$$S = \{|Wv_{init,s,t+1} - Wv_{init,s,t}|\},$$

$$\forall\, s\, \epsilon \{spring, summer, autumn, winter\}$$

$$\forall\, t\, \epsilon (\min(t_s), \max(t_s) - 1)$$

Where, Wv_{init}: initial Weather Variable (Wv) value, Wv_{dev}: deviated Wv value, S: the distribution of the differences between the same Wv_{init} for consecutive timesteps. The quantile value is seasonal and refers to S. Next, r: random number generator ($\{0,1\} \rightarrow$ 0 or 1, $ufm \rightarrow$ uniform distribution between [lower bound, upper bound)). If the updated Wv_{dev} of the initial weather variable distribution, subceeds or exceeds the minimum or the maximum seasonal value, respectively, then it receives that exact minimum or maximum value. Equation (6) is performed for each Wv in Table 9.

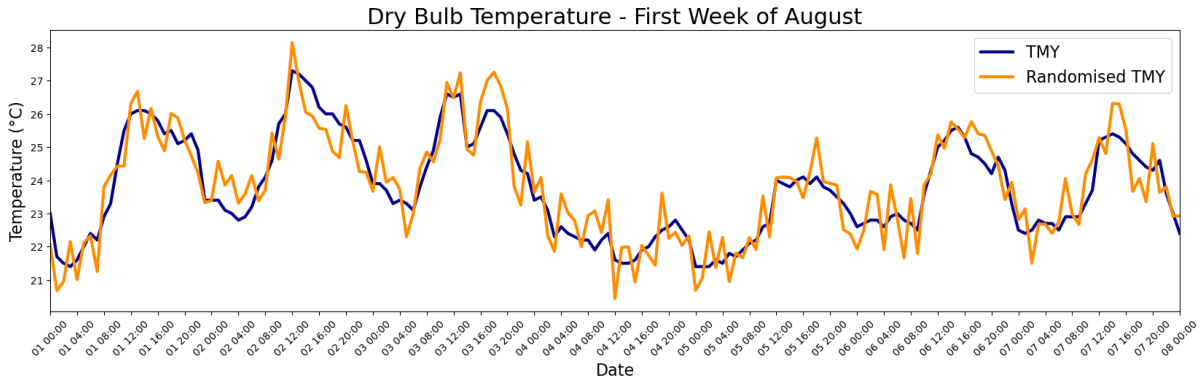

Figure 25. Example of processing of weather input variable (Dry-Bulb Temperature)

This resulting weather file is fed into the black-box E+ simulation, as part of the hybrid methodology described in 3.2, where the TZ ANN is built and trained to be finally reformulated and utilised in the optimisation problem.

Table 8. Season Date Ranges.

Season	Start Date	End Date
Spring	Mar 21	Jun 20
Summer	Jun 21	Sep 22

Autumn	Sep 23	Dec 20
Winter	Dec 21	Mar 20

Table 9. Outdoor weather Variables and respective seasonal calculated deviations.

Outdoor Weather Variable - Season	Spring	Summer	Autumn	Winter
Dry Bulb Temperature (ºC)	1.4	1.2	1.4	1.7
Dew Point Temperature (ºC)	1.8	2.9	1.74	2.8
Relative Humidity (%)	9	11	9	14
Atmospheric Station Pressure (Pa)	31.8	51	72.8	87.65
Horizontal Infrared Radiation Intensity (Wh/m^2)	17	12	20	21
Direct Normal Radiation (Wh/m^2)	230	240	231.4	214.3
Diffuse Horizontal Radiation (Wh/m^2)	58	46	43	46
Wind Direction ($degrees$)	142	240.6	133.4	301
Wind Speed (m/s)	2.1	1.2	1.5	2
Opaque Sky Cover ($tenths\ of\ coverage$)	2	7	3	6

5. Results

5.1. Thermal Zone Artificial Neural Network

5.1.1. Correlation analysis

As mentioned in the methods section, to comprehend the impact of the actions on the case study building TZ conditions (section 3.2.1), a correlation analysis was performed. A stable weather file was created by using the fixed median value of each weather variable given in the Ancona TMY weather file, throughout a whole year. The TZ was then exposed to this stable weather file while a single random action was implemented for a maximum of 4 timesteps (2 hours). The window and blind state are alternated between 0 and 1. The PTHP thermostat is alternated between being activated and deactivated. When enabled, the PTHP thermostat temperature value is set to 21°C. In the figures below each of the occupant actions' impact on the TZ conditions is examined over a one-month period. Because a stable weather file is used, the month of choice determines the solar angle and altitude characteristics as calculated internally by E+, and their subsequent impact on the TZ conditions. Specifically, January was chosen because it is the month during which the most radiation is measured to be transmitted through the TZ window. Throughout the year, the impact of the occupant actions on the TZ, create dynamics for the TZ ANN to be trained upon.

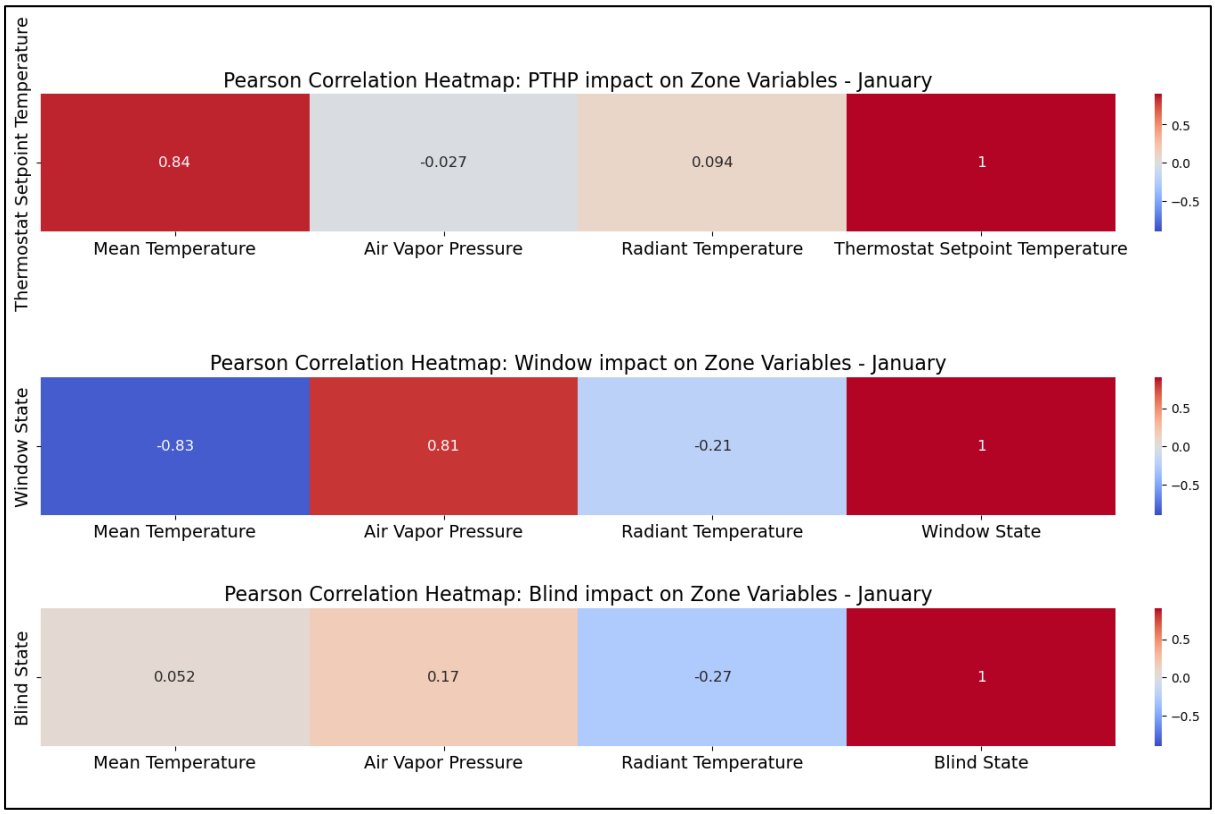

Figure 26. Example of Occupant Actions' impact on thermal zone conditions. Blind impact is only examined when there exists outdoor direct solar radiation.

Examining the Pearson correlation coefficients of the Heatmaps Figure 26, it is visible that moving from $t \rightarrow t+1$, when the thermostat temperature value is increased to 21°C, the Zone Mean Temperature also increases to a significant extend. This is a result of the low temperatures in the stable weather file. Therefore, zone heating is modelled. When the window is opened and its state changes from 0: closed to 1: open, the Zone Mean Temperature decreases significantly, the Zone Radiant Temperature decreases slightly. The Zone Air Vapor pressure increases. Regarding the blind action, in January, it impacts the thermal zone conditions to a lesser extent. The blind impact was examined only when direct solar radiation (part of the OWCs), is measured positive on the TZ of interest. During that time periods, seemingly, Zone Radiant Temperature decreases slightly when the blinds are applied (Blind state = 1.0).

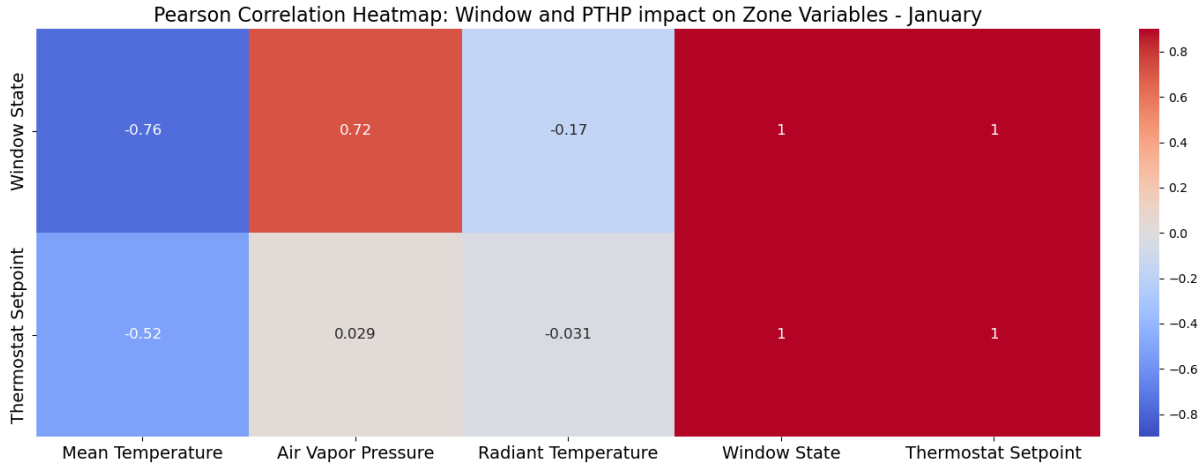

Figure 27. Example of simultaneous Occupant Actions' (Window and PTHP) impact on thermal zone conditions.

Because of the contradicting impact of the Window action and the PTHP action on the Mean Zone temperature, another stable weather simulation was implemented, during which both actions are applied simultaneously, again for a maximum period of 4 timesteps. As a result (Figure 27), it is obvious that during January, the window action, and its impact on the TZ conditions also due to the OWC, overpowers the impact of the PTHP heating attempt. Therefore, the Zone Mean Temperature still decreases when both actions are applied, though to a proportionally slighter extent.

5.1.2. Action impact analysis results – ANN preprocessing

To further investigate the impact of the adaptive TC occupant actions on the TZ indoor conditions on timestep scale a randomly chosen 2-day duration is examined. Specifically, the

range 10/01 –11/01 is chosen. The actions are applied separately on the TZ as explained in 5.1.1. As mentioned earlier, the OWC resulting from the simulation itself, do not remain completely stable because in E+, the building location and its date-dependent exposure to the sun, are of considerable importance.

In Figure 28, the TZ conditions are depicted when no occupant actions are applied to the TZ throughout the 2-day period, for them to be compared with the cases when the occupant actions are actually applied to the TZ (Figure 29, Figure 30, Figure 31)

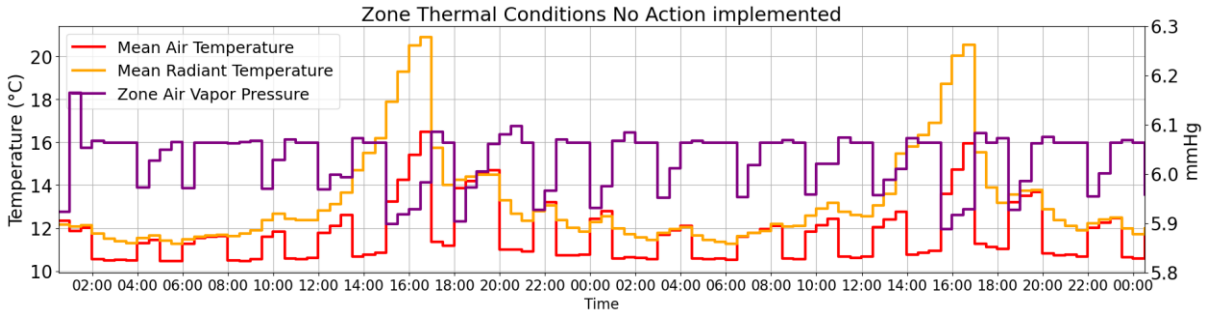

Figure 28. Thermal Zone conditions when no actions are implemented.

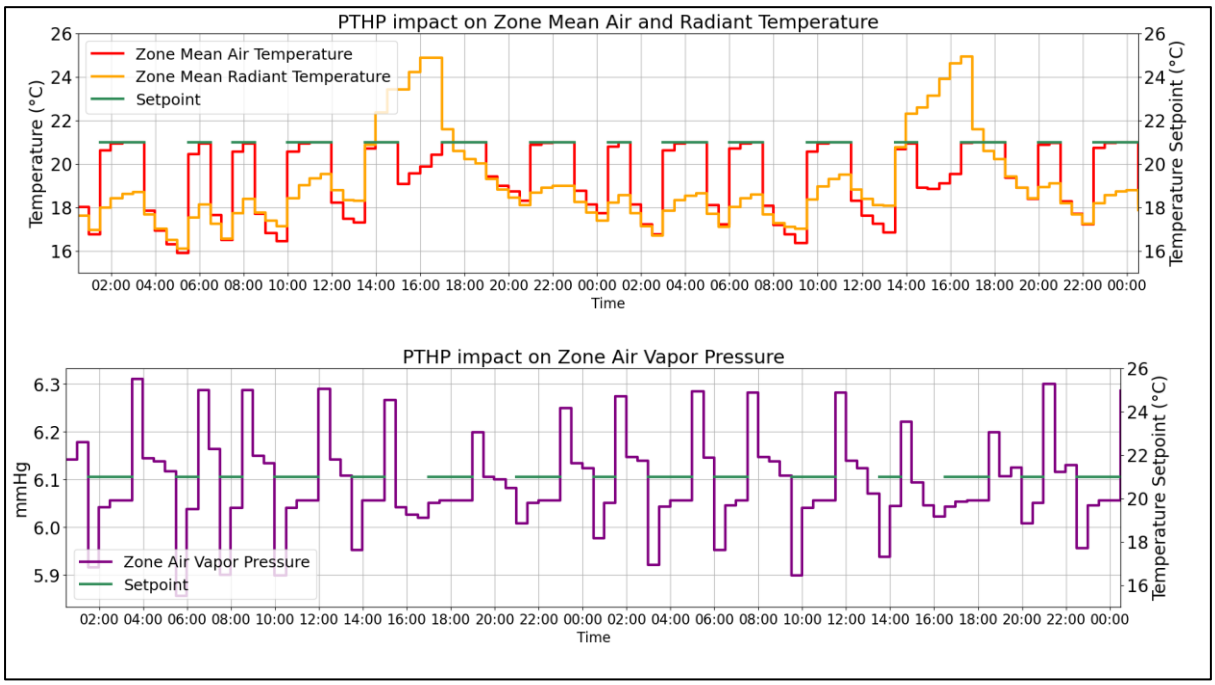

Figure 29. Impact of PTHP actions on thermal zone conditions (10/01 – 11/01).

Regarding the PTHP action, as observed in Figure 29, in this specific duration, it is obvious that once the PTHP is activated and the thermostat is set to the value of 21°C, the Zone Mean Air Temperature (T) is increasing up until that thermostat value. Similarly, the Zone Radiant Temperature (Tr) increases significantly when the thermostat is activated. On the contrary

Zone Air Vapor Pressure (P) seems to be decreasing every time the heating is activated. Following the deactivation of the PTHP system, T decreases gradually, as does Tr (the two peaks are a result of the solar radiation angle during that time of the day) while P increases.

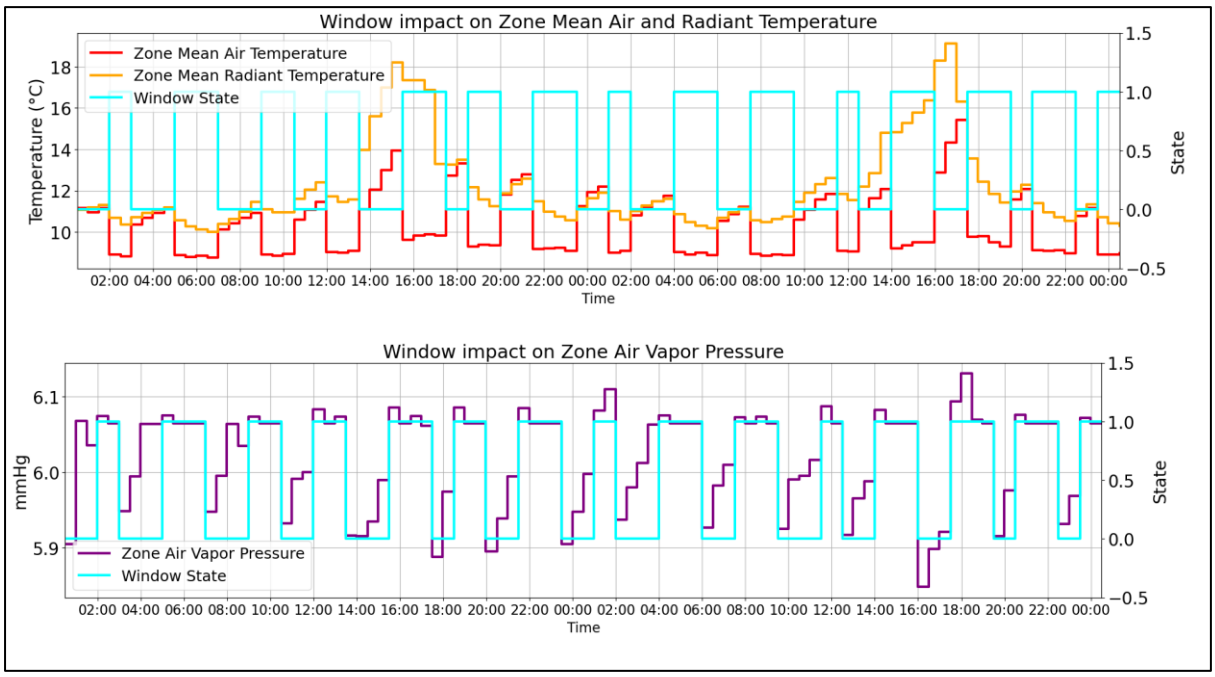

Figure 30. Impact of Window action on thermal zone conditions (10/01 – 11/01).

Regarding window usage (Figure 30), when the window is opened (state = 1.0) T shows a substantial decrease, Tr shows a slight decrease, and P shows a slight increase. On the other hand, when the window is closed (state = 0.0), as expected the outcomes for each variable are reversed.

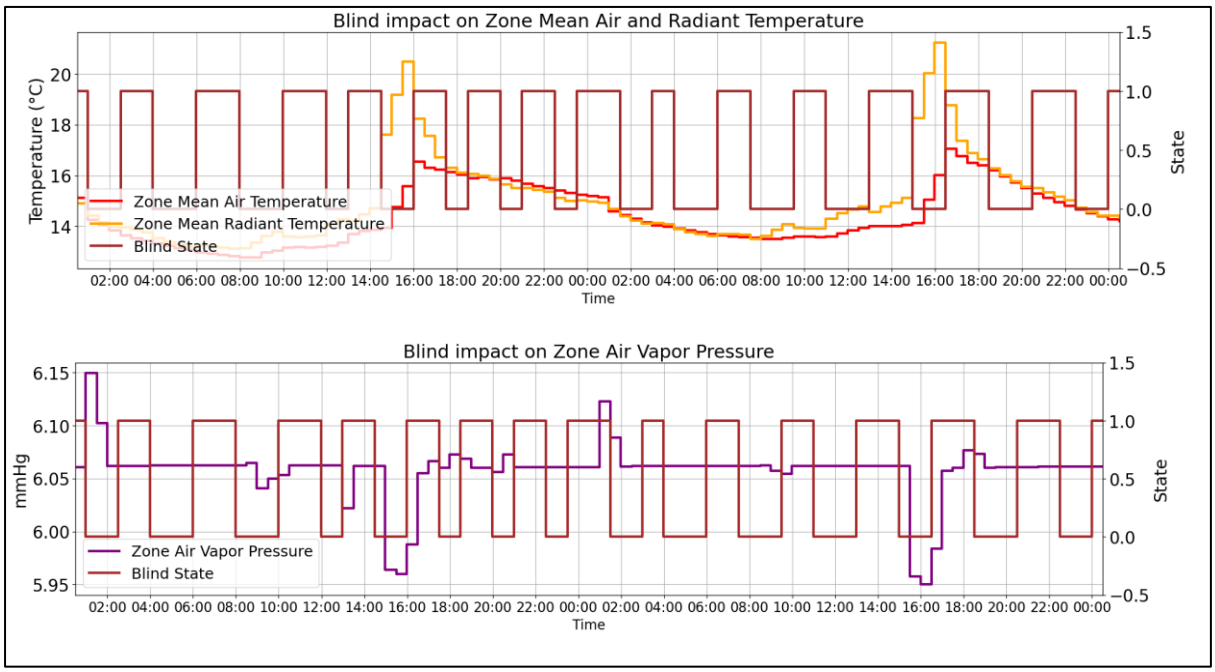

Figure 31. Impact of Blind Action on thermal zone conditions (10/01 – 11/01).

Finally, regarding the blind usage (Figure 31) is it evident that its impact is slighter compared to PTHP setpoint adjustments and window usage. Both when the blinds are applied (state 1.0) or retracted (state 0.0), all variables do not show significant alteration. Only during from 15:00 to 16:00, the increase in temperature is restrained.

Throughout the analysis though, it has been detected that during the hours of the day where the solar radiation outdoor variables, directly impact the thermal zone due to the solar angle, (that changes based on the E+ timestamp), blind usage restrains the impact of OWC on the TZ. This restraint can be captured though the ANN.

As mentioned before, the occupant clothing adjustments do not lead to any changes in the TZ indoor conditions but only affect the thermal sensation and comfort of the occupant itself. Therefore, there is no analysis for this specific adaptive TC actions to be examined in regard to its impact on the TZ.

5.1.3. Thermal Zone Artificial Neural Network training and validation

The architecture of the TZ ANN is described in 3.2.2.1. The TZ ANN model's hyperparameters were optimised using Bayesian Optimisation to balance model complexity. The neural network architecture consists of one hidden layer, comprising nine units, with ReLU activation functions applied to each node. Training utilised the Adam optimizer with a learning rate of 0.0113 and was performed for a maximum of 50 epochs, employing a batch size of 48 samples per iteration. Early stopping, with a patience of 10 epochs, was employed to prevent overfitting.

Results for the four output variables are summarized in Table 10 and Figure 33. Figure 33 illustrates the simulated output from E+ compared to the approximate output prediction from the ANN model for a randomly chosen 48 timestep (24 hour) period. For validation and in order to perform extrapolation, the comparison between actual values and predicted values is performed utilising a dataset that includes dynamics between TZ indoor conditions, as a result of exposure to random TC adaptive actions and the initial, non-deviated TMY Ancona weather file.

Table 10. Thermal Zone ANN prediction result metrics and standard deviation for each output variable.

Metric - Variable	EP	Tr	T	P
R2 score	0.94	0.96	0.96	0.95
MAE score	12.96	0.82	0.92	0.55
STD Value	97.63	5.48	5.70	3.76

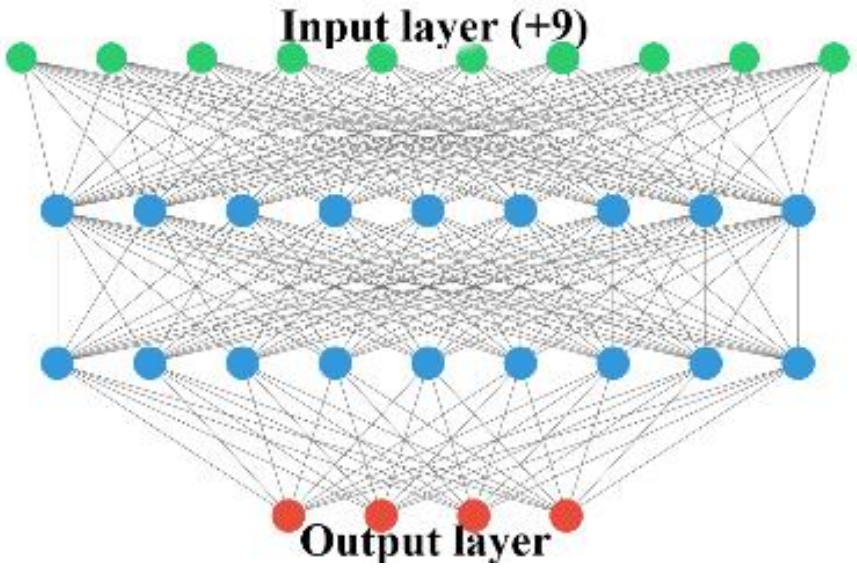

Figure 32. Artificial Neural Network Representation.

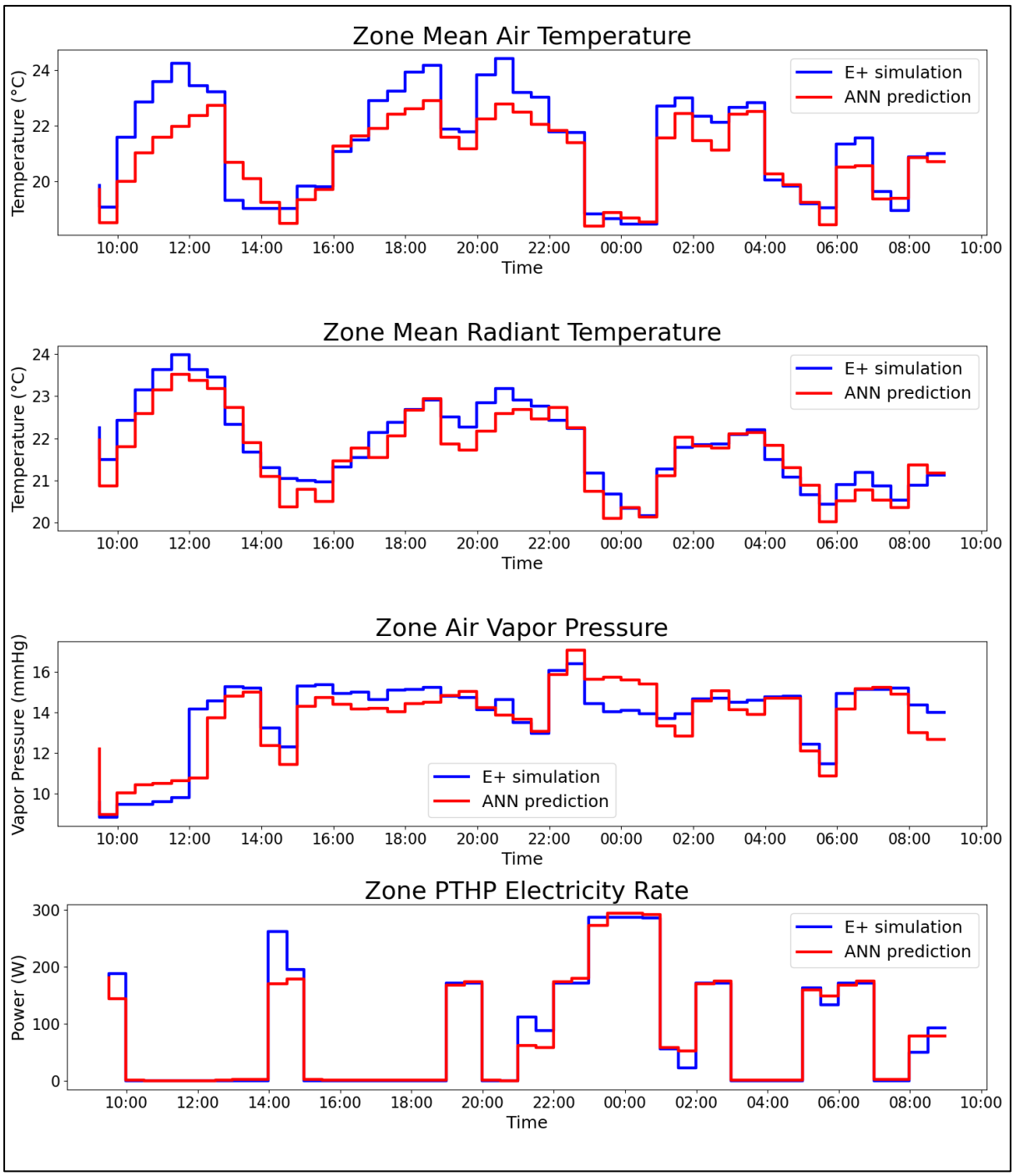

Figure 33. Examples of ANN prediction vs Energy Plus simulation for the 4 output variables (1 day duration).

5.2. PMV Artificial Neural Network training and validation

The architecture of the PMV ANN is described in 3.2.4.3.1. The hyperparameters for the training of the PMV ANN model were also suggested through BO while balancing model complexity. The neural network architecture comprises two hidden layers, each containing ten nodes, with ReLU activation functions applied to each node. Training was conducted using

the Adam optimizer with a learning rate of 0.0144, over a maximum of 50 epochs, and with a batch size of 48 samples per iteration. Early stopping was implemented, with a patience of 10 epochs, to prevent overfitting. Results for the PMV output variable are presented in Table 11 and Figure 34. Figure 34 illustrates the simulated output from calculated values given through the PMV ISO 7730 (2005) script [80], compared to the predicted output from the ANN model.

Table 11. PMV ANN prediction result metrics and standard deviation for PMV.

Metric - Variable	Predicted Mean Vote
R2 score	0.99
MAE score	0.058
STD Value	1.93

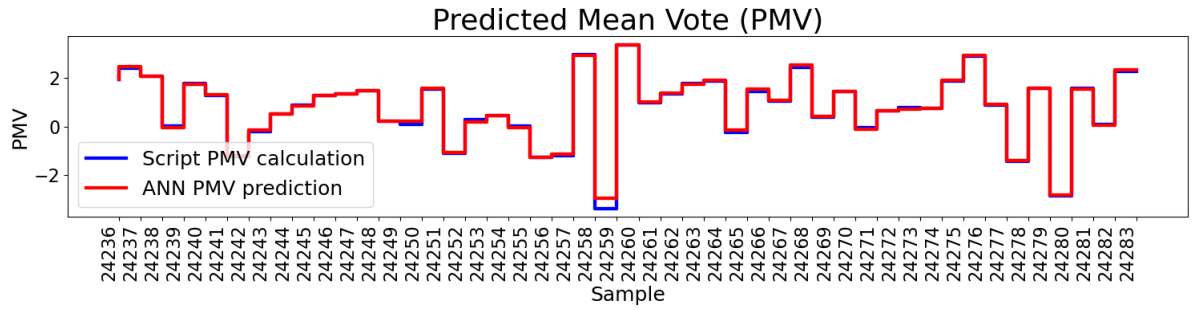

Figure 34. Example of PMV ANN prediction vs ISO PMV script calculation.

5.3. Closed loop simulation

A closed-loop simulation model is utilised to operate the HVAC-PTHP system and implement adaptive TC measures. This involves conducting simulations using E+, where optimal actions are determined and applied to regulate the thermal conditions of a zone at every 30-minute timestep through the solution of the optimisation problem. The performance of the optimisation process is evaluated by applying these actions over a single day, comprising 48 timesteps, for each season of the year. Specifically, four days representing transitional periods between seasons are selected for simulation. These days are chosen based on their high variation in OWC, as determined by the standard deviations in the original Ancona TMY weather file, normalised and equally weighted. Furthermore, to examine a heatwave day, specifically regarding the summer season, another day is chosen due to its high mean outdoor temperature. In each chosen day, two different values for α and subsequently two different OBs are examined, thus presenting the differences in occupant actions based on their preferences. From the objective function (4) it is obvious that higher α values prioritise TC,

while lower values prioritise energy saving actions. The results of the different examined scenarios are summarised in Table 12.

It is worth noting that, in each of the optimisation results below, the discrepancy between the first and the subsequent values is observed because the simulation is initiated at the beginning of the day. The initial system states impact the outcome before the system is controlled afterwards.

Table 12. Closed loop simulation results for specific days and α values.

Name	Date	α value	Mean absolute PMV	Total energy consumption ($\boldsymbol{kWh}$)
Spring shoulder day	23/03	0.975	0.45	0.23
		0.99	0.75	1.17
Summer shoulder day	05/07	0.993	0.53	0
		0.9992	0.16	1.74
Summer heatwave day	25/07	0.986	0.64	1.21
		0.9978	0.38	2.59
Autumn shoulder day	23/11	0.97	0.92	1.01
		0.99	0.47	1.59
Winter shoulder day	09/02	0.969	1.22	1.19
		0.99	0.55	2.29

5.3.1. Spring shoulder day analysis (23/03)

The spring shoulder day OWC (Figure 35) consist of relatively low and stable air-temperature and dewpoint temperature. Humidity is high during (00:00 – 6:00) and sinks to mid-range values during the day. Wind speed increases after (18:00) to reach around 8 m/s while pressure levels remain fairly stable. Direct and diffuse radiation, incoming from the sun follow the solar altitude angle pattern while horizontal infrared radiation has a mean value of 306 W/m^2.

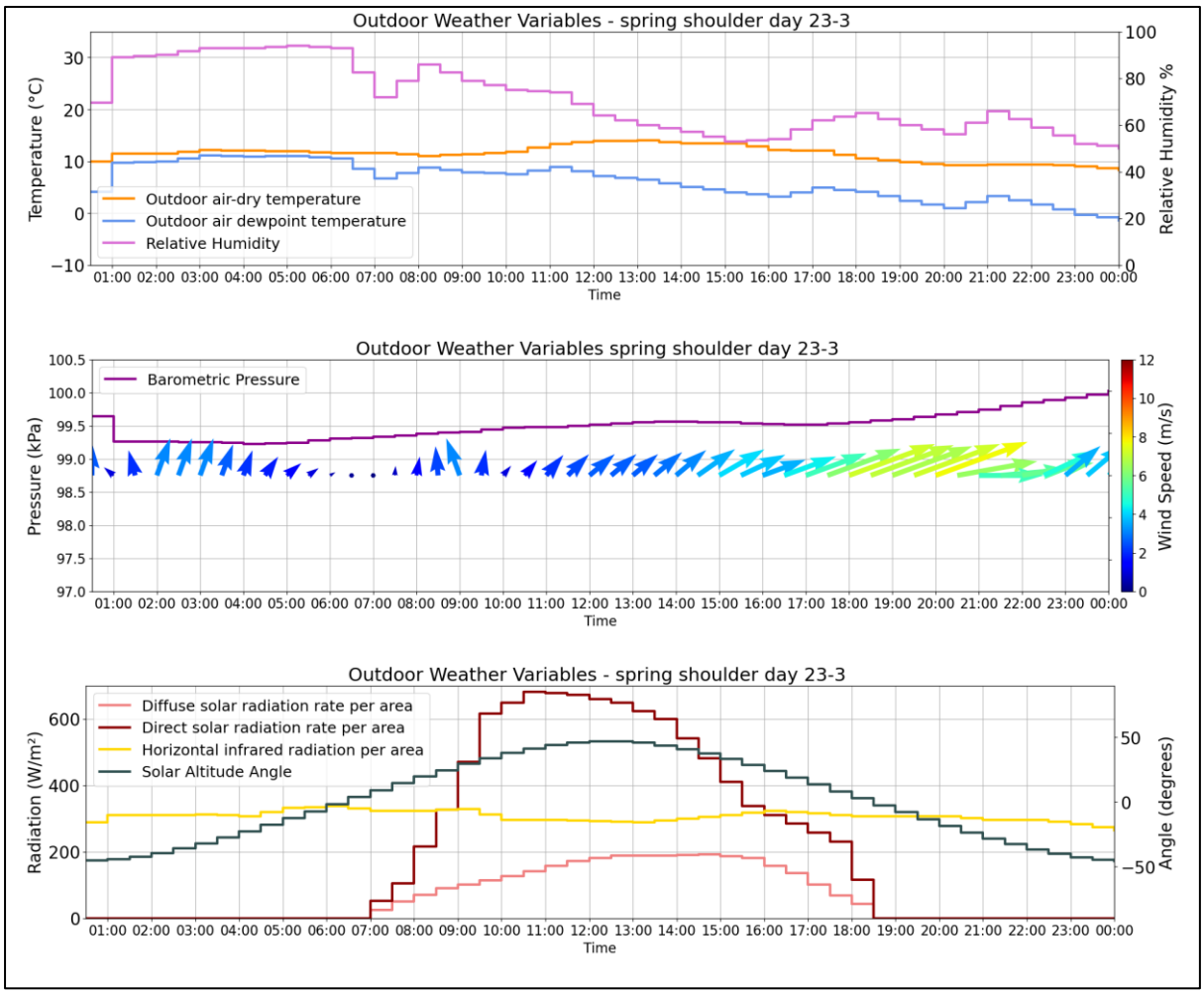

Figure 35. Spring shoulder day (23/03) outdoor weather conditions.

Examining the optimisation results on 23/03, firstly, when α = 0.975 (Figure 36), clothing is used to its maximum value throughout the day to cover for TC needs, as it does not consume any energy. At the beginning of the day, the setpoint temperature is deployed at just under 20°C, then it increases slightly towards the 14:00 hour mark until the HVAC is shut down between 14:30 – 19:30, to save energy. At 19:30 it is turned on again to cover the needs for TC maximisation. When α = 0.99, (Figure 37) the temperature setpoint is deployed a bit higher during (0:30-14:30) than at α = 0.975, and during the 14:30 – 19:30 period the PTHP is not turned off, but instead the thermostat temperature increased, and clothing is removed as the occupant clearly does not consider EC minimisation as its primary goal. No window or blind actions are implemented in either scenario.

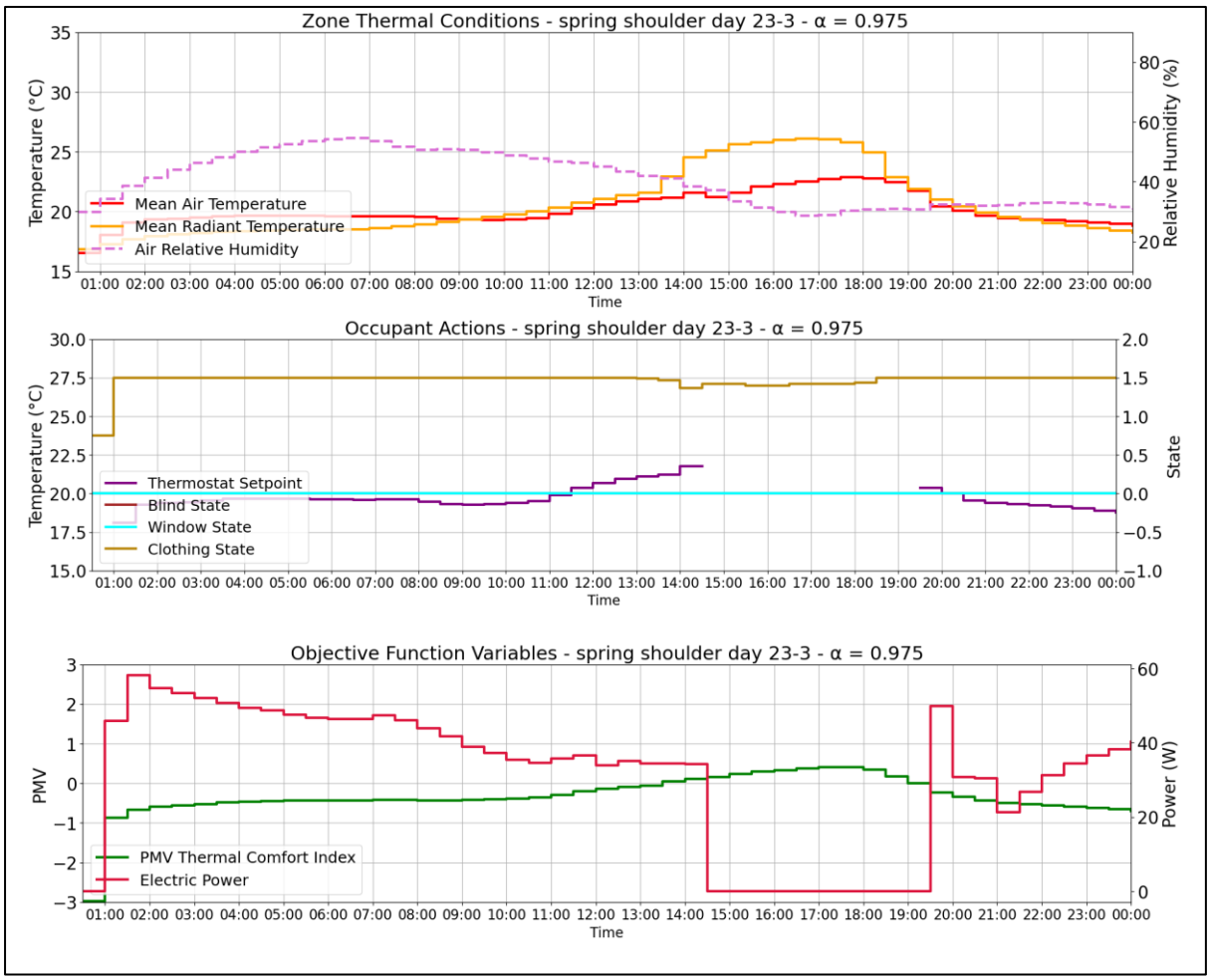

Figure 36. Spring shoulder day (23/03) thermal zone conditions, occupant actions and the resulting thermal comfort and energy consumption, α = 0.975

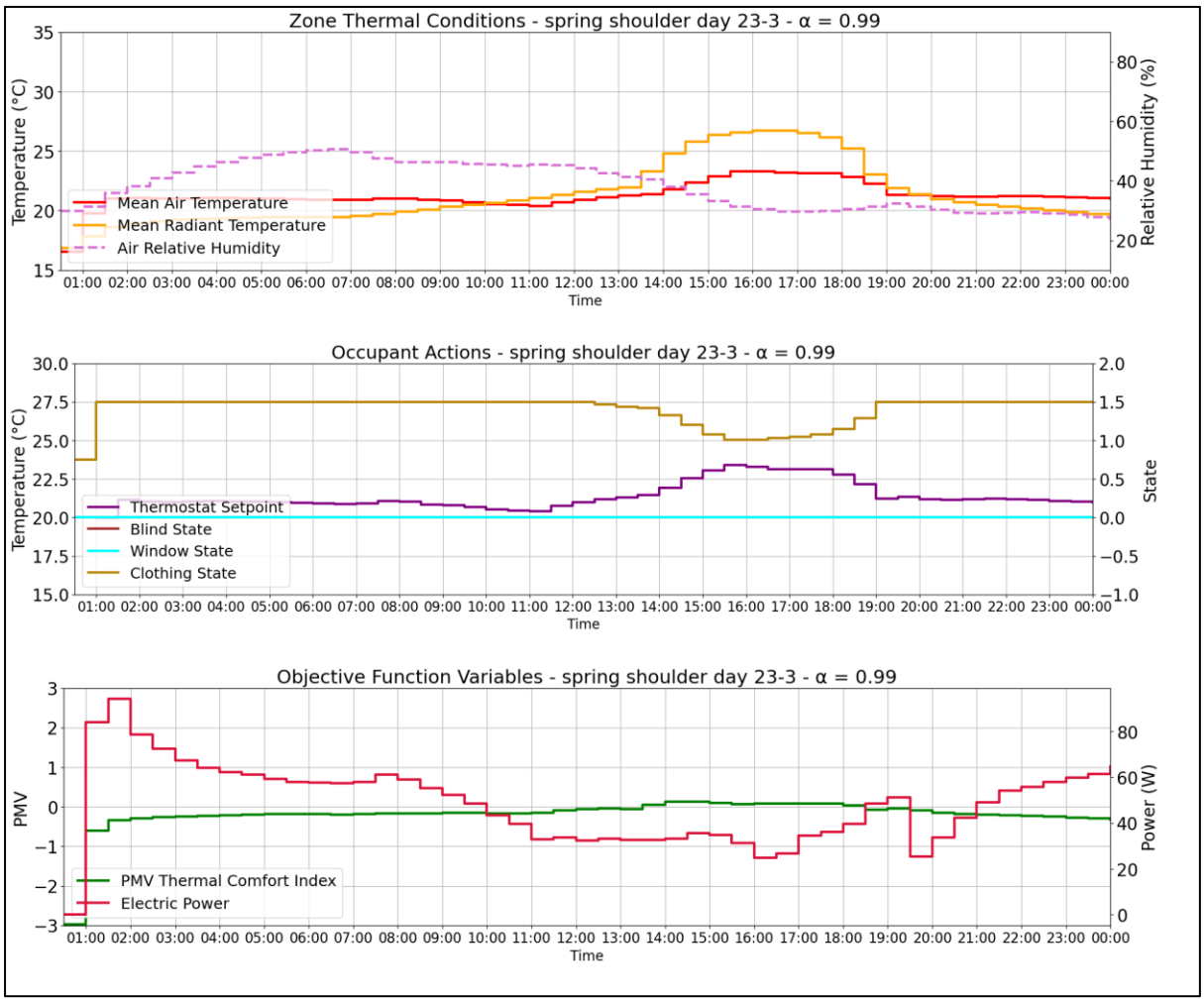

Figure 37. Spring shoulder day (23/03) thermal zone conditions, occupant actions and the resulting thermal comfort and energy consumption, α = 0.99.

5.3.2. Summer shoulder day analysis (05/07)

During the beginning of the summer shoulder day (Figure 38), outdoor air-dry bulb temperature is high and close to 28ºC, though it steadily decreases to below 20ºC until the end of the day. Outdoor dewpoint temperature remains below 20ºC throughout. Outdoor relative humidity stays at around 50% until the evening, where it peaks at 90%. During 6:00 – 9:00, there are relatively strong south-west wind speeds reaching ($10 m/s$) while pressure remains between 98.5-100 kPa, increasing towards the end of the day. Horizontal infrared radiation has a mean value of 368.75 W/m^2.

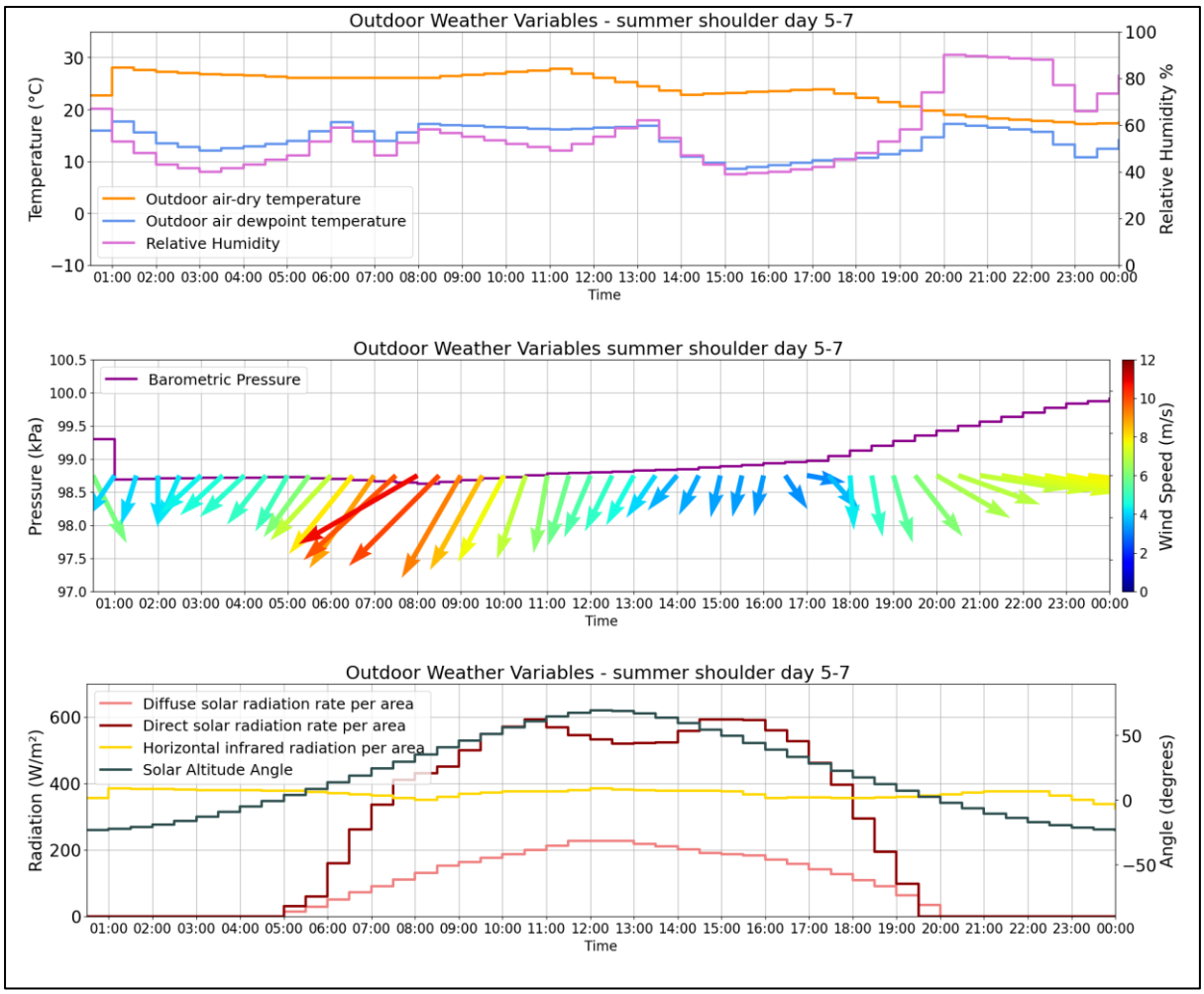

Figure 38. Summer shoulder day (05/07) outdoor weather conditions.

During the summer shoulder day, observing the closed-loop simulation when (α = 0.993 - Figure 39), because of its non-consumptive nature, clothing insulation, is reduced to combat the heat. Frequently, the window and the blinds are opened and applied throughout the day. When the windows are opened it is observed that the occupant is adding to its clothing insulation. Interestingly when α = 0.993, the PTHP is not enabled at all, as the other adaptive TC actions satisfy the TC objective adequately. On the other hand, when (α = 0.9992 -Figure 40), the windows are closed and the PTHP is in operation all day. Blinds are also applied most timesteps of the day. The PTHP thermostat setpoint is set to 27ºC for stable air-conditioning during the day. The clothing insulation is adjusted throughout the day to complement the air-conditioning and obtain optimal TC values.

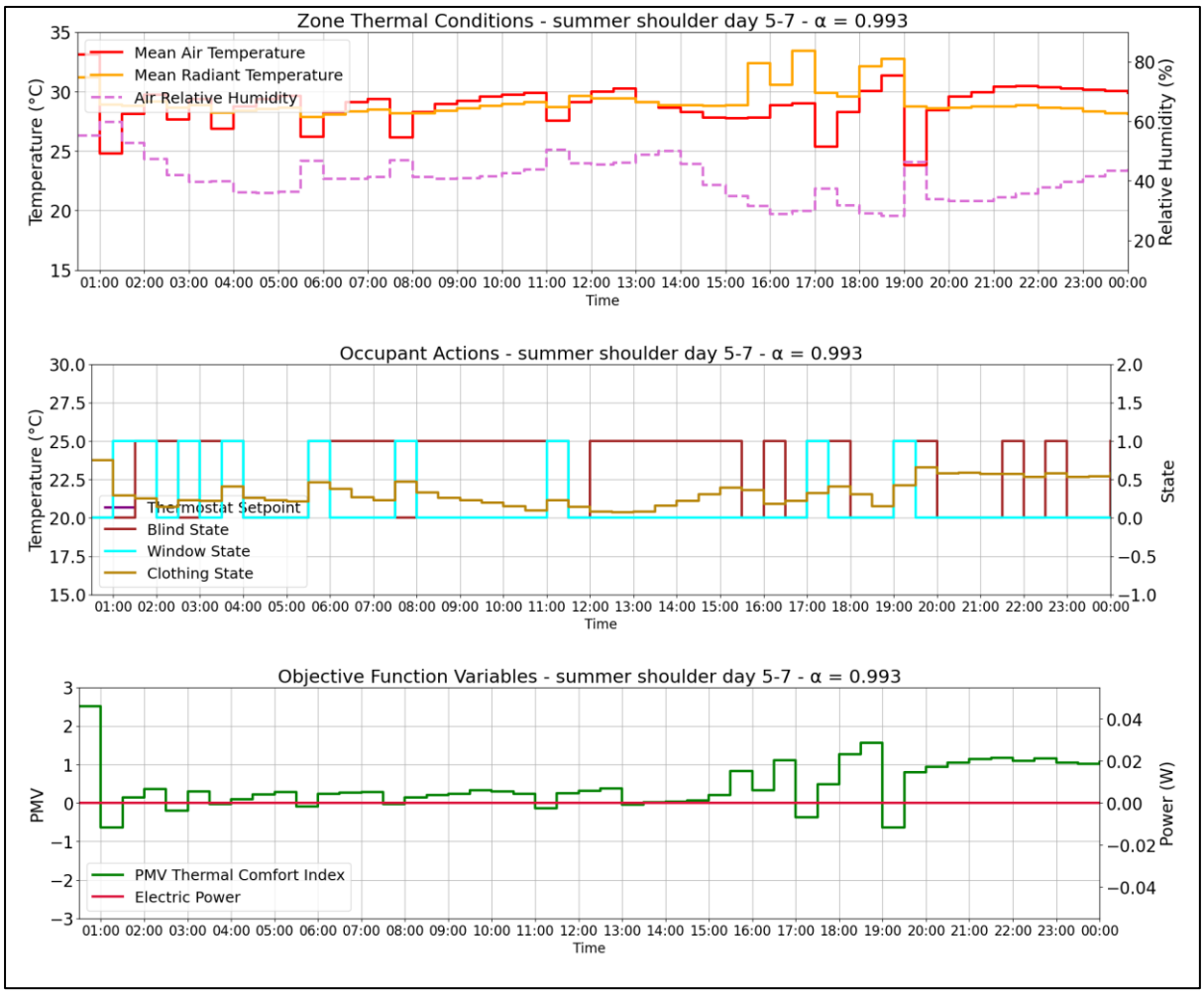

Figure 39. Summer shoulder day (05/07) thermal zone conditions, occupant actions and the resulting thermal comfort and energy consumption, α = 0.993

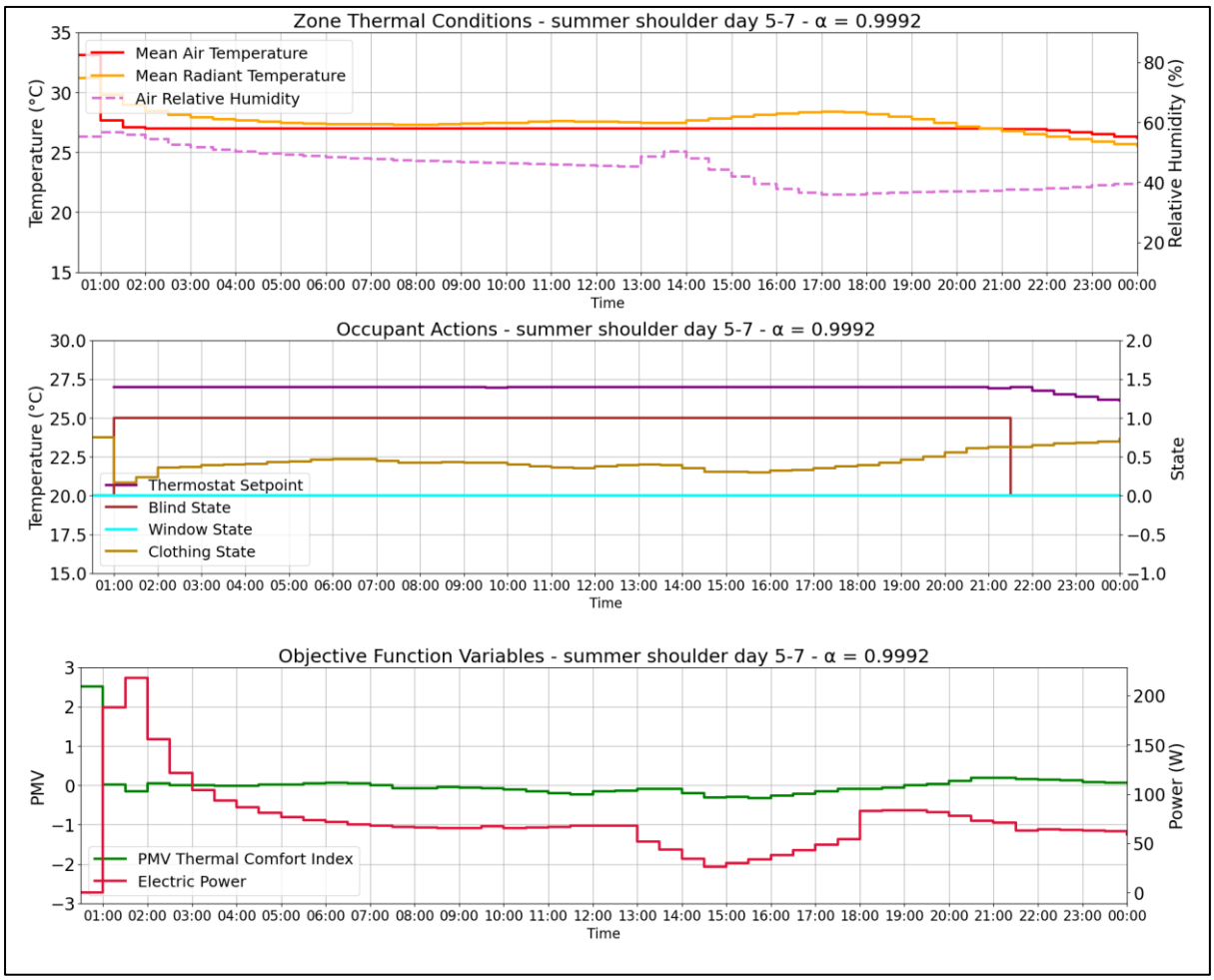

Figure 40. Summer shoulder day (05/07) thermal zone conditions, occupant actions and the resulting thermal comfort and energy consumption, α = 0.9992.

5.3.3. Summer heatwave day analysis (25/07)

Regarding the outdoor weather (Figure 41), the summer heatwave day is reporting the highest mean air-dry temperature (28ºC) in the entire year. It never falls below 24ºC. Between 12:00-18:00, it reaches values above 30ºC. Dewpoint temperature and relative humidity present similar patterns regarding their peaks and troughs, with values around the 20ºC and 60% mark respectively. The barometric pressure remains stable, in between 99.5–99.6 kPa while only exceptionally low wind speeds are observed. The horizontal infrared radiation intensity has a mean value of 376.2 W/m^2, the highest out of all the examined days.

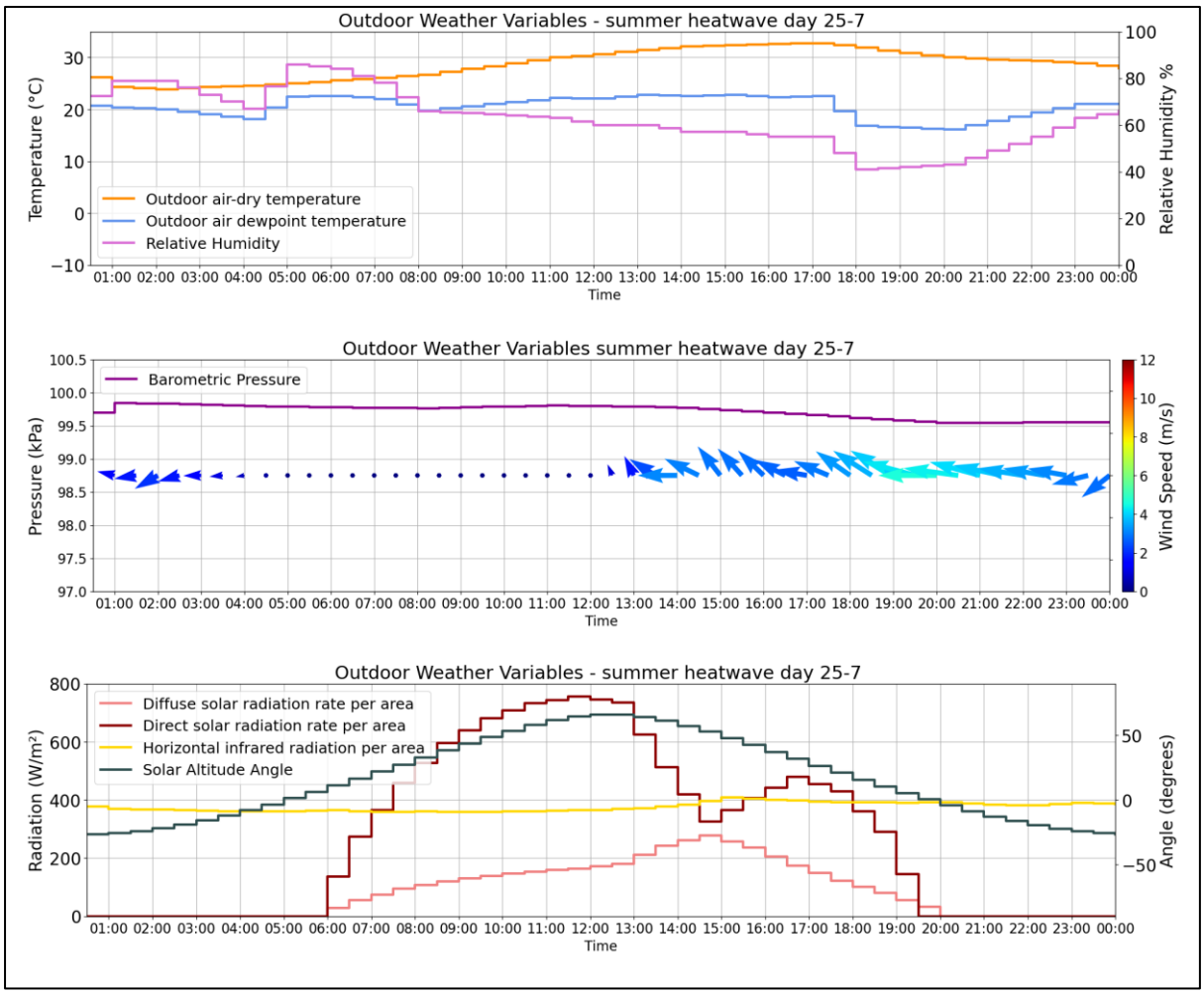

Figure 41. Summer heatwave day (25/07) outdoor weather conditions.

The analysis of the summer heatwave day optimisation outcomes, show that when α = 0.986 (Figure 42) the PTHP system is enabled sparingly. It is enabled once at 1:00 but turned off again right after. Between 2:00 and 13:30, energy is saved, and the attempt to satisfy TC is managed through window opening and clothing adjustment actions. After 14:00, the window usage impact is calculated to be insufficient and thus, the window is closed, and the PTHP is enabled again until 18:00 (thermostat setpoint = 27°C). After 18:00 the PTHP is disabled again, as considering the OWC, opening the window is again considered sufficient regarding TC satisfaction. On the contrary, when α = 0.9978 (Figure 43), EC minimisation in considered less, and therefore the PTHP is enabled for longer periods during the day (1:00-11:00 and 13:00-19:00). During these periods, often it is preferred to increment the clothing value rather that disable the PTHP system completely. Interestingly, in both cases (α = 0.986, α = 0.9978), when the PTHP system is enabled, the windows are closed and vice versa, indicating that for optimal operation of the PTHP system a more, stable environment is preferred. Finally, in both cases as well as in the summer shoulder day 5.3.2, blinds are applied to the window

throughout the day thus indicating that their impact on reducing the solar radiation influx and preserving thermal zone conditions' stability.

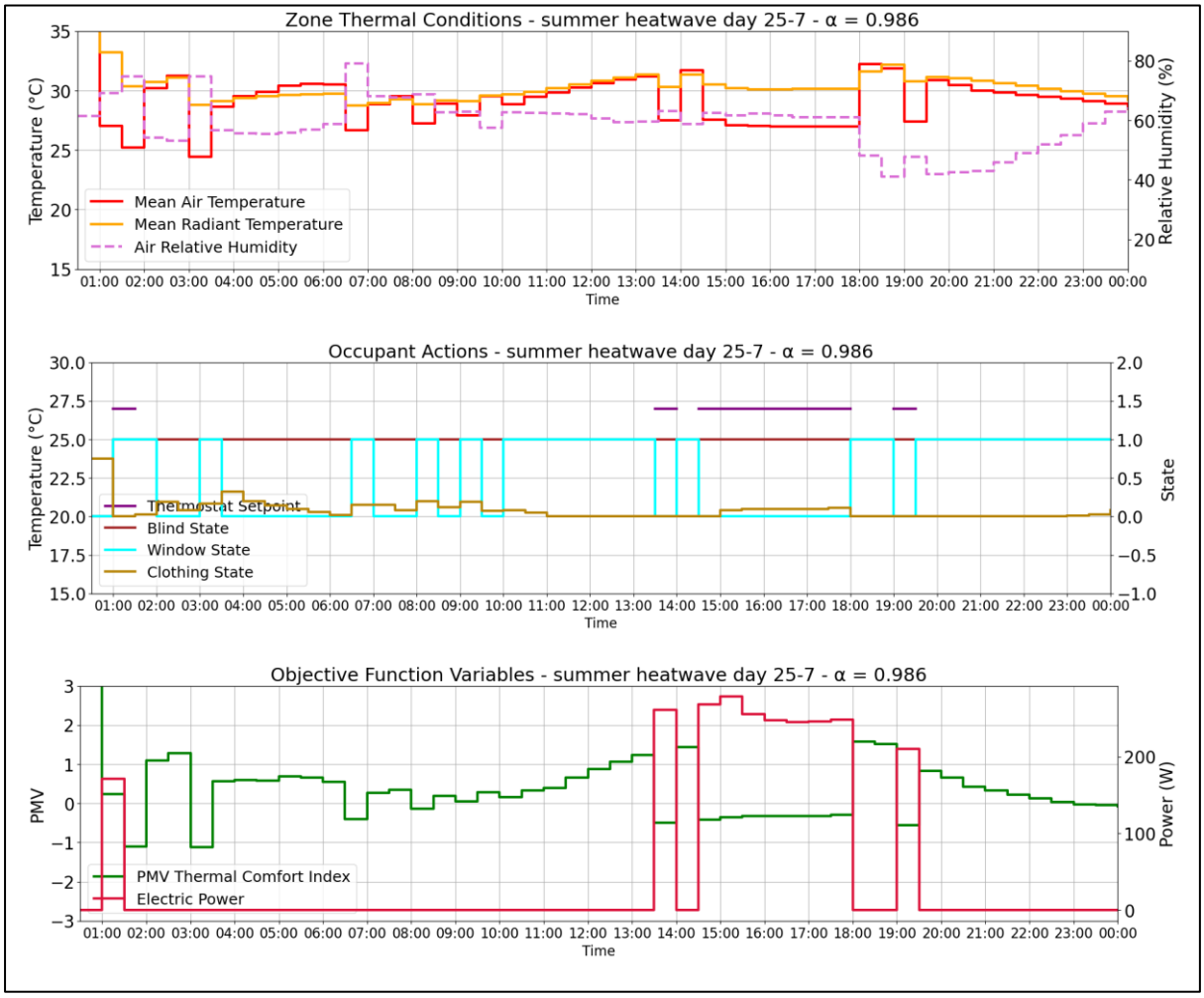

Figure 42. Summer heatwave day (25/07) thermal zone conditions, occupant actions and the resulting thermal comfort and energy consumption, α = 0.986.

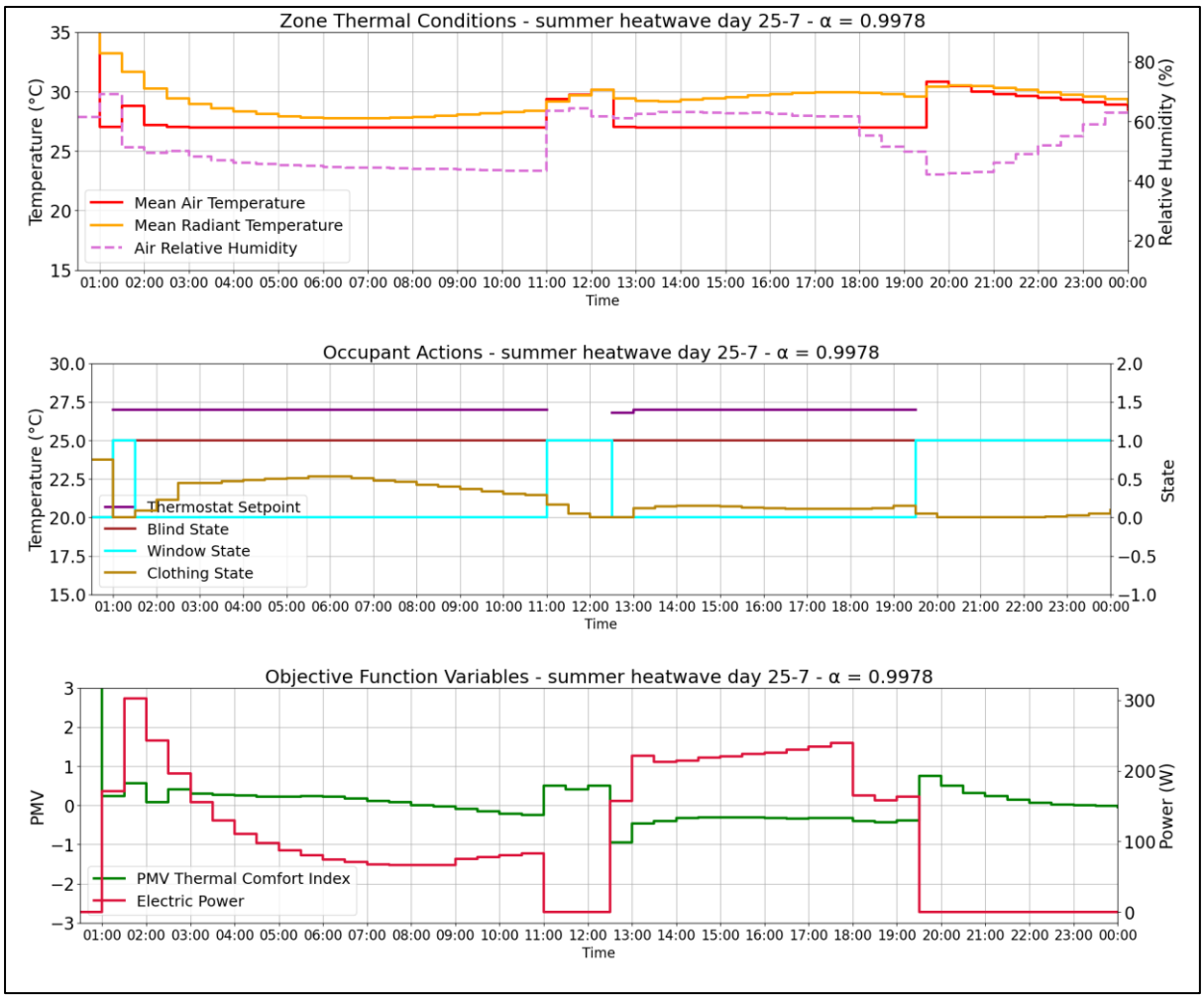

Figure 43.. Summer heatwave day (05/07) thermal zone conditions, occupant actions and the resulting thermal comfort and energy consumption, α = 0.9978.

5.3.4. Autumn shoulder day analysis (23/11)

Regarding the OWC during the autumn shoulder day (23/11, Figure 44), air temperature remains at around 10°C, while dewpoint temperature decreases significantly, reaching -10°C at noon. Relative humidity follows the dewpoint temperature trajectories and ranges between (25%-78%). Between 1:00 – 7:00 strong south and south-east winds are observed reaching the speed of 12m/s, while pressure levels reach the lowest out of the 4 days (97.2 kPa). In the afternoon wind speeds reduce. Throughout the day, horizontal infrared radiation has a mean value of 278.3 W/m^2.

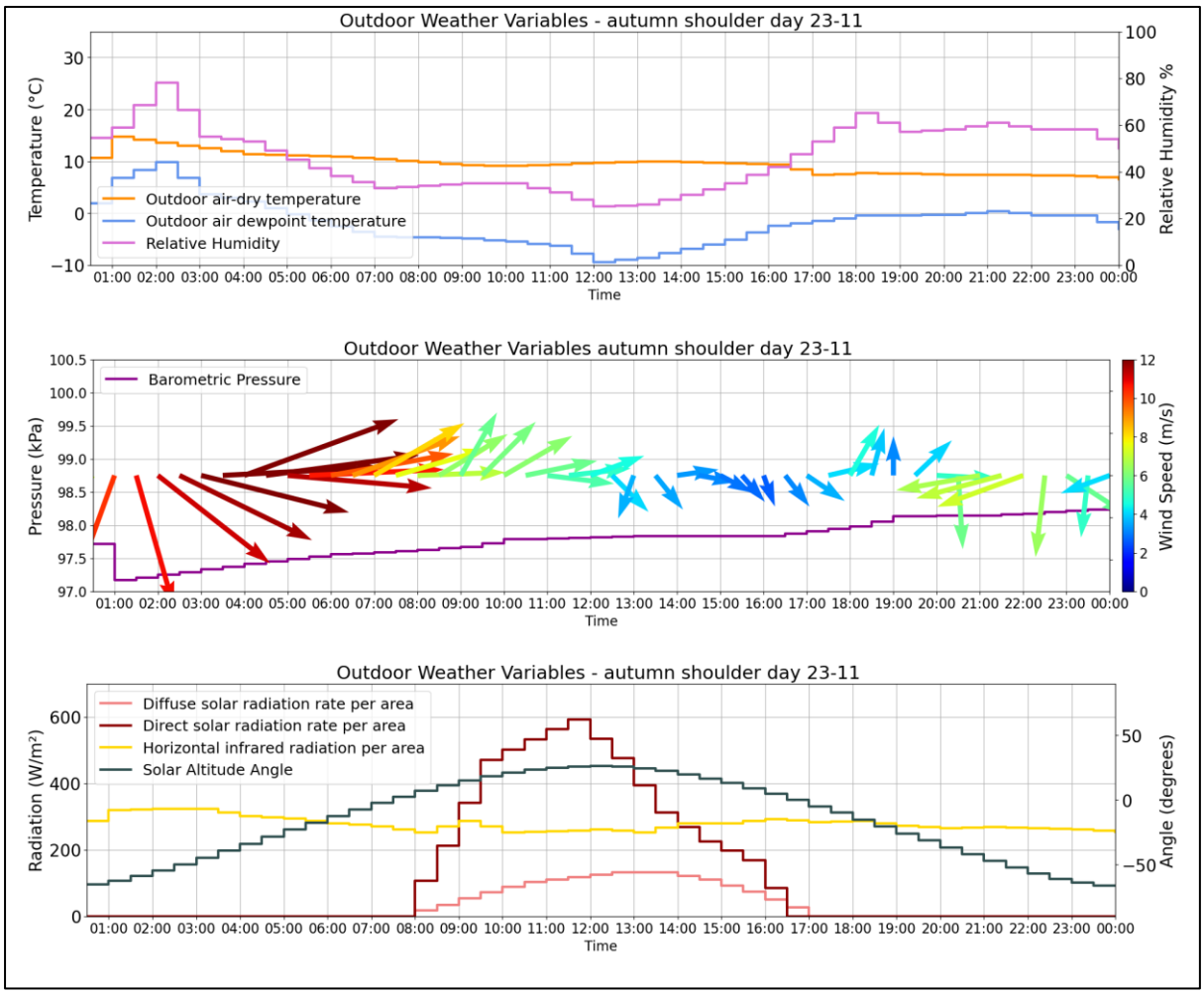

Figure 44. Autumn shoulder day (23/11) outdoor weather conditions.

Observing the optimisation outcomes on 23/11, in both scenarios (α = 0.97 - Figure 45, α = 0.99 - Figure 46), clothing is used to its maximum, receiving a value of 1.5 clo, and the PTHPs are enabled throughout the day. When α = 0.97, the PTHP thermostat is set below 20°C, and is used taking into consideration its effect on EC, as its value reaches the minimum allowed value (17°C), multiple times during the day. When α = 0.99, the thermostat value is always higher than when α = 0.97, only ever reaching below 20°C values, when outdoor radiation values are the highest. In general, the actions follow a similar pattern, with just the temperature value of the thermostat defining the trade-off between TC and EC. Blind and window actions are not utilized.

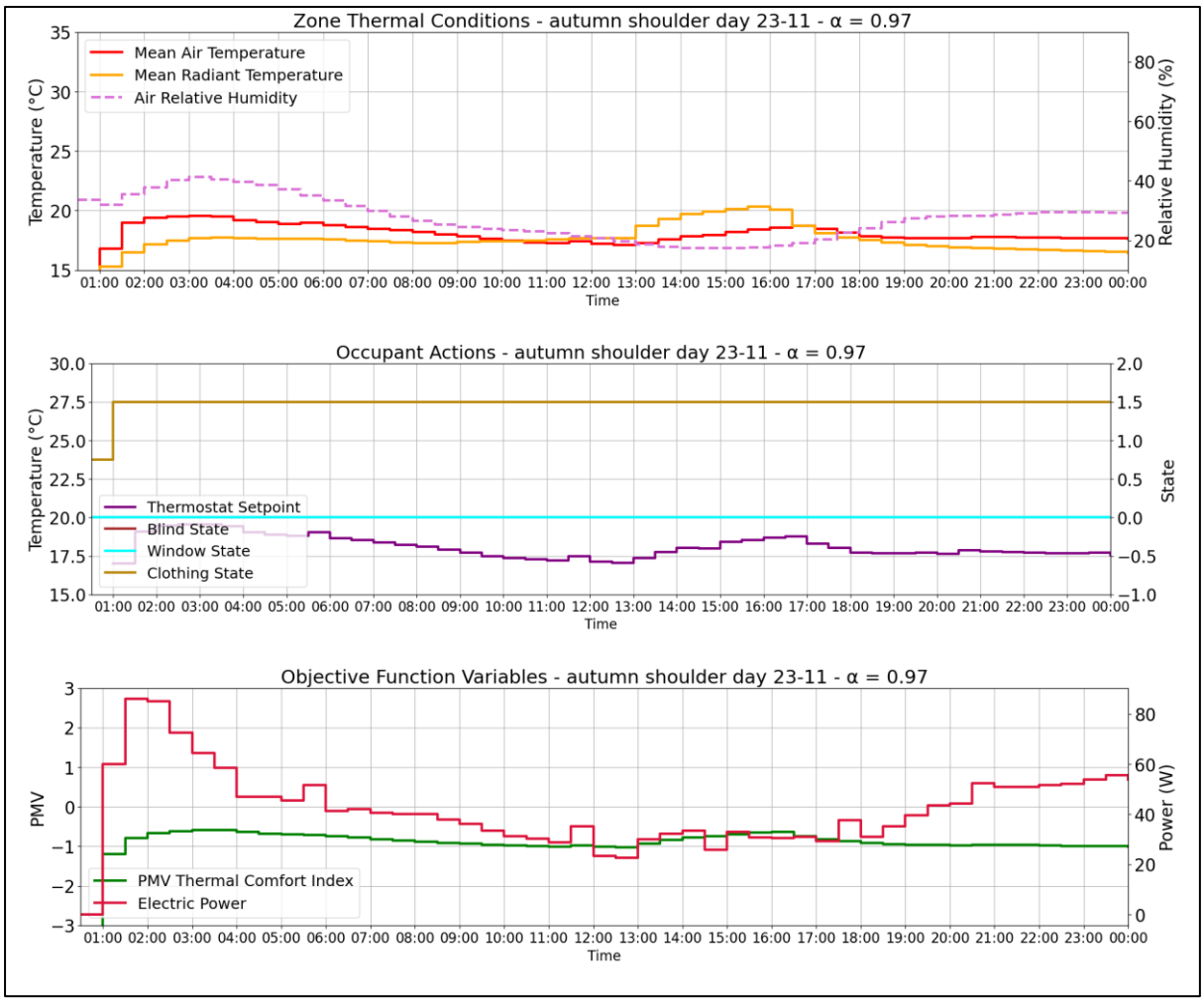

Figure 45. Autumn shoulder day (23/11) thermal zone conditions, occupant actions and the resulting thermal comfort and energy consumption, α = 0.97.

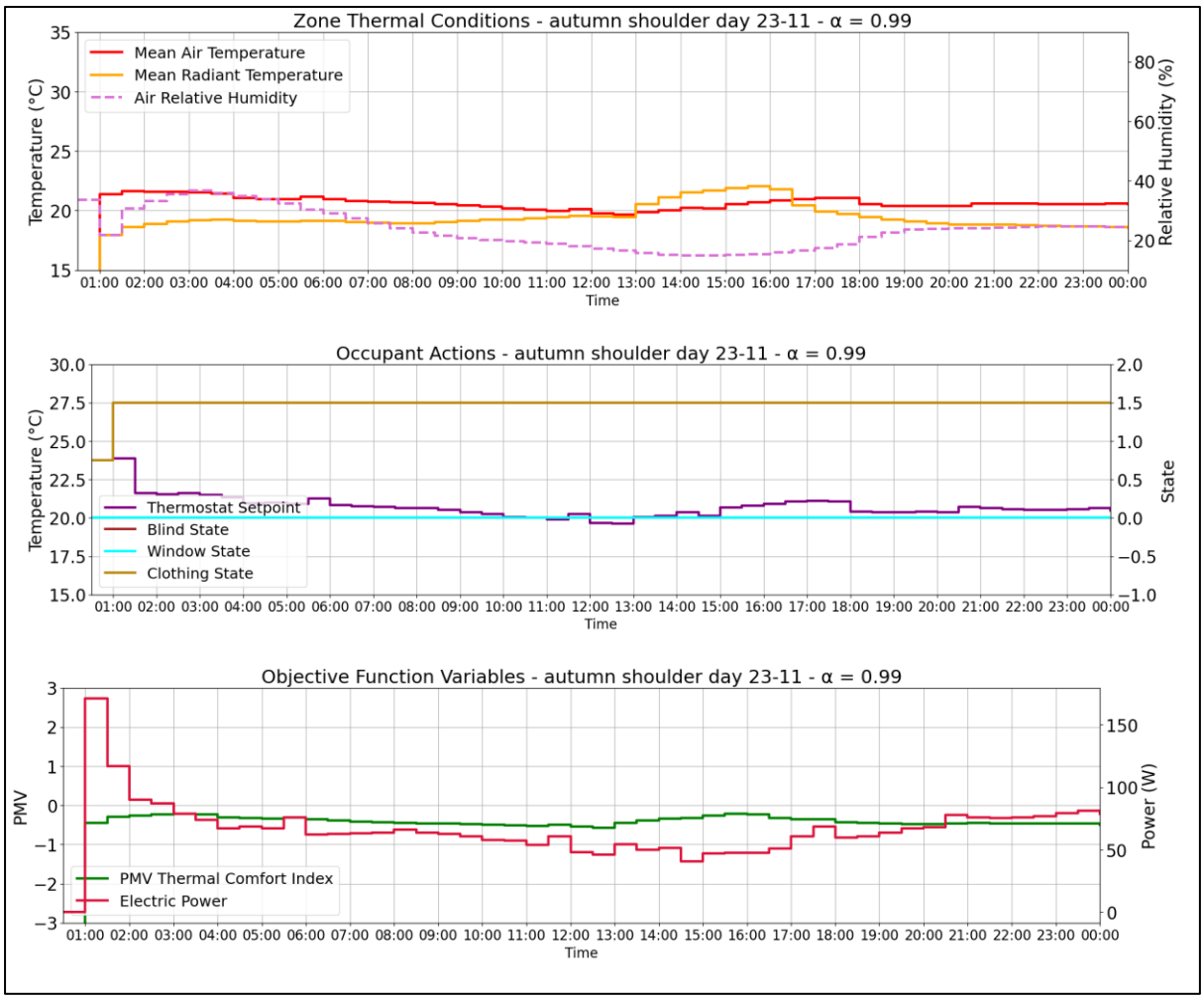

Figure 46. Autumn shoulder day (23/11) thermal zone conditions, occupant actions and the resulting thermal comfort and energy consumption, α = 0.99.

5.3.5. Winter shoulder day analysis (09/02)

During (09/02, Figure 47) outdoor air-dry temperature remains under 10ºC and outdoor dewpoint temperature, remains below 0ºC, with an observed mean value of -6ºC and -2.7ºC respectively. Again, outdoor relative humidity follows the patterns of dewpoint temperature with its lower values reaching 35%, during the time with high radiation. Outdoor pressure remains fairly stable, showing a similar value and trajectory as the outdoor pressure during the spring shoulder day. Strong northwest winds blow above $10 m/s$ in wind speed, are blowing after the 14:00 hour mark. Horizontal infrared radiation has a mean value of 275.8 W/m^2.

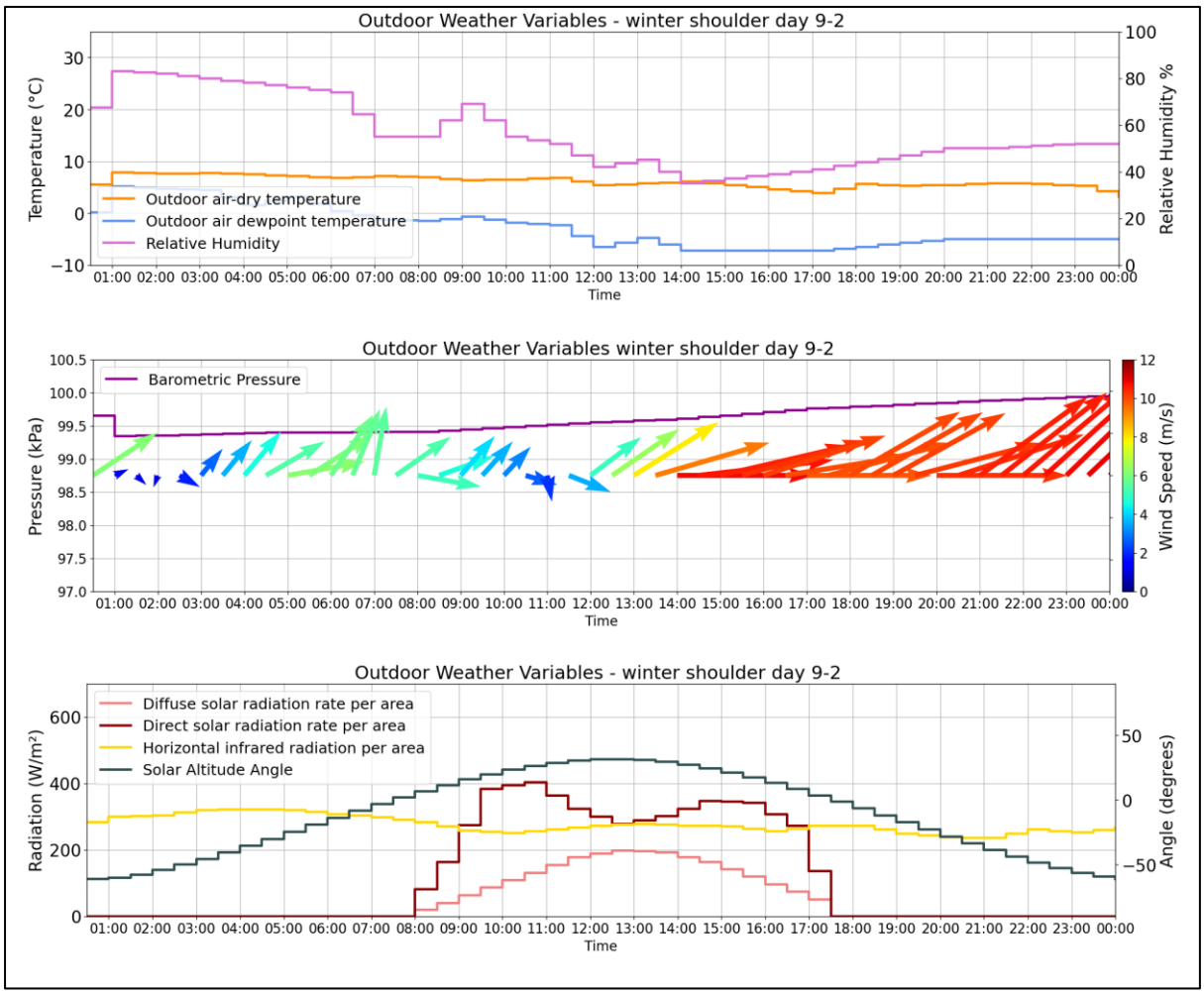

Figure 47. Winter shoulder day (09/02) outdoor weather conditions.

During the winter shoulder day, observing the closed-loop simulation results , because of the harsh OWC, again in both explored scenarios (α = 0.969 - Figure 48, α = 0.99 - Figure 49), and because of its non-consumptive nature, clothing insulation, is utilised to the maximum value. Regarding, the operation of the PTHP, when α = 0.969 it is turned off twice to save energy, once at 1:30 (after a high 27°C thermostat value) only for a few timesteps, and once after 23:00 till the end of the day. In between, the PTHP is in operation with its thermostat values relatively stably set around the 17°C mark. In contrast, when α = 0.99, the PTHP system is in operation throughout the day. In the beginning of the day, higher initial thermostat values, above 22°C, are observed, while later on between 3:00 – 19:00 the thermostat values stabilise between 19°C-21°C. After 19:00, 4 peaks are observed, as the thermostat values alternate between 20°C and 23°C. Observing the OWC, this behaviour is probably related to the strong west-facing winds applied to the west facing thermal zone and window. Blinds and window actions are not implemented in either scenario.

Figure 48. Winter shoulder day (09/02) thermal zone conditions, occupant actions and the resulting thermal comfort and energy consumption, α = 0.969.

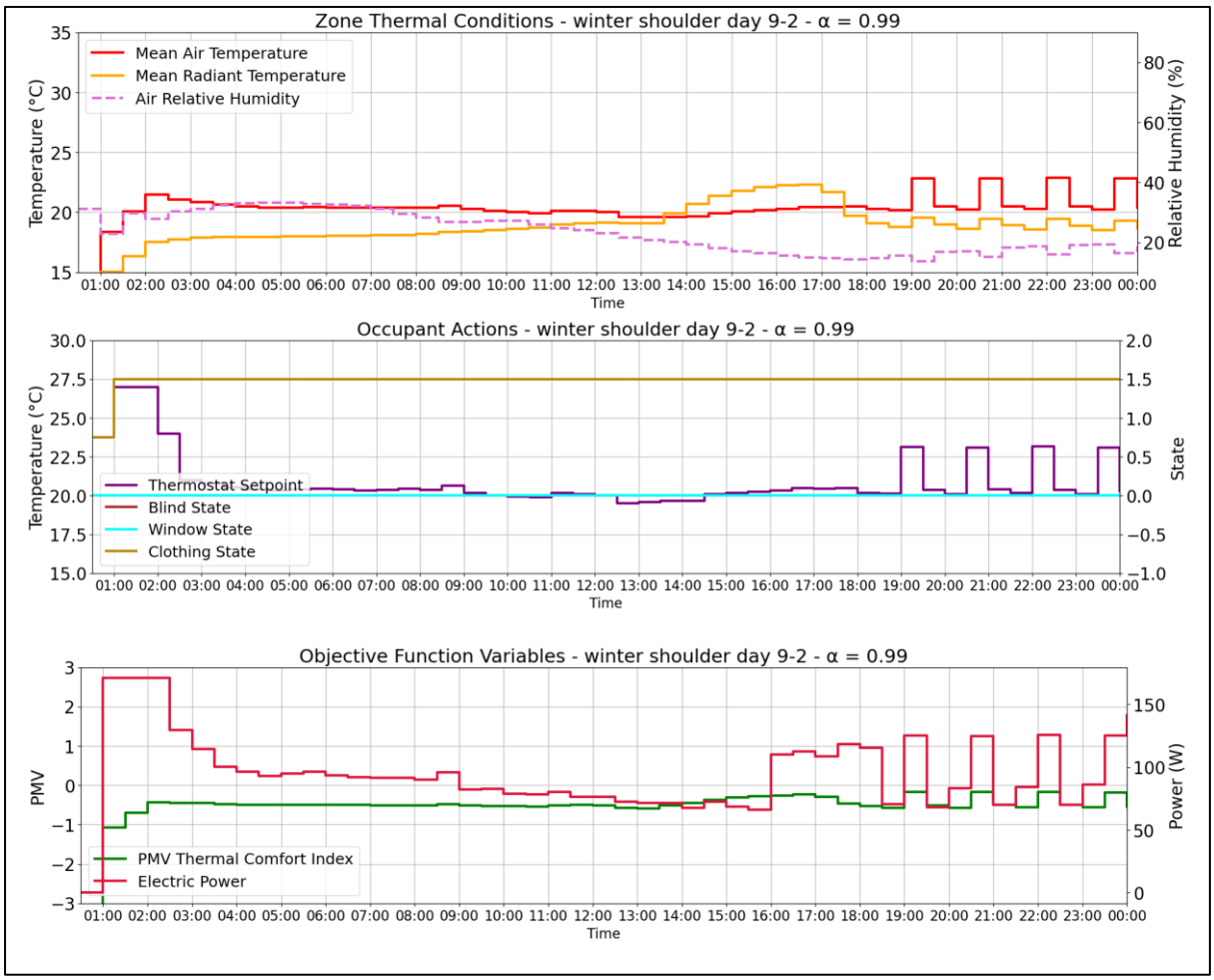

Figure 49. Winter shoulder day (09/02) thermal zone conditions, occupant actions and the resulting thermal comfort and energy consumption, α = 0.99.

5.4. Pareto Optimal Curves

The objective functions of the optimisation problem under consideration consists of three terms: (i) TC maximisation, (ii) EC minimisation and (iii) HVAC operation stabilisation. As the closed loop simulation analysis has demonstrated, (i), (ii) contradict with each other, and therefore a Pareto curve is generated to depict a set of optimal results. The problem is solved iteratively for each of the 4 shoulder days plus the summer heatwave day, with varying values assigned to the parameter α of the objective function Equation (4). The α parameter represents the trade-off between (i) and (ii), and characterises optimal OB profiles, and their respective preferences. Notably α, only affects (i), (ii). The extend to which (iii) is considered, is defined by the ratio between the weighting coefficients QR, R, (3.2.4, Equation (4)), which remains fixed throughout the iterative pareto curve derivation process. The Pareto curve graphs are produced by varying α from 0 to 1 mostly in increments of 0.001. In areas of interest, to obtain further insight, α is incremented by values as small as 0.0002. For each examined day the range of α's is utilised that best depicts the trade-off and dynamics between (i), (ii).

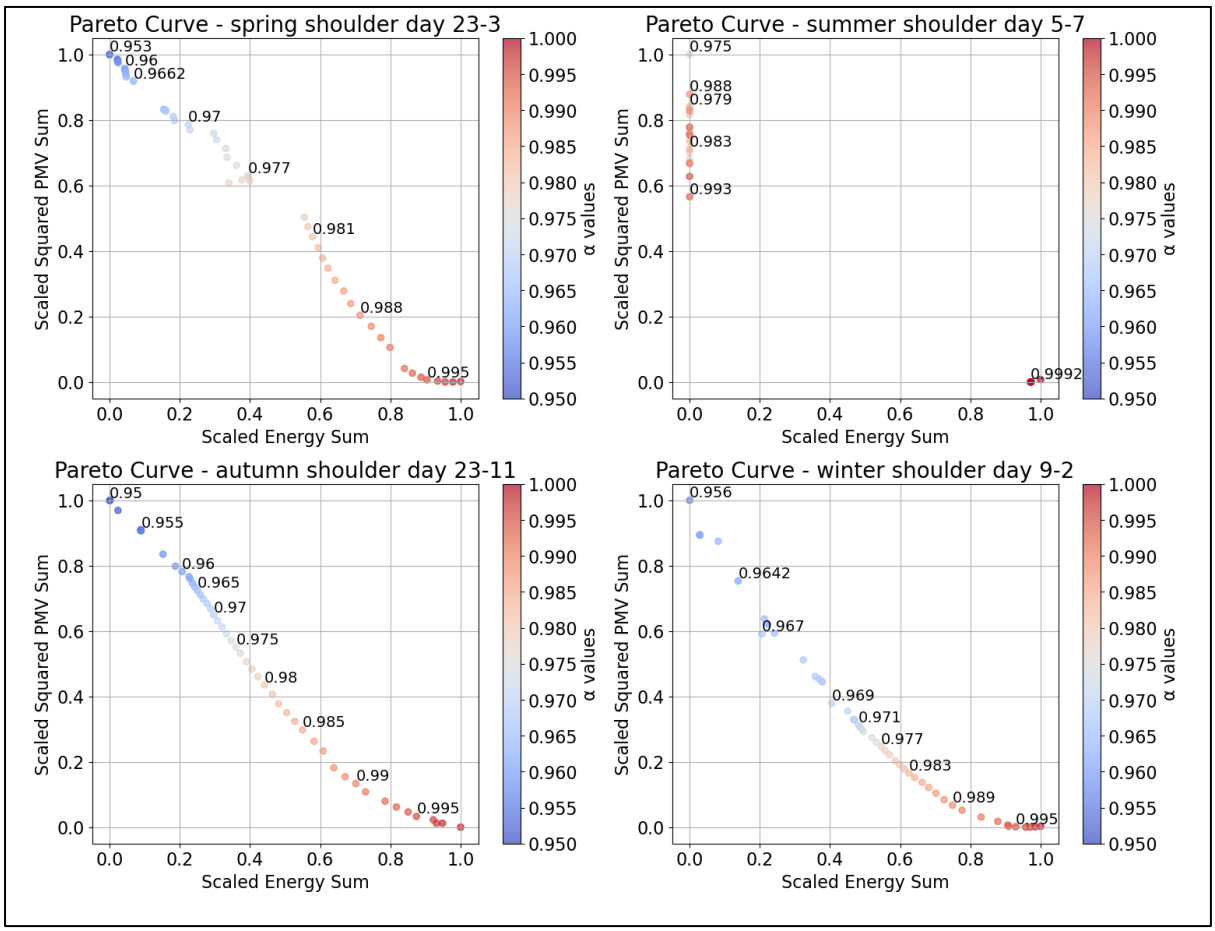

Figure 50. Pareto curves for shoulder days showing the trade-off between comfort and energy use.

During each of spring, autumn, winter shoulder day it is evident that by prioritising TC, EC is increasing in a non-linear fashion. Regarding the summer shoulder day though, it is evident, as mentioned in 5.3.2, that the non-consumptive adaptive TC actions in a lot of OB profiles (different α values) adequately cover the need for TC satisfaction and thus no energy is consumed. Only if the occupant preferences almost entirely focus on TC maximisation (Figure 50) a shift towards EC is observed. Another day was examined, to investigate the Pareto curve, for extreme heat weather conditions during summer. Examining the summer heatwave day, it is evident that for occupants prioritising TC satisfaction (gradually higher α values), a gradual need for HVAC enablement and increased energy consumption is depicted Figure 51.

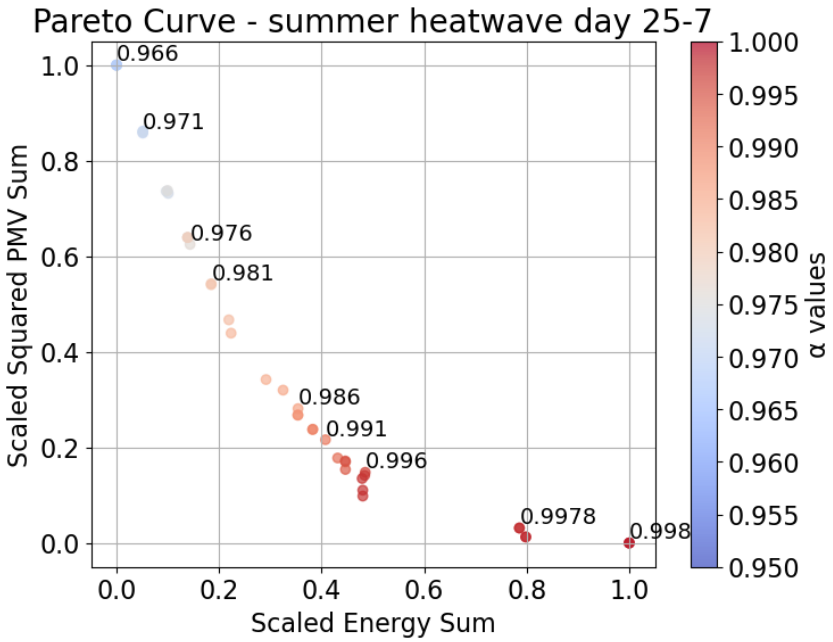

Figure 51. Pareto Curve for summer heatwave day showing trade-off between comfort and energy use.

6. Concluding Remarks and Future Work

In conclusion, this study introduces a comprehensive framework (Figure 17) aimed at understanding and simulating the intricate interplay between occupant behaviour, building conditions, thermal comfort, and energy efficiency. By integrating innovative dynamic methods and focusing on interventions centred around occupants, this research significantly advances scholarly understanding in building energy efficiency and indoor environmental quality.

The methodology employed integrates diverse techniques, including building energy simulations, occupant behaviour modelling, Python simulation coupling, machine learning methods, and mixed-integer optimisation. Notably, the optimisation process addresses the inherent challenge of balancing energy consumption minimisation with the maximisation of thermal comfort for the occupant, resulting in the derivation of optimised occupant behaviour profiles.

Results from the closed-loop simulations (section 5.3) underscore the effectiveness of the framework in optimising building performance under varying outdoor and indoor environmental conditions, as well as occupant preferences. Analysis conducted on specific days, including shoulder seasons and a summer heatwave, illustrates how different occupant behaviour profiles (objective function weighting factors), impact thermal comfort levels and energy consumption.

Moreover, the Pareto curves generated (section 5.4) through multi-objective optimisation provide valuable insights into the trade-offs between energy efficiency and thermal comfort. These curves depict how adjusting the weighting parameter, which governs the balance between these objectives, influences occupant behaviour profiles and overall building performance across different scenarios.

In summary, this study makes a significant contribution to advancing occupant-centric approaches in building design and operation. By integrating considerations of occupant behaviour into building energy simulations and optimisation strategies, this framework offers decision-making support for stakeholders and communities committed to achieving low-carbon goals. Ultimately, it facilitates the creation of healthier, more comfortable, and environmentally sustainable built environments.

To advance the introduced Occupant Behaviour Optimisation framework and its application, several key steps could be undertaken:

Enhanced Thermal Comfort Modelling: Incorporating varying metabolic rate values based on occupant activities into the Predicted Mean Vote (PMV) calculation will provide a more detailed understanding of thermal comfort dynamics in relation to different levels of physical exertion and activity.

Chance Constraints Optimisation: Integrating chance constraint optimisation techniques to maintain PMV and occupant clothing within predefined boundaries with a certain probability will ensure that thermal comfort and energy consumption remain within acceptable limits, accounting for uncertainties in occupant behaviour and environmental conditions.

Incorporation of multiple thermal zones and multiple occupants: Considering, analysing and modelling the behaviour of multiple occupants within multiple thermal zones of a building to further investigate the dynamics between outdoor weather conditions, multiple thermal zone building indoor conditions, occupant movement, actions and interactions, to scale the framework to a more holistic approach.

Application and validation to actual thermal zone: Deployment of the refined framework in a real-life thermal setting enables the validation of its performance in actual building-occupant dynamics scenarios. This validation process ascertains the model's accuracy and reliability in predicting building performance and occupant comfort under various conditions.

Development of a User-Friendly Recommendation System: Restructuring the framework to create a user-friendly recommendation system will enable the provision of actionable insights and recommendations based on occupant behaviour analysis, building conditions, and environmental factors.

7. References

[1] F. Lima, M. L. Nunes, J. Cunha, and A. F. P. Lucena, “Driving forces for aggregate energy consumption: A cross-country approach,” *Renew. Sustain. Energy Rev.*, vol. 68, pp. 1033–1050, Feb. 2017, doi: 10.1016/j.rser.2016.08.009.

[2] D. R. Easterling, G. A. Meehl, C. Parmesan, S. A. Changnon, T. R. Karl, and L. O. Mearns, “Climate Extremes: Observations, Modeling, and Impacts,” *Science*, vol. 289, no. 5487, pp. 2068–2074, Sep. 2000, doi: 10.1126/science.289.5487.2068.

[3] M. N. Uddin, Q. Wang, H. H. Wei, H. L. Chi, and M. Ni, “Building information modeling (BIM), System dynamics (SD), and Agent-based modeling (ABM): Towards an integrated approach,” *Ain Shams Eng. J.*, vol. 12, no. 4, pp. 4261–4274, Dec. 2021, doi: 10.1016/j.asej.2021.04.015.

[4] S. Chen, G. Zhang, X. Xia, Y. Chen, S. Setunge, and L. Shi, “The impacts of occupant behavior on building energy consumption: A review,” *Sustain. Energy Technol. Assess.*, vol. 45, p. 101212, Jun. 2021, doi: 10.1016/j.seta.2021.101212.

[5] J. Zuo and Z.-Y. Zhao, “Green building research–current status and future agenda: A review,” *Renew. Sustain. Energy Rev.*, vol. 30, pp. 271–281, Feb. 2014, doi: 10.1016/j.rser.2013.10.021.

[6] International Energy Agency, “World Energy Outlook 2023, IEA,” 2023.

[7] H. Wang, W. Chen, and J. Shi, “Low carbon transition of global building sector under 2- and 1.5-degree targets,” *Appl. Energy*, vol. 222, pp. 148–157, Jul. 2018, doi: 10.1016/j.apenergy.2018.03.090.

[8] P. Nejat, F. Jomehzadeh, M. M. Taheri, M. Gohari, and M. Z. Abd. Majid, “A global review of energy consumption, CO 2 emissions and policy in the residential sector (with an overview of the top ten CO 2 emitting countries),” *Renew. Sustain. Energy Rev.*, vol. 43, pp. 843–862, Mar. 2015, doi: 10.1016/j.rser.2014.11.066.

[9] C. Van Dronkelaar, M. Dowson, C. Spataru, and D. Mumovic, “A Review of the Regulatory Energy Performance Gap and Its Underlying Causes in Non-domestic Buildings,” *Front. Mech. Eng.*, vol. 1, Jan. 2016, doi: 10.3389/fmech.2015.00017.

[10] C. Klessmann, A. Held, M. Rathmann, and M. Ragwitz, “Status and perspectives of renewable energy policy and deployment in the European Union—What is needed to reach the 2020 targets?,” *Energy Policy*, vol. 39, no. 12, pp. 7637–7657, Dec. 2011, doi: 10.1016/j.enpol.2011.08.038.

[11] D. Yan *et al.*, “IEA EBC Annex 66: Definition and simulation of occupant behavior in buildings,” *Energy Build.*, vol. 156, pp. 258–270, Dec. 2017.

[12] E. Azar and C. C. Menassa, “Agent-Based Modeling of Occupants and Their Impact on Energy Use in Commercial Buildings,” *J. Comput. Civ. Eng.*, vol. 26, no. 4, pp. 506–518, Jul. 2012, doi: 10.1061/(ASCE)CP.1943-5487.0000158.

[13] A. C. Menezes, A. Cripps, D. Bouchlaghem, and R. Buswell, “Predicted vs. actual energy performance of non-domestic buildings: Using post-occupancy evaluation data to reduce the performance gap,” *Appl. Energy*, vol. 97, pp. 355–364, Sep. 2012, doi: 10.1016/j.apenergy.2011.11.075.

[14] A. Bueno, A. De Paula Xavier, and E. Broday, “Evaluating the Connection between Thermal Comfort and Productivity in Buildings: A Systematic Literature Review,” *Buildings*, vol. 11, no. 6, p. 244, Jun. 2021, doi: 10.3390/buildings11060244.

[15] J. Gupta and M. Chakraborty, “Energy efficiency in buildings,” in *Sustainable Fuel Technologies Handbook*, Elsevier, 2021, pp. 457–480. doi: 10.1016/B978-0-12-822989-7.00016-0.

[16] UNEP. Division of Technology, Industry and Economics, “ENERGY EFFICIENCY FOR BUILDINGS.”

[17] H. Yoshino, T. Hong, and N. Nord, “IEA EBC annex 53: Total energy use in buildings—Analysis and evaluation methods,” *Energy Build.*, vol. 152, pp. 124–136, Oct. 2017.

[18] M. E. Emetere, “Typical environmental challenges,” in *Numerical Methods in Environmental Data Analysis*, Elsevier, 2022, pp. 41–51. doi: 10.1016/B978-0-12-818971-9.00004-1.

[19] P. O. Fanger, “Thermal Comfort. Copenhagen, 1970”.

[20] American Society of Heating, Refrigerating and Air-Conditioning Engineers, “Standard 55-2017: Thermal Environmental Conditions for Human Occupancy (ANSI/ASHRAE Approved).” Atlanta, GA, 2017.

[21] SimScale, “What is PMV? what is PPD? the basics of Thermal comfort”.” [Online]. Available: https://www.simscale.com/blog/what-is-pmv-ppd/

[22] D. Bienvenido-Huertas and C. Rubio-Bellido, “Adaptive Thermal Comfort Models for Buildings,” in *Adaptive Thermal Comfort of Indoor Environment for Residential Buildings*, in SpringerBriefs in Architectural Design and Technology. , Singapore: Springer Singapore, 2021, pp. 13–33. doi: 10.1007/978-981-16-0906-0_2.

[23] M. Casini, “Building performance simulation tools,” in *Construction 4.0*, Elsevier, 2022, pp. 221–262. doi: 10.1016/B978-0-12-821797-9.00004-0.

[24] The Office of Energy Efficiency and Renewable Energy (EERE), “About Building Energy Modeling, Buildings.”

[25] X. Li and J. Wen, “Review of building energy modeling for control and operation,” *Renew. Sustain. Energy Rev.*, vol. 37, pp. 517–537, Sep. 2014, doi: 10.1016/j.rser.2014.05.056.

[26] A. H. Al Ka’bi, “Comparison of energy simulation applications used in green building,” *Ann. Telecommun.*, vol. 75, no. 7–8, pp. 271–290, Aug. 2020, doi: 10.1007/s12243-020-00771-6.

[27] A. Shahcheraghian, H. Madani, and A. Ilinca, “From White to Black-Box Models: A Review of Simulation Tools for Building Energy Management and Their Application in Consulting Practices,” *Energies*, vol. 17, no. 2, p. 376, Jan. 2024, doi: 10.3390/en17020376.

[28] Z. Afroz, G. Shafiullah, T. Urmee, and G. Higgins, “Modeling techniques used in building HVAC control systems: A review,” *Renew. Sustain. Energy Rev.*, vol. 83, pp. 64–84, Mar. 2018.

[29] N. Saha, A. Swetapadma, and M. Mondal, “A Brief Review on Artificial Neural Network: Network Structures and Applications,” in *2023 9th International Conference on Advanced Computing and Communication Systems (ICACCS)*, Coimbatore, India: IEEE, Mar. 2023, pp. 1974–1979. doi: 10.1109/ICACCS57279.2023.10112753.

[30] K. Amasyali and N. M. El-Gohary, “A review of data-driven building energy consumption prediction studies,” *Renew. Sustain. Energy Rev.*, vol. 81, pp. 1192–1205, Jan. 2018, doi: 10.1016/j.rser.2017.04.095.

[31] “Overview of optimization,” in *Process Systems Engineering*, vol. 7, Elsevier, 2006, pp. 285–314. doi: 10.1016/S1874-5970(06)80012-3.

[32] S. Boyd and L. Vandenberghe, *Convex optimization*. Cambridge university press, 2004.

[33] H. Ren and Y. Sun, “Building energy flexibility: modeling and optimization,” in *Building Energy Flexibility and Demand Management*, Elsevier, 2023, pp. 41–62. doi: 10.1016/B978-0-323-99588-7.00002-X.

[34] N. Collath, B. Tepe, S. Englberger, A. Jossen, and H. Hesse, “Aging aware operation of lithium-ion battery energy storage systems: A review,” *J. Energy Storage*, vol. 55, p. 105634, Nov. 2022, doi: 10.1016/j.est.2022.105634.

[35] J. D. Kelly and B. C. Menezes, “Automating a shuttle-conveyor for multi-stockpile level control,” in *Computer Aided Chemical Engineering*, vol. 46, Elsevier, 2019, pp. 1153–1158. doi: 10.1016/B978-0-12-818634-3.50193-4.

[36] C. A. Floudas, *Nonlinear and Mixed-Integer Optimization: Fundamentals and Applications*. Oxford University Press, 1995. doi: 10.1093/oso/9780195100563.001.0001.

[37] A. Iqbal, A. Nauman, R. Hussain, and M. Bilal, “Cognitive D2D communication: A comprehensive survey, research challenges, and future directions,” *Internet Things*, vol. 24, p. 100961, Dec. 2023, doi: 10.1016/j.iot.2023.100961.

[38] P. Limleamthong and G. Guillén-Gosálbez, “Combined Use of Bilevel Programming and Multi-objective Optimization for Rigorous Analysis of Pareto Fronts in Sustainability Studies: Application to the Redesign of the UK Electricity Mix,” in *Computer Aided Chemical Engineering*, vol. 43, Elsevier, 2018, pp. 1099–1104. doi: 10.1016/B978-0-444-64235-6.50192-3.

[39] H. Y. Alhammadi and J. A. Romagnoli, “Process design and operation,” in *Computer Aided Chemical Engineering*, vol. 17, Elsevier, 2004, pp. 264–305. doi: 10.1016/S1570-7946(04)80063-4.

[40] P. Chutima and P. Pinkoompee, “Multi-objective sequencing problems of mixed-model assembly systems using memetic algorithms,” *ScienceAsia*, vol. 35, no. 3, p. 295, 2009, doi: 10.2306/scienceasia1513-1874.2009.35.295.

[41] G. M. Kopanos and E. N. Pistikopoulos, “Reactive Scheduling by a Multiparametric Programming Rolling Horizon Framework: A Case of a Network of Combined Heat and Power Units,” *Ind. Eng. Chem. Res.*, vol. 53, no. 11, pp. 4366–4386, Mar. 2014.

[42] Z. Wang, T. Hong, and M. A. Piette, “Data fusion in predicting internal heat gains for office buildings through a deep learning approach,” *Appl. Energy*, vol. 240, pp. 386–398, Apr. 2019, doi: 10.1016/j.apenergy.2019.02.066.

[43] X. Luo, K. P. Lam, Y. Chen, and T. Hong, “Performance evaluation of an agent-based occupancy simulation model,” *Build. Environ.*, vol. 115, pp. 42–53, Apr. 2017, doi: 10.1016/j.buildenv.2017.01.015.

[44] D. Aerts, J. Minnen, I. Glorieux, I. Wouters, and F. Descamps, “A method for the identification and modelling of realistic domestic occupancy sequences for building energy demand simulations and peer comparison,” *Build. Environ.*, vol. 75, pp. 67–78, May 2014, doi: 10.1016/j.buildenv.2014.01.021.

[45] Y. Zhang, X. Bai, F. P. Mills, and J. C. V. Pezzey, “Rethinking the role of occupant behavior in building energy performance: A review,” *Energy Build.*, vol. 172, pp. 279–294, Aug. 2018, doi: 10.1016/j.enbuild.2018.05.017.

[46] D. Yan *et al.*, “IEA EBC Annex 66: Definition and simulation of occupant behavior in buildings,” *Energy Build.*, vol. 156, pp. 258–270, Dec. 2017, doi: 10.1016/j.enbuild.2017.09.084.

[47] J. Ouyang and K. Hokao, “Energy-saving potential by improving occupants’ behavior in urban residential sector in Hangzhou City, China,” *Energy Build.*, vol. 41, no. 7, pp. 711–720, Jul. 2009, doi: 10.1016/j.enbuild.2009.02.003.

[48] A. Khosrowpour, R. K. Jain, J. E. Taylor, G. Peschiera, J. Chen, and R. Gulbinas, “A review of occupant energy feedback research: Opportunities for methodological fusion at the intersection of experimentation, analytics, surveys and simulation,” *Appl. Energy*, vol. 218, pp. 304–316, May 2018, doi: 10.1016/j.apenergy.2018.02.148.

[49] S. Chen, G. Zhang, X. Xia, Y. Chen, S. Setunge, and L. Shi, “The impacts of occupant behavior on building energy consumption: A review,” *Sustain. Energy Technol. Assess.*, vol. 45, p. 101212, Jun. 2021, doi: 10.1016/j.seta.2021.101212.

[50] T. Hong, S. D’Oca, S. C. Taylor-Lange, W. J. N. Turner, Y. Chen, and S. P. Corgnati, “An ontology to represent energy-related occupant behavior in buildings. Part II: Implementation of the DNAS framework using an XML schema,” *Build. Environ.*, vol. 94, pp. 196–205, Dec. 2015, doi: 10.1016/j.buildenv.2015.08.006.

[51] T. Hong, S. D’Oca, W. J. N. Turner, and S. C. Taylor-Lange, “An ontology to represent energy-related occupant behavior in buildings. Part I: Introduction to the DNAs framework,” *Build. Environ.*, vol. 92, pp. 764–777, Oct. 2015, doi: 10.1016/j.buildenv.2015.02.019.

[52] T. Hong, D. Yan, S. D’Oca, and C. Chen, “Ten questions concerning occupant behavior in buildings: The big picture,” *Build. Environ.*, vol. 114, pp. 518–530, Mar. 2017, doi: 10.1016/j.buildenv.2016.12.006.

[53] M. Ala’raj, M. Radi, M. F. Abbod, M. Majdalawieh, and M. Parodi, “Data-driven based HVAC optimisation approaches: A Systematic Literature Review,” *J. Build. Eng.*, vol. 46, p. 103678, Apr. 2022.

[54] M. W. Ahmad, M. Mourshed, B. Yuce, and Y. Rezgui, “Computational intelligence techniques for HVAC systems: A review,” *Build. Simul.*, vol. 9, no. 4, pp. 359–398, Aug. 2016.

[55] M. Ning and M. Zaheeruddin, “Neuro-optimal operation of a variable air volume HVAC&R system,” *Appl. Therm. Eng.*, vol. 30, no. 5, pp. 385–399, Apr. 2010, doi: 10.1016/j.applthermaleng.2009.10.009.

[56] W.-S. Lee, Y.-T. Chen, and T.-H. Wu, “Optimization for ice-storage air-conditioning system using particle swarm algorithm,” *Appl. Energy*, vol. 86, no. 9, pp. 1589–1595, Sep. 2009.

[57] J. A. Wright, H. A. Loosemore, and R. Farmani, “Optimization of building thermal design and control by multi-criterion genetic algorithm,” *Energy Build.*, vol. 34, no. 9, pp. 959–972, Oct. 2002, doi: 10.1016/S0378-7788(02)00071-3.

[58] S. Shahnawazahmed, M. Shahmajid, H. Novia, and H. Abdrahman, “Fuzzy logic based energy saving technique for a central air conditioning system,” *Energy*, vol. 32, no. 7, pp. 1222–1234, Jul. 2007, doi: 10.1016/j.energy.2006.07.025.

[59] Z. Wang, R. Yang, and L. Wang, “Intelligent multi-agent control for integrated building and micro-grid systems,” in *ISGT 2011*, Anaheim, CA, USA: IEEE, Jan. 2011, pp. 1–7. doi: 10.1109/ISGT.2011.5759134.

[60] M. Mokhtar, M. Stables, X. Liu, and J. Howe, “Intelligent multi-agent system for building heat distribution control with combined gas boilers and ground source heat pump,” *Energy Build.*, vol. 62, pp. 615–626, Jul. 2013, doi: 10.1016/j.enbuild.2013.03.045.

[61] G. Serale, M. Fiorentini, A. Capozzoli, D. Bernardini, and A. Bemporad, “Model Predictive Control (MPC) for Enhancing Building and HVAC System Energy Efficiency: Problem

Formulation, Applications and Opportunities," *Energies*, vol. 11, no. 3, p. 631, Mar. 2018, doi: 10.3390/en11030631.

[62] C. C. W. Ham, S. P. N. Singh, and M. Kearney, "Learning-based model predictive control and user feedback in home automation," in *2013 IEEE/RSJ International Conference on Intelligent Robots and Systems*, Tokyo: IEEE, Nov. 2013, pp. 2718–2724. doi: 10.1109/IROS.2013.6696740.

[63] I. Hazyuk, C. Ghiaus, and D. Penhouet, "Optimal temperature control of intermittently heated buildings using Model Predictive Control: Part I – Building modeling," *Build. Environ.*, vol. 51, pp. 379–387, May 2012, doi: 10.1016/j.buildenv.2011.11.009.

[64] INCAS − National Institute for Aerospace Research "Elie Carafoli" B-dul Iuliu Maniu 220, Bucharest 061126, Romania iursu@incas.ro, U. Ioan, N. Ilinca, C. Sorin, I. Andreea, and T. Adrian, "Intelligent control of HVAC systems. Part I: Modeling and synthesis," *INCAS Bull.*, vol. 5, no. 1, pp. 103–118, Mar. 2013, doi: 10.13111/2066-8201.2013.5.1.11.

[65] R. Yang and L. Wang, "Multi-objective optimization for decision-making of energy and comfort management in building automation and control," *Sustain. Cities Soc.*, vol. 2, no. 1, pp. 1–7, Feb. 2012, doi: 10.1016/j.scs.2011.09.001.

[66] E. T. Maddalena, Y. Lian, and C. N. Jones, "Data-driven methods for building control — A review and promising future directions," *Control Eng. Pract.*, vol. 95, p. 104211, Feb. 2020, doi: 10.1016/j.conengprac.2019.104211.

[67] G. Halhoul Merabet *et al.*, "Intelligent building control systems for thermal comfort and energy-efficiency: A systematic review of artificial intelligence-assisted techniques," *Renew. Sustain. Energy Rev.*, vol. 144, p. 110969, Jul. 2021.

[68] F. Chollet and others, "Keras." 2015. [Online]. Available: https://keras.io

[69] "EnergyPlus™. Computer software. https://www.osti.gov//servlets/purl/1395882. Vers. 00. USDOE Office of Energy Efficiency and Renewable Energy (EERE), Energy Efficiency Office. Building Technologies Office. 30 Sep. 2017. Web."

[70] B. Pang, E. Nijkamp, and Y. N. Wu, "Deep Learning With TensorFlow: A Review," *J. Educ. Behav. Stat.*, vol. 45, no. 2, pp. 227–248, Apr. 2020, doi: 10.3102/1076998619872761.

[71] A. Subasi, "Machine learning techniques," in *Practical Machine Learning for Data Analysis Using Python*, Elsevier, 2020, pp. 91–202. doi: 10.1016/B978-0-12-821379-7.00003-5.

[72] F. Pedregosa *et al.*, "Scikit-learn: Machine Learning in Python," *J. Mach. Learn. Res.*, vol. 12, no. 85, pp. 2825–2830, 2011.

[73] M. L. Bynum *et al.*, *Pyomo — Optimization Modeling in Python*, vol. 67. in Springer Optimization and Its Applications, vol. 67. Cham: Springer International Publishing, 2021.

[74] Gurobi Optimization, LLC, "Gurobi Optimizer Reference Manual." 2023.

[75] A. Butt, "The Stack Effect - Fine Homebuilding — finehomebuilding.com." [Online]. Available: https://www.finehomebuilding.com/project-guides/insulation/how-it-works-the-stack-effect

[76] J. Katz, I. Pappas, S. Avraamidou, and E. N. Pistikopoulos, "Integrating Deep Learning and Explicit MPC for Advanced Process Control," in *2020 American Control Conference (ACC)*, Denver, CO, USA: IEEE, Jul. 2020, pp. 3559–3564.

[77] M. Fischetti and J. Jo, "Deep neural networks and mixed integer linear optimization," *Constraints*, vol. 23, no. 3, pp. 296–309, Jul. 2018, doi: 10.1007/s10601-018-9285-6.

[78] B. Grimstad and H. Andersson, “ReLU Networks as Surrogate Models in Mixed-Integer Linear Programs,” 2019, doi: 10.48550/ARXIV.1907.03140.

[79] C. Federspiel, “User-adaptable and minimum-power thermal comfort control,” Massachusetts Institute of Technology, 1992.

[80] International Organization for Standardization [ISO], “Ergonomics of the thermal environment — Analytical determination and interpretation of thermal comfort using calculation of the PMV and PPD indices and local thermal comfort criteria ISO-7730.” 2005.

[81] N. Kampelis *et al.*, “Evaluation of the performance gap in industrial, residential & tertiary near-Zero energy buildings,” *Energy Build.*, vol. 148, pp. 58–73, Aug. 2017.

[82] World Meteorological Organization, *Guide to meteorological instruments and methods of observation*, 6th ed. 1996.

Appendix

```python
def calculate_vapor_pressure_mmhg(temperature_C, relative_humidity):
    """
    This function calculates vapor pressure.

    Args:
        temperature_C (float): Temperature (°C).
        relative_humidity (float): Relative humidity (%).

    Returns:
        float: Vapor pressure (mmHg).
    """
    # Constants for Tetens formula
    A = 17.27
    B = 237.7

    # Convert relative humidity to fraction
    RH_fraction = relative_humidity / 100.0

    # Calculate saturation vapor pressure using Tetens formula
    saturation_vapor_pressure = 6.105 * math.exp((A * temperature_C) / (B + temperature_C))

    # Calculate actual vapor pressure using relative humidity
    actual_vapor_pressure = RH_fraction * saturation_vapor_pressure

    # Convert vapor pressure from hPa to mmHg
    actual_vapor_pressure_mmHg = actual_vapor_pressure * 0.750062

    return actual_vapor_pressure_mmHg
```

Figure 52. Vapor pressure calculation script.

```python
def pmv_custom(air_velocity, clothing_insulation, metabolic_rate, vp_mmhg, zone_temp, zone_temp_radiant):
        """
        Calculates Predicted Mean Vote (PMV) based on script in ISO 7730, 2005.

        Args:
            air_velocity (float): Air velocity in meters per second (m/s).
            clothing_insulation (float): Clothing insulation in clo units.
            metabolic_rate (float): Metabolic rate in met units.
            vp_mmhg (float): Vapor pressure in millimeters of mercury (mmHg).
            zone_temp (float): Zone temperature in Celsius (°C).
            zone_temp_radiant (float): Mean radiant temperature in Celsius (°C).

        Returns:
            float: Predicted Mean Vote (PMV) value.
        """
        metabolic_rate = metabolic_rate * 58.15           #Convert met to W/m^2
        Ta = zone_temp
        Tr = zone_temp_radiant
        P_a = vp_mmhg * 133.322133        #Convert water vapor pressure to Pa
        EW = 0
        v_air = air_velocity
        M = metabolic_rate
        W = EW
        MW = M - W  #Internal heat production in the human body
        ICL = clothing_insulation * 0.155   #Thermal insulation of clothing in m^2K/W
        #Calculate clothing area factor
        if ICL <= 0.078:
            FCL = 1 + 1.29 * ICL
        else:
            FCL = 1.05 + 0.645 * ICL
        HCF = 12.1 * math.sqrt(v_air)           #Heat transfer coefficient by forced convection
        TaA = Ta + 273  #Air temperature in Kelvin
        TrA = Tr + 273  #Radiant Temperature in Kelvin
        TCLA = TaA + (35.5 - Ta) / (3.5 * ICL + 0.1) #First guess for surface temperature for clothing
        P1 = ICL * FCL
        P2 = P1 * 3.96
        P3 = P1 * 100
        P4 = P1 * TaA
        P5 = 308.7 - 0.028 * MW + P2 * (TrA / 100) ** 4
        XN = TCLA / 100
        XF = XN
        N = 0
        EPS = 0.00015   #stop criteria in iteration
        #Calculate surface temperature for clothing by iteration
        while abs(XN - XF) > EPS or N == 0:
            XF = (XF + XN) / 2
            HCN = 2.38 * abs(100 * XF - TaA) ** 0.25
            if HCF > HCN:
                HC = HCF
            else:
                HC = HCN
            XN = (P5 + P4 * HC - P2 * XF ** 4) / (100 + P3 * HC)
            N += 1
            if N > 200:
                PMV = 999   #Dummy return value
                return PMV
        TCL = 100 * XN - 273 #Surface temperature of clothing
        #Heat loss components
        Ediff = 3.05 * 0.001 * (5733 - 6.99 * MW - P_a)     #Heat loss diff through skin
        Esw = 0.42 * (MW - 58.15) if MW > 58.15 else 0      #Heat loss by sweat
        LRES = 1.7 * 0.00001 * M * (5867 - P_a)             #Latent respiration heat loss
        DRES = 0.0014 * M * (34 - Ta)                       #Dry respiration heat loss
        R = 3.96 * FCL * (XN ** 4 - (TrA / 100) ** 4)       #Heat loss by radiation
        C = FCL * HC * (TCL - Ta)                           #Heat loss by convection
        TS = 0.303 * math.exp(-0.036 * M) + 0.028           #Thermal sensation transfer coefficient
        PMV = TS * (MW - Ediff - Esw - LRES - DRES - R - C) #Predicted Mean Vote
        PPD = 100 - 95 * math.exp(-0.03353 * PMV ** 4 - 0.2197 * PMV ** 2)  #Predicted Percentage of Dissatisfied

        return PMV
```

Figure 53. Predicted Mean Vote script calculation.

Table 13. Garment clothing insulation acquired from [20].

Garment Description	Clothing insulation (clo)	Garment Description	Clothing insulation (clo)
Underwear		**Dress and Skirts**	
Bra	0.01	Skirt (thin)	0.14
Panties	0.03	Skirt (thick)	0.23
Men's briefs	0.04	Sleeveless, scoop neck (thin)	0.23
T-shirt	0.08	Sleeveless, scoop neck (thick), i.e., jumper	0.27
Half-slip	0.14	Short-sleeve shirtdress (thin)	0.29
Long underwear bottoms	0.15	Long-sleeve shirtdress (thin)	0.33
Full slip	0.16	Long-sleeve shirtdress (thick)	0.47
Long underwear top	0.2		
Footwear		**Sweaters**	
Ankle-length athletic socks	0.02	Sleeveless vest (thin)	0.13
Pantyhose/stockings	0.02	Sleeveless vest (thick)	0.22
Sandals/thongs	0.02	Long-sleeve (thin)	0.25
Shoes	0.02	Long-sleeve (thick)	0.36
Slippers (quilted, pile lined)	0.03		
Calf-length socks	0.03	**Suit Jackets and Vests**	

Knee socks (thick)	0.06	Sleeveless vest (thin)	0.1
Boots	0.1	Sleeveless vest (thick)	0.17
Shirts and Blouses		Single-breasted (thin)	0.36
Sleeveless/scoop-neck blouse	0.12	Single-breasted (thick)	0.44
Short-sleeve knit sport shirt	0.17	Double-breasted (thin)	0.42
Short-sleeve dress shirt	0.19	Double-breasted (thick)	0.48
Long-sleeve dress shirt	0.25		
Long-sleeve flannel shirt	0.34	**Sleepwear and Robes**	
Long-sleeve sweatshirt	0.34	Sleeveless short gown (thin)	0.18
Trousers and Coveralls		Sleeveless long gown (thin)	0.2
Short shorts	0.06	Short-sleeve hospital gown	0.31
Walking shorts	0.08	Short-sleeve short robe (thin)	0.34
Straight trousers (thin)	0.15	Short-sleeve pajamas (thin)	0.42
Straight trousers (thick)	0.24	Long-sleeve long gown (thick)	0.46
Sweatpants	0.28	Long-sleeve short wrap robe (thick)	0.48

Overalls	0.3	Long-sleeve pajamas (thick)	0.57
Coveralls	0.49	Long-sleeve long wrap robe (thick)	0.69

Table 14. Thermal Zone Information

Zone Name	EAST_2SMALLOFFICE 1
North Axis (deg)	0
Origin X-Coordinate (m)	4.41
Origin Y-Coordinate (m)	-7.68
Origin Z-Coordinate (m)	5.37
Centroid X-Coordinate (m)	5.81
Centroid Y-Coordinate (m)	-5.73
Centroid Z-Coordinate (m)	6.72
Type	1
Zone Multiplier	1
Zone List Multiplier	1
Minimum X (m)	4.5
Maximum X (m)	7.09
Minimum Y (m)	-7.58
Maximum Y (m)	-3.87
Minimum Z (m)	5.37

Maximum Z (m)	8.07
Ceiling Height (m)	2.7
Volume (m^3)	24.74
Zone Inside Convection Algorithm	TARP
Zone Outside Convection Algorithm	DOE-2
Floor Area (m^2)	9.16
Exterior Gross Wall Area (m^2)	16.63
Exterior Net Wall Area (m^2)	14.23
Exterior Window Area (m^2)	2.4
Number of Surfaces	9
Number of SubSurfaces	1
Number of Shading SubSurfaces	0
Part of Total Building Area	Yes

Table 15. Thermal Zone Sizing information

Zone Name	WEST_2SMALLOFFICE 1	WEST_2SMALLOFFICE 1
Load Type	Cooling	Heating
Calc Des Load (W)	604.833	89.03931
User Des Load (W)	695.55795	111.29913
Calc Des Air Flow Rate (m^3/s)	0.0492184	0.00402971
User Des Air Flow Rate (m^3/s)	0.0566012	0.00503714
Design Day Name	ANCONA ANN CLG .4% CONDNS DP=>MDB	ANCONA ANN HTG 99.6% CONDNS DB
Date/Time of Peak	1/8/2024 17:30	1/2/2024 7:00
Temperature at Peak (°C)	31.155	1.7
Humidity Ratio at Peak (kgWater/kgDryAir)	0.0194667	0.00434421
Floor Area (m^2)	9.1615	9.1615
Calc Outdoor Air Flow Rate (m^3/s)	0	0
Calc DOAS Heat Addition Rate (W)	0	0

Table 16. Thermal Zone Nominal Internal Gains

Zone Name	WEST_2SMALLOFFICE 1
Floor Area (m²)	9.16
Interior Lighting (W/m²)	5
Electric Load (W/m²)	6.5
Gas Load (W/m²)	0
Other Load (W/m²)	0
Hot Water Eq (W/m²)	0
Steam Equipment (W/m²)	0
Sum Loads per Area (W/m²)	11.5
Outdoor Controlled Baseboard Heat	No